

Intracellular Peptide Trafficking in Yeast

Vom Fachbereich Biologie
der Johann Wolfgang Goethe-Universität Frankfurt
zur Erlangung des akademischen Grades eines Doktors
genehmigte

DISSERTATION

vorgelegt
von

Eva Janas
2002

meiner Mutter

1	Introduction.....	9
1.1	Function and organisation of ABC transporters.....	9
1.2	ABC transporters in the yeast <i>S. cerevisiae</i>	12
1.3	ABC transporters associated with cellular peptide transport.....	14
1.4	Cooperation of the subunits during the transport process.....	15
1.5	Structure and function of the NBDs.....	15
1.6	Quality control in mitochondria.....	18
2	Motivation and aims.....	20
3	Material.....	21
3.1	Chemicals.....	21
3.2	Oligomers.....	23
3.3	Peptides.....	25
4	Methods.....	27
4.1	<i>E. coli</i> methods.....	27
4.1.1	<i>E. coli</i> media, culture conditions and methods.....	27
4.1.2	Competent <i>E. coli</i> cells.....	27
4.1.3	Transformation of competent <i>E. coli</i>	27
4.1.4	Plasmid construction.....	27
4.1.5	Plasmids encoding for <i>MDL1</i> and their expression conditions in <i>E. coli</i>	28
4.1.6	Plasmids encoding for <i>MDL1</i> and their expression in yeast.....	31
4.1.7	Plasmids encoding for <i>YLL048</i>	32
4.1.8	Plasmids containing different constructs of the α -factor.....	33
4.2	Yeast methods.....	35
4.2.1	Yeast media and growth conditions.....	35
4.2.2	Competent yeast cells.....	35
4.2.3	Transformation of yeast cells.....	35
4.2.4	Preparation of genomic DNA of yeast.....	36
4.3	RNA methods.....	37
4.3.1	Random-primed labelling of DNA-fragments.....	37
4.3.2	Isolation of total RNA.....	37
4.3.3	Northern blot.....	38
4.4	Cell biology of yeast.....	38
4.4.1	Preparation of crude cell extract.....	38
4.4.2	Preparation of total membranes.....	39
4.4.3	Cultivation of yeast cells for mitochondria preparation.....	39
4.4.4	Preparation of spheroplasts.....	39
4.4.5	Preparation of mitochondria.....	40

Table of contents

4.4.6	Generation of mitoplasts by osmotic swelling	40
4.4.7	Digitonin fractionation of mitochondria and proteinase K digestion	41
4.4.8	Preparation of microsomes	41
4.4.9	Preparation of vacuoles	41
4.4.10	Marker enzyme for vacuole	42
4.4.11	Subcellular fractionation	42
4.4.12	Preparation of transport-competent cells	43
4.5	Biochemical methods	43
4.5.1	SDS-PAGE	43
4.5.2	Western blotting	44
4.5.3	Stripping of immunoblots	45
4.5.4	Generation of Mdl1p-specific antiserum	46
4.5.5	Solubilization of membrane proteins from mitochondria	46
4.5.6	Enrichment of Mdl1p from solubilized mitochondria by gelfiltration	46
4.5.7	Affinity-isolation of Mdl1p from solubilized mitochondria	47
4.5.7.1	ATP-agarose	47
4.5.7.2	Metal affinity chromatography	47
4.5.7.3	Streptactin chromatography	47
4.5.8	Reconstitution into preformed liposomes	48
4.5.9	8-azido-ATP photolabelling of Mdl1p	48
4.5.10	Peptide labelling with NaI ¹²⁵	49
4.5.11	Peptide transport assay	49
4.5.12	Purification of His ₆ -tagged NBDs	50
4.5.13	8-azido-ATP photolabelling of the Mdl1p-NBD	50
4.5.14	ATPase assay	50
4.5.15	Dimerization Assays	51
4.5.16	Determination of the ATP/ADP composition of the dimer	51
4.5.17	Thiol-specific labelling of NBDs for FRET	51
5	Results	53
5.1	Characterisation of the ABC transporter Mdl1p	53
5.1.1	Expression and purification of wild type and mutant Mdl1p-NBDs	53
5.1.2	Activity of wild type Mdl1p-NBD	55
5.1.3	The active form of NBD is a dimer	58
5.1.4	Analysis of mutant NBDs	60
5.1.5	Nucleotide composition of the dimer	62
5.1.6	ATP hydrolysis cycle of Mdl1p-NBD	66
5.1.7	Expression and purification of full-length Mdl1p	68
5.1.8	Reconstitution of Mdl1p	70
5.1.9	Specific ATP binding of Mdl1p	74

5.1.10	Expression, purification and activity of recombinant Mdl1p.....	75
5.1.11	Deletion of mitochondrial targeting sequence	76
5.1.12	Expression and purification of His-tagged Mdl1p	80
5.1.13	Heterologous expression of Mdl1p in <i>E. coli</i>	81
5.2	Characterisation of an intracellular peptide transporter of <i>S. cerevisiae</i>	83
5.2.1	Characterisation of the ABC transporter encoded by <i>YLL048</i>	84
5.2.2	Substrate specificity	86
5.2.3	Subcellular localisation of the ABC transporter encoded by <i>YLL048</i>	88
5.2.4	Physiological function of YLL048p in yeast	91
5.3	<i>In vivo</i> screen of TAP mutants based on an autocrine stimulation assay	94
5.3.1	Pheromones mediate mating in the yeast	94
5.3.2	TAP-mediated α -factor secretion	95
5.3.3	Functionality of the autocrine stimulation assay	96
6	Discussion	99
6.1	Characterisation of the ATPase cycle of isolated Mdl1p-NBDs.....	99
6.1.1	Analysis of mutants in the ATPase cycle	100
6.1.2	Model of the ATPase cycle	102
6.2	Characterisation of yeast ABC transporter Mdl1p	103
6.2.1	Expression and reconstitution of Mdl1p	104
6.2.2	Deletion of the mitochondrial targeting sequence	106
6.3	Characterisation of an intracellular peptide transporter of <i>S. cerevisiae</i>	107
7	ZUSAMMENFASSUNG.....	109
8	Summary	115
9	Appendix	117
9.1	Thiol-specific labelling of NBDs to assay dimerization by FRET	117
9.2	Heterologous expression of transmembrane domain in <i>E.coli</i>	119
9.3	Abbreviations	121
10	References	123
11	Curriculum vitae	141

1 Introduction

1.1 Function and organisation of ABC transporters

ATP binding cassette (ABC) transporters comprise a large family of membrane proteins that catalyze the active transfer of a variety of solutes across biological membranes (Higgins, 1992). ABC transporters operate in all living cells from bacteria to human and fulfil a lot of cellular functions. Most of them act as ATP-driven transporters, which use the energy of ATP hydrolysis to pump substrates against a concentration gradient. However, ABC proteins can also function as ion channels, channel regulators, receptors, proteases and even as sensors of the environment (Higgins, 1995). A large variety of molecules is recognized as substrates ranging from ions, anticancer drugs, phospholipids, and peptides to antibiotics (Dean and Allikmets, 1995; Kuchler and Thorner, 1992). ABC transporters can function as importers and exporters. In bacteria, ABC transporters often work as nutrient uptake systems like the maltose importer MalFGK₂ from *E. coli* or the histidine permease HisQMP₂ from *S. typhimurium* (Bavoil *et al.*, 1980; Ames and Lever, 1970). ABC pumps like LmrA or HlyB confer resistance to antibiotics and toxins by exporting them out of the bacterium (van Veen *et al.*, 2001; Blight *et al.*, 1995).

The dysfunction of ABC transporters has been reported to be central to various human pathologies such as cystic fibrosis (CFTR), adrenoleukodystrophy (ALD), familial hyperinsulinemic hypoglycemia of infancy (SUR), and Stargardt's disease (hABCR). A separate class of ABC transporters is implicated in multidrug resistance (MDR) as P-glycoprotein (P-gp) whose overexpression in tumour cells causes resistance to various cytotoxic agents used in chemotherapy (Gottesman *et al.*, 1995). Another clinically relevant human ABC transporter is TAP (transporter associated with antigen processing), which translocates peptides from the cytosol to the ER and plays a key function in the presentation of antigenic peptides at the cell surface (Lankat-Buttgereit and Tampé, 2002).

The ABC transport family shares a common modular architecture consisting of two polytopic transmembrane domains (TMD) and two nucleotide binding domains (NBD). The four domains can be arranged in any possible combination (Fig.1). The subunits may be encoded as separate polypeptides as in the case of several bacterial transporters. The histidine permease complex of *S. typhimurium* comprises the membrane channel subunits HisQ and HisM and two ATP-binding subunits HisP. The majority of eukaryotic ABC transporters are expressed as a single polypeptide (P-gp). In half-size transporters like TAP each TMD is fused to an NBD. Several different arrangements are also observed but they are less frequent. In addition to the four core components, prokaryotic ABC transporters involved in solute uptake employ a periplasmic binding protein to capture the substrate (Van Der Heide and Poolman, 2002).

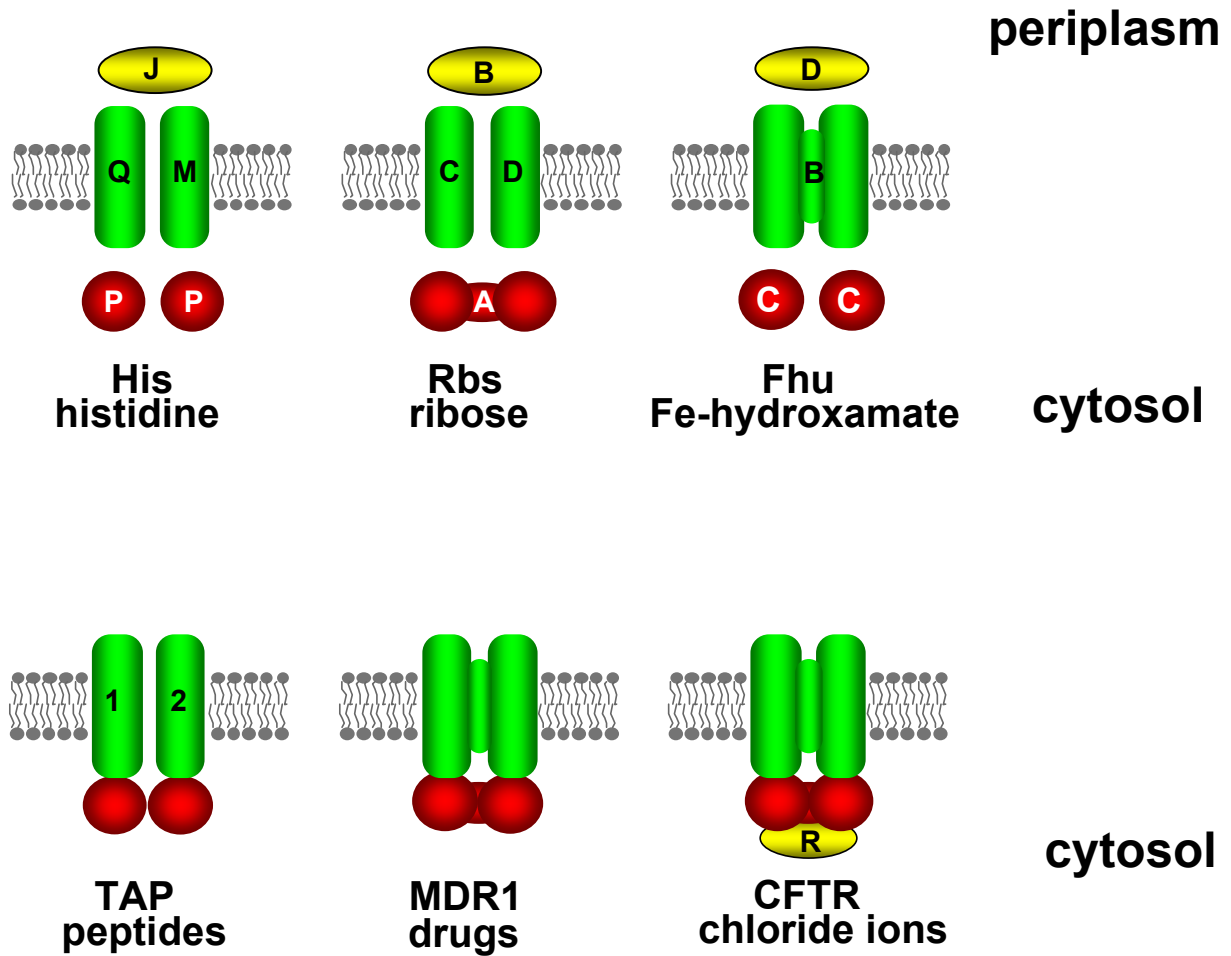


Fig.1: Organisation of ABC transporters.

The typical ABC transporter has two membrane-associated domains (TMDs), two ATP-binding domains (NBD) and in some cases the periplasmic substrate binding protein. The domains can be fused in different combinations: i) they can be encoded as four separate polypeptides (as for the histidine permease), ii) fused NBDs (as for the ribose transporter RbsA) iii) fused TMDs (as for the iron-chelate transporter FhuCB) iv) half-size transporter with one NBD fused to one TMD (as for the peptide transporter TAP) v) all four domains fused into a single polypeptide (as for the drug transporter MDR1) vi) intercalating R domain (only known for the chloride channel CFTR).

The TMDs span the membrane multiple times via putative α -helices forming the substrate translocation pore across the membrane (Fig.2). The majority of ABC transporters contain twelve predicted α -helices. However, examples of ABC-transporters with a different number of α -helices are known. Each TMD of the vitamin B₁₂ transporter BtuCDE of *E. coli* consists of 10 α -helices and the TMDs of human TAP1 and TAP2 are predicted to possess 10 and 9 α -helices, respectively (Locher *et al.*, 2002; Lankat-Buttgereit and Tampé, 2002). Some of the predicted membrane-spanning α -helices may not be crucial to the core function of substrate

translocation but may serve auxiliary functions such as membrane insertion or regulation of the transporter (Higgins, 2001). The substrate specificity is determined by the TMD or the periplasmic binding protein. As the substrate spectrum of the ABC transporter family is very broad, the TMDs generally share little homology (Holland and Blight, 1999).

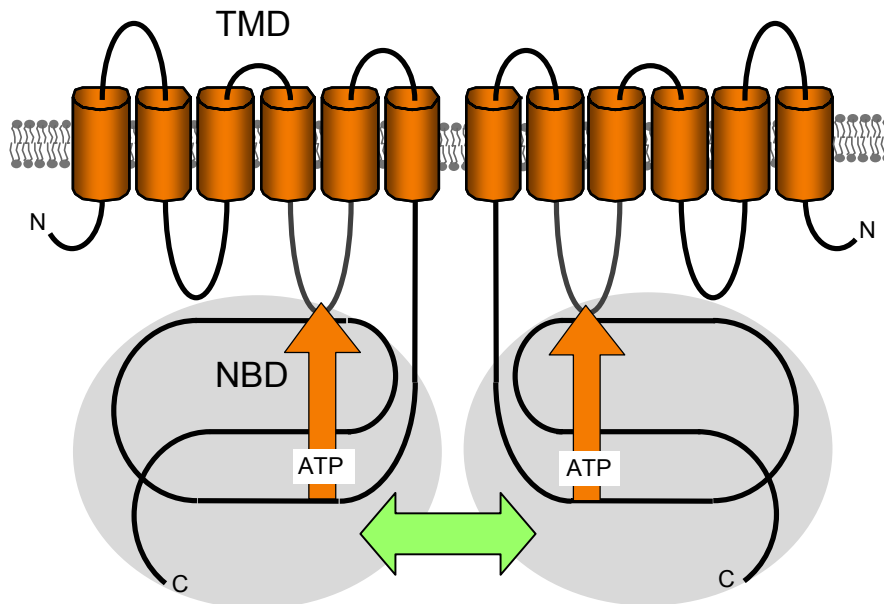


Fig.2: Predicted membrane topology of a half-size ABC transporter.

Typically, there are six predicted membrane spanning α -helices per domain (twelve per transporter). The TMDs form the pathway through which solutes cross the membrane and determine the specificity of the transporter through the substrate-binding sites. Two other domains, the NBDs, are hydrophilic and energize the transport by hydrolysis of ATP.

The NBDs act as molecular motors which drive the transport process by hydrolysis of ATP (for details, see below). The amino acid identity of NBDs is over 25%, suggesting that even in transporters of unrelated function the structure and function of NBDs is highly conserved (Schneider and Hunke, 1998).

1.2 ABC transporters in the yeast *S. cerevisiae*

The yeast *S. cerevisiae* was the first eukaryotic organism whose complete genome was sequenced and revealed the presence of 30 ABC protein genes (Tab.1) (Decottignies and Goffeau, 1997; Taglicht and Michaelis, 1998). Fungal ABC proteins are implicated in a variety of cellular functions ranging from drug resistance, pheromone secretion, stress response to cellular detoxification (Fig.3). Here only a brief overview of the ABC subfamilies in *S. cerevisiae* will be provided (for review see Bauer *et al.*, 1999). Based on phylogenetic analysis, yeast ABC proteins were classified into six subfamilies: MDR, PDR; MRP/CFTR, ALDp, YEF3, and RLI subfamily (Decottignies and Goffeau, 1997).

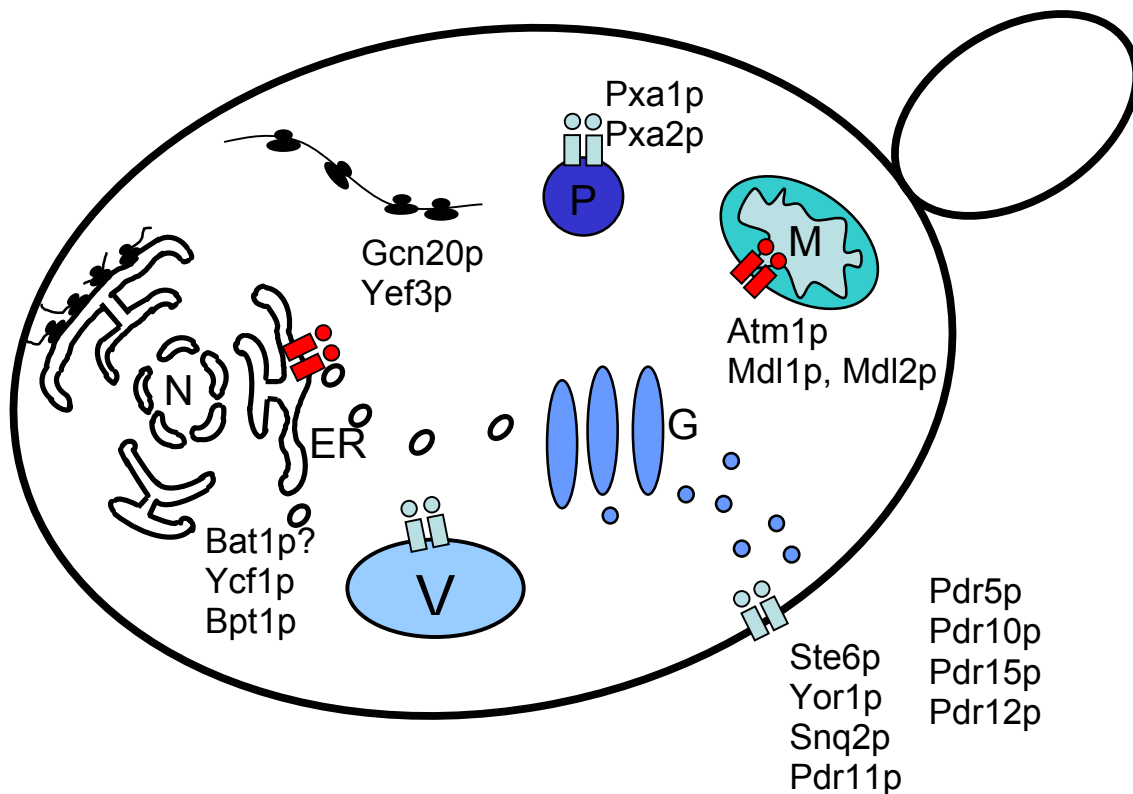


Fig.3: Subcellular localisation of *S. cerevisiae* ABC transporters.

ER, endoplasmic reticulum; G, Golgi apparatus; M, mitochondria; N, nucleus; P, peroxisome; V, vacuole.

Tab.1: Functional classification of *S. cerevisiae* ABC transporters and their homologues.

Abbreviations: conj., conjugates; Cyto, cytoplasm; Es, endosome; GS, glutathione; GV, Golgi vesicle; Hs, hypersensitivity; LC, long chain; M, mitochondria; PM, plasma membrane; Ps, polysomes; Px, peroxisome, R, regulatory domain; Ribo, ribosome; TMS, transmembrane segment; V, vacuole.

ABC Protein	Substrate(s)	Length	Topology	Localisation	Phenotype
MDR family					
Ste6p	a-factor	1290	(TMS ₆ -ABC) ₂	PM, GV, Es	Sterile
Atm1p	Fe/S proteins	694	TMS ₆ -ABC	M	slow-growth
Ssh1p/Mdl2p	?	820	TMS ₆ -ABC	M	Viable
Mdl1p	peptide	696	TMS ₆ -ABC	M	Viable
PDR family					
Pdr5/Sts1/Ydr1/Lem1p	Drugs, steroids, antifungals	1511	(ABC-TMS ₆) ₂	PM	Drug ^{Hs}
Pdr10p	Weak acids	1564	(ABC-TMS ₆) ₂	PM	Viable
Pdr15p	?	1529	(ABC-TMS ₆) ₂	PM	Viable
Snq2p	Drugs, steroids, mutagens	1501	(ABC-TMS ₆) ₂	PM	Drug ^{Hs}
Pdr12p	weak acids	1511	(ABC-TMS ₆) ₂	PM	weak acid ^{Hs}
Pdr11p	?	1411	(ABC-TMS ₆) ₂	PM(?)	Viable
Adp1p	?	1049	TMS ₂ -ABC-TMS ₇	?	Viable
YNR070w	?	1333	(ABC-TMS ₆) ₂	?	?
YOR011w	?	1394	(ABC-TMS ₆) ₂	?	?
YOL075c	?	1095	(ABC-TMS ₆) ₂	?	?
MRP/CFTR family					
Yor1p	Oligomycin, Reveromycin	1477	(TMS ₆ -ABC) ₂	PM	Drug ^{Hs}
Ycf1p	GS-conj./Cd ²⁺	1515	(TMS ₆ -R-ABC) ₂	V	Cd ^{Hs}
YLL048	Bile acids	1661	(TMS ₆ -ABC) ₂	V	Viable
YLL015w	?	1559	(TMS ₆ -ABC) ₂	?	?
YHL035c	?	1592	(TMS ₆ -ABC) ₂	?	?
YKR103w/YKR104w	?	1524	(TMS ₆ -ABC) ₂	?	?
ALDp family					
Ssh2/Pal1/Pxa1/Pat2p	LC-fatty acids	870	TMS ₆ -ABC	Px	Oleate-
YKL741/Pxa2/Pat1p	LC-fatty acids	853	TMS ₆ -ABC	Px	Oleate-
YEF3 family					
Yef3p	Drugs	1044	ABC ₂	Ribo?, Cyto?	Essential
Gcn20p	?	752	ABC ₂	Ps	Viable
YNL014w/Hef3p	?	1044	ABC ₂	Cyto?	Viable
YPL226w	?	1196	ABC ₂	?	?
YER036c	?	610	ABC ₂	?	?
RLI family					
YDR091c	?	608	ABC ₂	?	?
Others					
YDR061w	?	539	ABC	?	?
YFL028c	?	289	ABC	?	?

Ste6p, which belongs to the multidrug resistance (**MDR**) subfamily, was the first known yeast ABC transporter and is one of the best characterised (Kuchler *et al.*, 1989; McGrath and Varshavsky, 1989). While steady state localisation of Ste6p appears to be the Golgi apparatus and endosome-like compartments, it functions at the plasma membrane and mediates ATP-dependent secretion of the yeast **a**-factor pheromone (Kuchler *et al.*, 1993; Kuchler *et al.*, 1989). The other members of the MDR subfamily are mitochondrial half-size ABC transporters. Atm1p is localised in the inner mitochondrial membrane with its NBD facing the mitochondrial matrix (Leighton and Schatz, 1995) and functions as an exporter of Fe/S precursors (Kispal *et al.*, 1999). Two other members have been detected in the mitochondrial inner membrane, Mdl1p and Mdl2p. Mdl1p has been identified as an intracellular peptide exporter, while the function of Mdl2p has not been defined so far (Young *et al.*, 2001).

The pleiotropic drug resistance (**PDR**) subfamily is the largest subfamily of ABC-proteins in *S. cerevisiae*. Pdr5p and Snq2p mediate PDR through an ATP-dependent drug efflux pumping hundreds of structurally and functionally unrelated compounds. They are functional homologues of mammalian P-gp (Balzi and Goffeau, 1995).

The best-characterised members of the multidrug resistance related protein (**MRP/CFTR**) family are Yor1p and Ycf1p (Katzmann *et al.*, 1999; Szczypka *et al.*, 1994). Overexpression of Yor1p confers resistance to oligomycin, reveromycin A and organic anions (Cui *et al.*, 1996). Ycf1p plays a role in the detoxification of the cytosol by translocation of metal ions (cadmium), glutathione-S-conjugates and metal-containing peptides into the vacuole (Li *et al.*, 1996). The ORF *YLL048* encodes a full-length transporter (Bat1p) that was reported to translocate bile acids into vacuoles (Ortiz *et al.*, 1997), but also transports peptides as described in this thesis.

The adrenoleukodystrophy family (**ALD**) consists of two members, namely the *PXA1/PAR2/SSH2/PAL1* (Shani *et al.*, 1995) and *PXA2/PAT1/YKL741* (Shani *et al.*, 1996) genes. Both of them are half size transporters and putative orthologues of human ALDP and PMP70. They import long-chain fatty acids into the peroxisomes for subsequent β -oxidation (Hetteema *et al.*, 1996).

1.3 ABC transporters associated with cellular peptide transport

The transporter associated with antigen processing (TAP) has been for a long time the only known intracellular peptide transporter which mediates the import of peptides into the lumen of the endoplasmatic reticulum (Lankat-Buttgereit and Tampé, 2002). As potential homologous of TAP, two candidates, Mdl1p and Mdl2p, have been found in yeast (Dean *et al.*, 1994). The function of the mitochondrial Mdl2p has not been assigned so far, but it was excluded that Mdl2p

forms a heterodimer with Mdl1p. Mdl1p has been identified as a mitochondrial peptide exporter (Young *et al.*, 2001). Mdl1p and TAP2 share 35% identity and 55% similarity. Both transporters translocate peptides of a similar size (6-21 amino acids for Mdl1p and 8-16 amino acids for TAP). So far, Mdl1p is the only characterised member of the Mitochondrial Peptide Exporter (MPE) family. Members of this family have also been found in other species as *Asperigillus fumigatus* (MDR2), *Candida albicans* (MDL1), *Homo sapiens* (M-ABC2) (Zhang *et al.*, 2000) and *Mus musculus* (ABC-me: mitochondrial erythroid) (Shirihai *et al.*, 2000).

By investigation of peptide transport in yeast microsomes, we discovered a new peptide uptake activity which was mediated by ORF *YLL048*. This ORF encodes a full-length ABC transporter belonging to the MRP family. Surprisingly, this protein was reported to work as vacuolar bile acid transporter (Bat1p) (Ortiz *et al.*, 1997).

To obtain insight into the mechanism of peptide transport, the yeast ABC transporter Mdl1p as well as the newly discovered peptide pump encoded by *YLL048* has been studied in detail in this PhD thesis.

1.4 Cooperation of the subunits during the transport process

The ability to mediate vectorial transport of substrates requires intricate coupling between the TMDs and NBDs (and the periplasmic binding protein where applicable) (Higgins, 2001). The mechanism by which the conformational changes of NBDs in response to ATP hydrolysis are transmitted to conformational rearrangement at the TMDs to mediate substrate translocation is not well understood. One of the recent focuses on ABC transporter research is to gain insights into the inter-domain communication. Three types of inter-domain communications of the subunits have been described (Kerr, 2002): i) TMD-TMD interactions which may influence binding and release of substrate ii) NBD-TMD interactions which are proposed to mediate the coupling of nucleotide hydrolysis with substrate translocation iii) NBD-NBD interactions which are essential for coordination of ATP-hydrolysis of the complex.

1.5 Structure and function of the NBDs

Much of the mechanism how ABC motor domains work and communicate was learned from the characterisation of isolated NBDs. Based on their primary structure the NBDs are characterised by five consensus motifs. The Walker A and Walker B motif are found in all nucleotide binding proteins (Walker *et al.*, 1982). The Walker A motif has the sequence 'GxxGxGKS/T', where x is any amino acid. The Walker B motif is less stringent with the sequence 'Rx(6-8)ΦΦΦΦD', where Φ represents any hydrophobic residue. A subset of ATP-

binding proteins contains an extended Walker B site with the consensus 'Rx(6-8)ΦΦΦΦDEATSALD' (Michaelis and Berkower, 1995). The diagnostic hallmark of the ABC family is the 'C-loop' with the consensus sequence 'LSGGQ', which is unique to ABC transporters and also known as the ABC signature motif (Bianchet *et al.*, 1997; Higgins, 1992; Michaelis and Berkower, 1995). The C-loop has been described as a hot spot for mutations which causes loss of function in ABC transporters (Hoof *et al.*, 1994).

An invariant histidine is placed downstream of the Walker B motif in the so-called switch II region, which is proposed to be involved in the ATPase hydrolysis (Nikaido and Ames, 1999). Between the Walker A motif and the C-loop a conserved Q-loop is located. The Q-loop might undergo conformational changes during the catalytic cycle and function as a signal transducer between TMDs and NBDs (Jones and George, 2002).

Crystal structures of monomeric NBDs (e.g. HisP, MalK, TAP1) showed as a consensus fold an L-shaped molecule with two arms, one including the ATP-binding domain containing the Walker A and B motifs, and the other including the signature motif (Fig. 4a) (Hung *et al.*, 1998; Diederichs *et al.*, 2000; Gaudet and Wiley, 2001). The hinge region between the two arms contains the H-loop (Switch) and Q-loop. Mutagenesis studies of HisP implicated arm II in the interaction with the membrane-spanning domain. The mutations in arm II were characterised by a loss of regulatory control by TMDs resulting in a constitutive ATPase activity (Hung *et al.*, 1998).

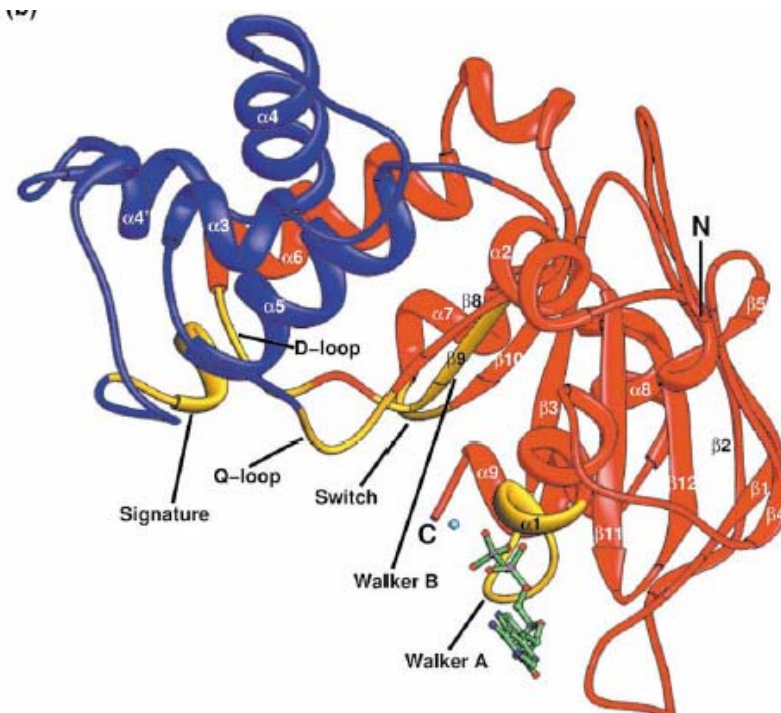


Fig.4a: Structure of the monomer of TAP1-NBD

The structure is displayed in ribbon format. The L-shaped monomer is divided into a RecA-like domain (red, arm I) and a helical domain (blue, arm II). Conserved sequence motifs are depicted in yellow. The co-crystallized ADP is green and the Mg^{2+} ion is cyan (Gaudet and Wiley, 2001).

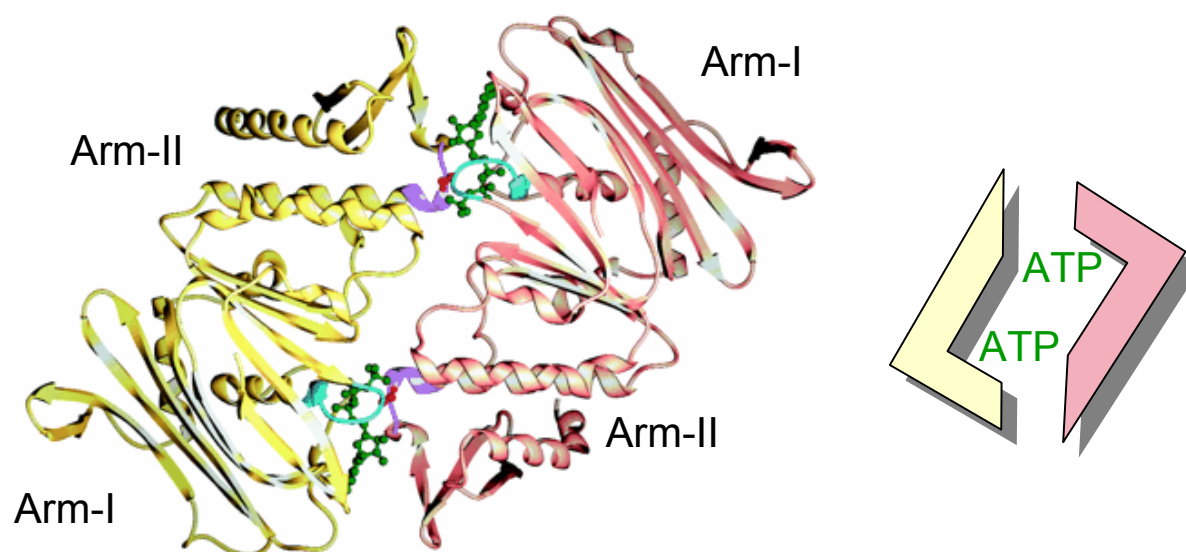


Fig.4b: Dimeric structure of a DNA repair ABC transporter-like domain, Rad50cd.

The structure is displayed in ribbon format. The L-shape of the monomer including the two arms is indicated. The two monomers are coloured in yellow and red. Two ATP molecules are sandwiched at the dimer interface and are coloured green and rendered in a space-filling style (Hopfner *et al.*, 2000).

Crystal structures of different NBD dimers have been solved, but they differ significantly in the manner how the monomers are associated (Kerr, 2002). The dimer of Rad50cd, a DNA repair enzyme that shares homology with the NBDs of ABC proteins, is assumed to be the ‘functional’ dimer (Fig.4b). This dimer contains two nucleotides, which are clamped at the interface between two monomers causing them to dimerize in a head-to-tail manner (Hopfner *et al.*, 2000). The ATP molecules are sandwiched between the Walker A and B motifs from one monomer and the LSGGQ-motif from the other monomer. The crystal structure shows that the Walker A lysine and Walker B aspartate/ glutamate pair closely interact with the β - and γ -phosphate of ATP, while the signature motif of the other monomer provides interactions with the adenine ring, ribose and triphosphate. Mutagenesis studies suggest that this dimer represents a true physiological association state since mutation of the serine of the signature motif to arginine prevented ATP-dependent dimerization (Hopfner *et al.*, 2000).

This proposed functional dimer configuration was very recently found in the crystal structure of the mutant NBD MJ0796 (E171Q) from *Methanococcus jannaschii* (Smith *et al.*, 2002) and of the NBDs of the vitamin B₁₂ transporter BtuCDE from *E. coli* (Locher *et al.*, 2002). Biochemical data on the maltose transporter (MalFGK₂) and on P-gp further confirmed the involvement of the C-loop in ATP binding (Fetsch and Davidson, 2002; Loo *et al.*, 2002). While the crystallographic dimer of HisP does not show the sandwiched ATP, an equivalent dimer formation for HisP as described for Rad50 was modelled based on comparative sequence

analysis (Jones and George, 1999). The association of the NBDs is regarded as a central step of the ATPase cycle, but it still remains controversial how both NBDs cooperate and coordinate ATP hydrolysis. Based on the high resolution structures of different NBDs it was proposed that two ATPs are bound to a dimer at the same time. Whether the motor domains work as equivalent modules hydrolysing both ATPs synchronically, sequentially or alternating is still under discussion. An alternating model based on P-gp, LmrA and HisMQP₂ was proposed in which only one NBD hydrolyses ATP at a time (Senior *et al.*, 1995; Urbatsch *et al.*, 1995a; van Veen *et al.*, 2000; Higgins, 2001; Jones and George, 2002).

In addition to the alternative modus, non-equivalency of the NBDs has been proposed. Functional non-equivalency of NBDs was shown for HisP although both NBDs have complete sequence identity (Kreimer *et al.*, 2000). P-gp is a full-length ABC transporter which consists of two different NBDs located at the N-half and C-half of this protein. Chimeras of P-gp containing two identical N-half NBDs showed full activity. The two N-half NBDs showed asymmetric behaviour which did not result from the difference in primary sequence but rather from their localisation inside P-gp (Hrycyna *et al.*, 1999). It was suggested that hydrolysis of one ATP in the dimer provides energy for the translocation of the substrate whereas hydrolysis of the ATP in the second binding pocket might have regulatory functions, possibly returning the complex to the ground state of the ATPase cycle (Hrycyna *et al.*, 1999; Jones and George, 1999).

To obtain insight into the mechanism of NBD interaction and communication, the NBD of the yeast ABC transporter Mdl1p has been studied in detail in this work.

1.6 Quality control in mitochondria

Mdl1p (multidrug resistance like) is localised in the inner mitochondrial membrane of *S. cerevisiae*. This transporter is required for the export of peptides derived from the degradation of non-assembled membrane proteins (Fig.5) (Young *et al.*, 2001). These peptides are generated by ATP-dependent m-AAA proteases (*YTA10-12*) (matrix-oriented ATPases associated with a variety of cellular activities), which are responsible for the degradation and turnover of inner mitochondrial membrane proteins and short-lived regulatory proteins in an ubiquitin/proteasome-independent manner (Arnold and Langer, 2002; Langer *et al.*, 2001). Mdl1p translocates the breakdown products ranging from 6 to 21 amino acids into the intermembrane space from where they are released into the cytosol probably through porins or the TOM complex (translocase of the outer mitochondrial membrane). Alternatively, unfolded membrane proteins of the inner mitochondrial membrane are degraded by i-AAA proteases (*YME1*) which expose their catalytic site to the intermembrane space.

This quality control consisting of two homologous proteolytic complexes and Mdl1p ensures the selective removal of non-assembled or short-lived polypeptides from mitochondria. But no accumulation of peptides has been observed in $\Delta mdl1 \Delta yme1$ double deletion mutant due to the fact that mitochondrial proteolysis system is capable of degrading proteins to amino acids. As the peptide export pump Mdl1p is not essential for cell viability, it is tempting to speculate that its physiological role might be in the communication between the mitochondrion and the cellular environment. Mitochondrially derived peptides could be major players in signal transduction between the mitochondrion and the nucleus coordinating mitochondrial and nuclear gene expression (Arnold and Langer, 2002).

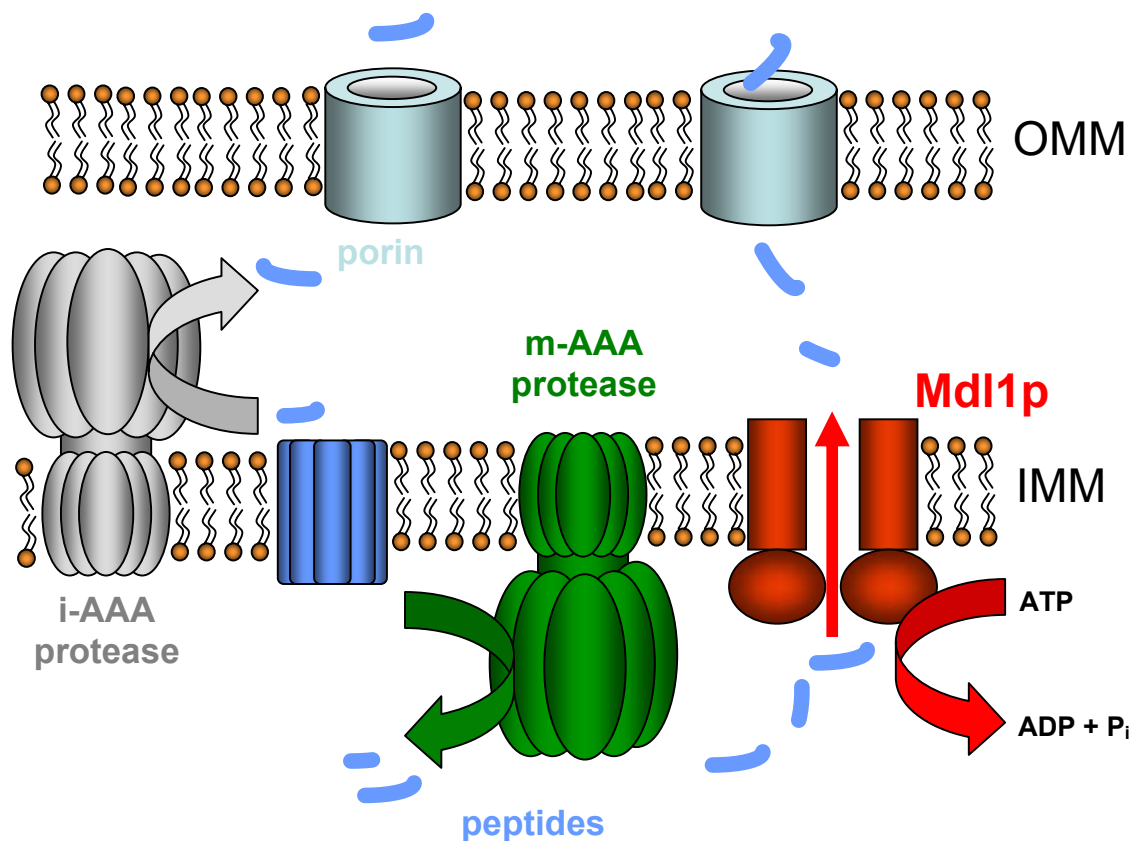


Fig.5: Quality control of mitochondria.

The key components of the quality control are two membrane embedded ATP-dependent proteolytic systems, i- and m-AAA proteases, which expose their catalytic sites to the intermembrane space and matrix, respectively and degrade not correctly assembled or misfolded inner membrane proteins. The breakdown products are exported from the matrix into the intermembrane space by the ABC transporter, Mdl1p.

OMM: outer mitochondrial membrane; IMM: inner mitochondrial membrane

The presence of ABC transporters homologous to Mdl1p in mammalian mitochondria e.g. ABC-me, M-ABC2, and M-ABC1 suggests a similar pathway in mitochondria of higher eukaryotic cells (Shirihai *et al.*, 2000; Zhang *et al.*, 2000; Hogue *et al.*, 1999). Peptides derived from mitochondrially encoded membrane proteins have been detected at the cell surface of mammalian cells where they are presented by class I major histocompatibility molecules (MHC) (Fischer Lindahl, 1997). It is possible that mitochondrially encoded minor histocompatibility antigens are generated by AAA proteases and released into the cytosol, from where they enter the conventional class I antigen processing and presentation pathway. The fact that the TMDs, which typically defined substrate specificity, of M-ABC2 show strong similarity to TAP2 (24% identity) might be due to a coevolution of both proteins, indicating that they might work in concert in antigen presentation.

2 Motivation and aims

The principles of peptide transport have been studied in detail on TAP which translocates antigenic peptides from the cytosol into the lumen of the ER. TAP has been functionally expressed in the yeast *S. cerevisiae*. To receive a fast and efficient method to characterise a broad spectrum of TAP mutants, one aim of this PhD thesis was to establish a genetic *in vivo* screen. The strategy was to develop an autocrine stimulation assay based on the TAP-mediated secretion of peptide pheromones.

By investigation of peptide trafficking in yeast, a new peptide uptake activity mediated by the ORF *YLL048* has been discovered (in our group). Relatively little is known about the physiological relevance of peptide metabolism in yeast. Therefore, one task of this PhD thesis was the genetic and biochemical characterisation of this peptide pump YLL048p.

Based on sequence alignments two potential homologs to TAP have been identified in yeast, Mdl1p and Mdl2p (Dean *et al.*, 1994). As Mdl1p has been recently described as a peptide transporter (Young *et al.*, 2001), we set out to characterise Mdl1p on molecular level. The main focus was put on the mechanism by which ATP hydrolysis drives the translocation of peptides. Inter-domain communication and signalling during transport process mediated by conformational changes of the individual domains are not well understood. The question how NBDs cooperate and coordinate the ATP hydrolysis in order to translocate substrate is of major interest. I tried to gain insights into the ATPase cycle of Mdl1p-NBD by characterisation of the interaction between the domains and by visualizing different catalytic transition states. A central target was to develop a model for the ATPase cycle of isolated Mdl1p-NBD.

3 Material

3.1 Chemicals

Chemicals	Company
[α - ³² P]-ATP or [γ - ³² P]-ATP	ICN
4-hydroxyazobenzen-2-carboxyl-acid (HABA)	Sigma-Aldrich GmbH
8-azido-[α - ³² P]-ATP	ICN
8-azido-biotin-ATP	Affinity labelling technology
acrylamid 30% (w/v)	National Diagnostics
adenosine-5'-diphosphate (ADP)	Fluka Chemie GmbH
adenosine-5'-triphosphate (ATP)	Fluka Chemie GmbH
apyrase	Sigma-Aldrich GmbH
ATP- agarose (C8 or N6 linked)	Sigma-Aldrich GmbH
BCA-kit	Pierce
benzonase	Merck
Biobeads SM-2	New England Biolabs
BL21(DE3)	Novagen
BSA	Sigma-Aldrich GmbH
calf intestine alkine phosphatase	Fermentas
cardiolipin	Sigma-Aldrich GmbH
carrier salmon testis DNA	Sigma-Aldrich GmbH
centrifugal filters (ultrafree)	Millipore S.A
chloramine T	Riedel-de Haen
concanavalin A-sepharose	Sigma-Aldrich GmbH
D-(+)-desthiobiotin	Sigma-Aldrich GmbH
β -D-decylmaltoside	Calbiochem
DeepVent	Biolabs
digitonin	Calbiochem
dimethylsulfoxide	Fluka Chemie GmbH
Dowex 1 x 8 anion exchange	Sigma-Aldrich GmbH
Enhanced ChemiLuminescence system (ECL)	Amersham Pharmacia
ethylendiamintetraacid (EDTA)	Carl Roth GmbH
Ex-Taq polymerase	Takara
hexokinase	Sigma-Aldrich GmbH
HiTrap desalting column	Amersham Pharmacia
hyperfilm chemiluminescence film	Amersham Pharmacia
isopropyl- β -D-thiogalactopyranoside (IPTG)	BTS-BioTech Trade& Service GmbH
Klenow fragment	New England biolabs
megaprime DNA labelling system	Amersham Pharmacia
N,N,N',N'-tetramethylethylendiamin (TEMED)	Sigma-Aldrich GmbH
Na ¹²⁵ I	Amersham Pharmacia
Ni-NTA beads	Qiagen GmbH

Material

nucleospin plasmid kit	Machery-Nagel GmbH & Co. KG, Düren
β -D-octylglycoside	Calbiochem
Oregon Green	Molecular Probes
pASK-IBAI	IBA
pBAD-His	Invitrogen
PEG 3350	Sigma-Aldrich GmbH
pET28, 26	Novagen
Pfu DNA polymerase	Promega
phosphatidylcholine	Avanti Lipids
phosphatidylethanolamine	Avanti Lipids
plasmid midi kit	Qiagen GmbH
polycarbonate filters (200 nm)	Avestin
polyethylenimine cellulose plates	Merck
Ponceau Red S	Sigma-Aldrich GmbH
Proteinase K	Sigma-Aldrich GmbH
pV1L392	Invitrogen
Pwo DNA polymerase	Roche Diagnostics
QIAquick gel extraction kit	Qiagen GmbH
QIAquick spin PCR purification kit	Qiagen GmbH
reactive RED 120	Sigma-Aldrich GmbH
restriction enzymes	MBI fermentas
sephadex G-50 columns	Amersham Pharmacia
sepharose A	Sigma-Aldrich GmbH
sequencing kit, big dye	Perkin Elmer
streptactin	IBA GmbH
streptavidin alkine phosphatase conjugate	IBA GmbH
Superdex 75 30/10	Amersham Pharmacia
Superose 200 HR 11/15	Amersham Pharmacia
Superose 6	Amersham Pharmacia
T4 DNA ligase	MBI fermentas
TA-cloning kit	Invitrogen
Texas Red	Molecular Probes
Top 10 cells	Invitrogen

3.2 Oligomers

Tab.2: Primer sequences used for cloning and sequencing of *MDL1*

formdl1 fl	ATTGAATTCATGATTGTAAGAATGATACGTCTTTGTAAA <i>EcoRI</i>
formdl1-mt	ATTGAATTCATGCAATCAGACATTGCGCAAGGAAAGAAG <i>EcoRI</i>
revmdl1	TACTCGAGAAGCTTTATACTTCCCGGGCAACACTA <i>XhoI HindIII</i>
revmdl1-Strept	ATACTCGAGAAGCTTTATTTTTCAAAGTGC GGATGAGACCAGCCGTT <i>XhoI HindIII</i> ACCACGTGGATAATACACTTCTCCCGGGCACCCTATTGTCCAAATC
formdl1 fl Nco1 new	CATATCCATGGGTATGATTGTAAGAATGATACGTCTTTG <i>NcoI</i>
formdl1-mt Nco1 new	CATATCCATGGGTCAATCAGACATTGCGCAAGG <i>NcoI</i>
pASK2revmdl	ATCCTAGGTCTCAGCGCTTACTTCCCGGGCAACACTATTGTC <i>BsaI</i>
pASK2for-mt	AGTCTAGGTCTCAGGCCCAATCAGACATTGCGCAAGGAAAG <i>BsaI</i>
pET22/6bmdl- mtfor	ATTACGAATTCGCAATCAGACATTGCGCAAGGAAAG <i>EcoRI</i>
pET22/6bmdlrev	ACGAAGCTTTACTTCCCGGGCAACACTATTGTC <i>HindIII</i>
revD598A	GGCACTGGTTGCTTCAGCTAAAATAAGGACGGC
forD598A	GCCGTCCTTATTTTAGCTGAAGCAACCAGTGCC
forH631R	CTACTAATATCAAATGCACGTAGGCTTTTCGACGATC
revH631R	GATCGTCGAAAGCCTACGCCTACGTGCAATTGATATAGTAG
forE599Q	GCCGTCCTTATTTAGATCAAGCAACCAGTGCC
revE599Q	GGCACTGGTTGCTTCATGTAATAAGGACGGC
revmdl1pXY	ATAGTCTGACTAAGCTTTACTTCCCGGGCAACACTAT <i>Sall HindIII</i>

Material

	primer for sequencing
Seq1 mdl1 f	GAAGTCCACCAAGCCCACTT
Seq2 mdl1 f	CGTGTCGGTGATTTGATCTC
Seq3 mdl1 f	GGAAGTACTGGGCTAGTTGG
Seq4 mdl1 f	CTTTGTTGCTCAGGTACTAC
Seq5 mdl1 f	GAATTGCATTAGCTAGAGCG
Seq mdl1 r	TTAGATAAGACGAATAGCCG
mdl1rev1	GGAAGGTACAGCCATACT
mdl1rev2	TGTCTTTAAACCCCGACG
T7 promotor	TTAATACCACTCACTATAGG
T7 terminator	CGATCAATAAGCAGTCGG
pBadfor	ATGCCATAGCATTTTTATCC

Tab.3: Primer sequences applied in the *YLL048* gene construction

Yll Nterm pRSc	TCCCCCGGGGGACTAGTCTGAAGAAAAAGCCACTC <i>XmaI</i> <i>SpeI</i>
Yll Cterm pRSc	CGGGGTACCCCGCTAATT(AAGATCCTCTCCGGAAATGAG <i>KpnI</i> (myc-tag) CTTTTGTTG)GTCCTTTTGTAGACTTCAATTTTCC
NtermXhoSiYll	GTCGTCCCCAGCTCTCGAGCCAAGGCAGGAACTAATA <i>XhoI</i>
CtermXhoSiYll	GTTCTTGCCTTGGCTCGAGAGCTGGGACGACAACCTTAC <i>XhoI</i>
YLL forward1	CCGACGAAGACGAACAGA
YLL forward2	AATCTATGGTTCGGTATC
YLL forward3	ATTTTGTGGACCATAAGG
YLL forward4	ATTTCCACCAACAAGACT
YLL forward5	GCTGCGATTGTGGGTGTC
YLL forward6	CGTTCAAGGCGAGGTATT
YLL forward7	TGGCATTATTAGGTGAAA
YLL forward8	GGTGGTCAAAGCAGAGA
YLL forward9	TAACCTACCCGCTGTCAA
YLL forward10	TTATTCCCAGAGCACAAC
YLL forward11	TGATGCTACTTCACCAGG

YLL forward12	ATGAAGGGAGGTTTATGC
YLL forward13	GCCATACAACGAACACAA
YLL forward14	ATTCACAGGGACCATTTA

Tab.4: List of α -factor constructs as sense and antisense nucleotide sequence

α -MOD1/H	GTCAATGGATCCATGAACGCTACTTTGGCTAAGAGAGAAGCTGAAGCT TGGCATTGGCTGCAGCTGAAGCCTGGCCAACCAATGTACTAAATCGAT AAGTCAA
α -MOD1/R	TGACTTATCGATTTAGTACATTGGTTGGCCAGGCTTCAGCTGCAGCCA ATGCCAAGCTTCTCTCTTAGCCAAAGTAGCGTTCATGGATCCATTGAC
α -MOD2/H	GTCAATGGATCCATGAAGAGAGAAGCTGAAGCTGAAGCTTGGCAGTG GCAGTGGCTGCAGCTGAAGCCTGGCCAACCAATGTACTAAATCGATAA GTCAA
α -MOD2/R	TGACTTATCGATTTAGTACATTGGTTGGCCAGGCTTCAGCTGCAGCCA ATGCCAAGCTTCAGCTTCTCTCTTCATGGATCCATTGACA
α -MOD3/H	GTCAATGGATCCATGTGGCATTGGCTGCAGCTGAAGCCTGGCCAACAA ATGTACAAGAGAAACGCTACTTAAATCGATAAGTCAA
α -MOD3/R	TGACTTATCGATTTAAGTAGCGTTTCTCTTGACATTGGTTGGCCAGGC TTCAGCTGCAGCCAATGCCACATGGATCCATTGACA
α -MOD4/H	GTCATTGGATCCATGTGGCATTGGCTGCAGCTGAAGCCTGGCCAACCA ATGTACTAAATCGATAAGTCAA
α -MOD4/R	TGACTTATCGATTTAGTACATTGGTTGGCCAGGCTTCAGCTGCAGCCA ATGCCACATGGATCCATTGACA
TOPO-Hin	AGCGCCCAATACGCAA
TOPO-Rück	CCAAGCGGCCGGAGAACC
Insert-alpha	TACATTGGTTGGCCAGGC

3.3 Peptides

Tab.5: Peptide sequence used for transport assays

Peptide	Sequence
R9LQK	RRYQKSTEL
R10T	RYWANATRST
α -factor	WHWLQLKPGQPMY

4 Methods

4.1 *E. coli* methods

4.1.1 *E. coli* media, culture conditions and methods

E. coli cells were grown in LB-medium (10 g trypton, 5 g yeast extract, 10 g NaCl per liter) at 37°C. If indicated, 100 µg/ml ampicillin or 50 µg/ml kanamycin were added after autoclaving. For selection with zeocin (50 µg/ml) LB-medium with reduced salt concentration was used (5 g NaCl per liter).

4.1.2 Competent *E. coli* cells

An *o/n*-culture of *E. coli* DH5α cells was diluted 1:50 in 100 ml LB-medium and grown at 37°C to an OD₆₀₀ of 0.5. The culture was incubated on ice for 10 min and the cells were harvested at 1,000 x g at 4°C for 10 min. The cell pellet was carefully resuspended in 10 ml sterile, ice-cold 0.1 M CaCl₂ and incubated on ice for 90 min. After centrifugation the pellet was resuspended in 2 ml sterile ice-cold 0.1 M CaCl₂ and 400 µl 87% glycerol. Cell aliquots of 100 µl were frozen in liquid nitrogen and stored at -80°C.

4.1.3 Transformation of competent *E. coli*

Competent *E. coli* cells were thawed on ice for 10 min. Plasmid DNA (10 ng to 1 µg) was dissolved in 10 µl water, mixed with 100 µl of competent cells and incubated on ice for 30 min. The suspension was transferred to 42°C for 90 sec (heat shock). The cells were regenerated in 1 ml LB-medium for 1 h at 37°C with vigorous shaking. The cell suspension was centrifuged (1,000 x g, 10 min, 25°C) and plated on prewarmed (37°C) LB-agar plates supplemented with the appropriate antibiotic and incubated overnight at 37°C.

4.1.4 Plasmid construction

Plasmid purification was performed using Mini or Midi-kits. Restriction enzyme digestion was performed using the amount of enzyme and the incubation temperature suggested by the manufacturer. Before electrophoresis DNA samples were mixed with 1x loading buffer (10x: 40% sucrose (w/v), 0.25% bromphenol blue, xylene cyanol in TE-buffer). DNA fragments were analysed in 0.8%-2% agarose gels in TAE-buffer (40 mM Tris-acetate pH 8, 1 mM EDTA) and

stained with ethidium bromide. If indicated, fragments were extracted from gel using QIAEX extraction kit.

To create blunt end from sticky end DNA, the digested DNA was incubated with 1 unit Klenow fragment and 200 μ M dNTPs in 1x manufacturer's reaction buffer for 15 min at 25°C.

To reduce religation of vector with blunt ends, dephosphorylation was performed. Routinely, 1-2 μ g DNA in a total volume of 50 μ l was incubated with 1 unit phosphatase (calf intestine) in 1x manufacturer's reaction buffer for 1 h at 37°C. The enzyme was heat inactivated at 72°C for 10 min.

Ligation was performed by incubating vector DNA with a 3-10x excess of insert DNA with T4-DNA ligase in 1x manufacturer's reaction buffer overnight at 16°C.

PCR (polymerase hain reaction) was used to amplify insert DNA using chromosomal yeast DNA or plasmid DNA as template. For PCR high fidelity Ex-Taq, Pwo-polymerase or DeepVent were used according to manufacturers' instructions. Site-directed mutagenesis was performed by PCR and a polymerase system producing blunt ends at the PCR fragments (e.g. DeepVent, for details see mutagenesis, NBD(E599Q)). Alternatively, PCR products with a 5'-end A-overhang produced by Ex-Taq were cloned using the TA-cloning kit.

Clones were checked via restriction analysis or colony-PCR. Positive clones were verified by DNA sequencing. For cloning and amplification of DNA the *E. coli* strain DH5 α was used. For gene expression different *E. coli* strains were applied in this thesis. Expression under the control of a T7 promotor was performed in BL21(DE3) cells or C41. For expression of genes under the control of the arabinose inducible promotor, the strain TOP10 was used which has a deletion in the *ara*-operon and is therefore unable to metabolize arabinose .

4.1.5 Plasmids encoding for *MDL1* and their expression conditions in *E. coli*

The *MDL1* gene (ORF *YLR188W*) was amplified by PCR from the genomic DNA of *S. cerevisiae*. Unless indicated otherwise, PCR was performed with the Ex-Taq using 1 μ l concentrated genomic DNA (200 ng/ μ l) as template and 10 pmol primers, respectively following this protocol: 2 min denaturation at 92°C, 30 cycles of 1 min denaturation at 92°C, 1 min annealing at 55°C, 2.5 min extension at 72°C, 10 min final extension at 72°C. The PCR fragments were cloned into different expression vectors of *E. coli*.

To clone *MDL1* into the pBAD vector the PCR was performed according to standard procedure with the primers (formdl1 fl) and (revmdl1). The PCR fragment was ligated into the pBAD-HisB using the restriction sites *EcoRI* and *HindIII* resulting in the construct **pBAD_{His}-mdl1**.

In this construct *MDL1* was fused at the 5' end with a His₆-tag derived from the vector. The affinity tag can be cleaved by enterokinase.

To delete the N-terminal predicted mitochondrial targeting sequence of *MDL1*, a PCR was carried out according to standard procedure using the primers (formdl1-mt) and (revmdl1). The PCR fragment truncated in 180 bp at the 5' end was cloned into pBAD-HisB using *EcoRI* and *HindIII*. The construct **pBAD_{His}-Δmt-mdl1** contains an N-terminal His₆-tag which can be cleaved by enterokinase.

A C-terminal StrepII-tag was introduced to *MDL1* by PCR using the primers (formdl1 fl Nco1 new) and (revmdl1-Strep). The PCR insert was cloned into the pBAD vector using *NcoI* and *HindIII* and obtaining the construct **pBAD-mdl1_{StrepII}**.

MDL1 deleted in the mitochondrial targeting sequence was obtained by PCR with the primers (formdl1-mt Nco1 new) and (revmdl1-Strep). By this PCR a C-terminal StrepII-tag was introduced to *MDL1*. The PCR insert was cloned into the pBAD vector using *NcoI* and *HindIII* and resulting in the construct **pBAD-Δmt-mdl1_{StrepII}**.

The expression of all *MDL1* constructs in the pBAD-vector was performed in *E. coli* strains TOP10 or C41. Transformed bacteria were grown at 30°C in LB-medium with 100 µg/µl ampicillin. At an OD₆₀₀ of 0.5 bacteria cells were induced with 0.02 % arabinose, and after different time points of induction the cells were harvested by centrifugation.

The *MDL1* gene was amplified by PCR using the primers (pASK2for-mt) and (pASK2revmdl) deleting the mitochondrial targeting sequence. The PCR fragment was cloned into the pASK-IBA2 vector using *BsaI* resulting in the recombinant plasmid **pASK-IBA2-Δmt-mdl1_{StrepII}**. *BsaI* is a restriction enzyme cutting outside its recognition site thus determining the final orientation of the insert in the vector. Mdl1p was fused N-terminally with the OmpA periplasmic leader sequence and C-terminally with a StrepII-tag (WSHPQFEK). Both features were encoded by the pASK-IBA2 vector.

The expression of *MDL1* in this construct is under the control of the *tet*-promotor. *E. coli* strain C41 was transformed with the plasmid and grown at 30°C in LB-medium with 50 µg/µl kanamycin. At an OD₆₀₀ of 0.5 cells were induced with 200 ng/ml anhydrotetracycline (AHT) (1:10000 dilution from 2 mg/ml AHT stock solved in DMF, stored at -20°), and after 3 h the cells were harvested by centrifugation.

MDL1 truncated in the mitochondrial targeting sequence (180 bp) was amplified by PCR using the primers (pET22/6bmdl-mtfor) and (pET22/6bmdlrev). The PCR fragment was cloned into the pET22 vector using *EcoRI* and *HindIII* resulting in the construct **pET22-Δmt-mdl1_{His}**.

Methods

Using this approach Mdl1p was fused N-terminally with a periplasmic leader sequence (PepB) and C-terminally with a His₆-tag. Both features were derived from the pET22 vector.

The expression of Mdl1p in pET22 was under the control of a T7-promotor. *E. coli* strain BL21(DE3) was transformed and grown at 30°C in LB-medium with 100 µg/µl ampicillin. At an OD₆₀₀ of 0.5 cells were induced with 0.2 mM isopropyl-β-D-thio-galacto-pyranoside (IPTG), and after 3 h the cells were harvested by centrifugation.

The transmembrane domain of Mdl1p without the mitochondrial targeting sequence was subcloned from the pBAD_{His}-Δmt-mdl1 into the pET28b using the *Nco*I and the *Bam*HI site derived from position 1266 inside the *MDL1*. The new construct **pET28_{His}-Δmt-TMD_{His}** contains an N-terminal His₆-tag derived from the pBAD vector and a C-terminal His₆-tag encoded by pET28b. BL21(DE3) cells were transformed and were grown at 30°C in LB-medium with 50 µg/µl kanamycin. At an OD₆₀₀ of 0.5 cells were induced with 0.2 mM IPTG, and after 3 h the cells were harvested by centrifugation.

The C-terminal domain of Mdl1p (amino acids 427 to 695) corresponding to the NBD was subcloned from the pBAD_{His}-Δmt-mdl1 into pET28b using *Bam*HI and *Hind*III. The resulting construct **pET28_{His}-NBD** includes a 30 residues N-terminal extension with His₆-tag, thrombin cleavage site and a T7-tag encoded by the vector. A conserved glutamate 599 downstream of the Walker B motif was changed to glutamine via site directed mutagenesis resulting in the construct **pET28_{His}-NBD(E599Q)** (Fig.6). To introduce the mutation into the gene, three different PCRs were performed. In PCR1 and PCR2 pET28-NBD was used as template and the primers, (T7 promotor) and (revE599Q) or (forE599Q) and (revmdl1), respectively. For amplification DeepVent polymerase creating blunt ends of the PCR fragments was used. Both PCR products were purified from agarose gel, mixed in an equimolar ratio and used as a template for a third PCR using the primers (T7 promotor) and (revmdl1). The resulting PCR fragment of 800 bp was sequenced to confirm the mutation and cloned *Bam*HI and *Hind*III into pET28b. The conserved aspartate 598 in the Walker B motif was changed to alanine according to the procedure described above resulting in the construct **pET28_{His}-NBD(D598A)**. For PCR1 the primer set (T7 promotor) and (revD598A), for PCR2 the set (forD598A) and (revmdl1) and PCR3 (T7 promotor) and (revmdl1) were used. The conserved histidine 631 in the switch region was changed to arginine resulting in **pET28_{His}-NBD(H631R)**. PCR1 was performed with the primer set (T7 promotor) and (revH631R), PCR2 with (forH631R) and (revmdl1) and PCR3 with (T7 promotor) and (revmdl1).

BL21(DE3) cells were transformed by the plasmids encoding the NBDs and bacteria were grown at 30°C in LB-medium with 50 µg/µl kanamycin. At an OD₆₀₀ of 0.5 cells were induced with 0.2 mM IPTG, and after 3 h the cells were harvested by centrifugation.

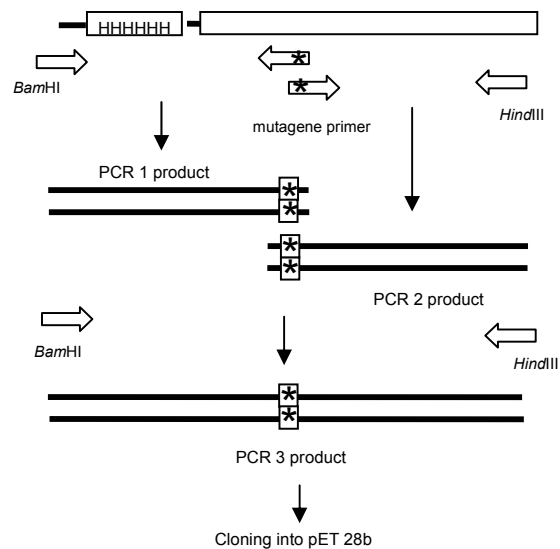


Fig.6: PCR based mutagenesis. Point mutations were introduced into the gene (NBD) by 3 step PCR. The gene of interest was subdivided into 2 fragments by PCR1 and 2 introducing the mutation. To avoid a frame-shift a PCR polymerase was used which creates blunt ends of the PCR products. In the PCR3 the full-length gene was re-amplified.

4.1.6 Plasmids encoding for *MDL1* and their expression in yeast

MDL1 was amplified by PCR with the primers (formdl1 fl) and (revmdl1-Strept) and cloned into the p426 vector using *EcoRI* and *HindIII*. In the resulting construct **p426-mdl1_{StreptII}** the gene was fused at the 3' end with a StreptII-tag derived from the reverse primer. The same cloning procedure was performed with *MDL1* deleted in the mitochondrial targeting sequence. The primers (formdl1-mt) and (revmdl1-Strept) were used to obtain the construct **p426-Δmt-mdl1_{StreptII}**. The yeast strain Δ*mdl1* was transformed by the recombinant plasmids and the clones were selected on URA drop out agar plates. The expression of *MDL1* is under the control of the strong, constitutive GDP promotor (680 bp). The transformed yeast cells were grown at 25°C in selective medium to OD₆₀₀ of 1-1.5 and harvested.

MDL1 was subcloned from the pBAD_{His}-Δmt-mdl1 into the pXY113 vector using *NcoI* and *HindIII*. The resulting construct **pXY113_{His}-Δmt-mdl1** contains an N-terminal His₆-tag derived from the pBAD. As Mdl1 kept its natural stop codon, the HA-tag at the C-terminus encoded by pXY113 was not expressed. The expression of the gene is under the control of the strong

inducible *GAL* promotor. The induction of *MDL1* was performed with 2% galactose for different times in selective media in the absence of Uracil.

4.1.7 Plasmids encoding for *YLL048*

As it was not successful to obtain a DNA fragment of the full length gene *YLL048* (including a 1000 bp promotor region) by PCR from the genomic DNA, the gene was subdivided into two fragments: a 5'-fragment of 3290 bp (nt -1001 to +2290) and the 3'-fragment of 2724 kb (nt 2291-4015) including a myc-tag. The 5'-part of the ORF *YLL048* was cloned by TA-cloning into the pCR-XL-Topo vector resulting in the construct **pCR-Topo-F1**. In the PCR Ex-Taq polymerase, 1 µl concentrated genomic yeast DNA as template and 10 pmol primers (pRS-N) and (C-termXho) were used and the following protocol applied: 2 min initial denaturation at 94°C, 30 cycles of 30 sec denaturation at 94°C, 1 min annealing at 60°C, 3.5 min extension at 72°C, a final extension for 10 min. The reverse primer contained a silent mutation creating a unique *XhoI* into the gene. This restriction site was later used to fuse the two gene fragments. As TA-cloning does not direct the orientation of the insert in the vector, the orientation of the insert was checked by *XhoI* digestion. Digestion of the plasmid, which contained the insert in sense orientation, resulted in a 6.8 kb fragment. When the insert was cloned in the opposite direction, a digestion resulted in a 3290 bp and a 3500 bp fragment. For further cloning, clones with the anti-sense orientation were used.

The 3'-part of the ORF *YLL048* was amplified by PCR using the primers (N-termXho) and (pRS-C). The same protocol as above was applied. The forward primer introduced a silent *XhoI* site into the 5'-end of the PCR product. The PCR product with ligated with pCR-XL-Topo resulting in the construct **pCR-Topo-F2**. The constructs were checked for orientation of the fragment inside the vector by *XhoI*. In sense orientation two fragments of the size of 2.7 kb and 3.5 kb were obtained, while in the case of the anti-sense orientation a 6 kb fragment was obtained. For further cloning, fragments with anti-sense orientation were used. The 3'-fragment (2.7 kb) from pCR-Topo-F2 was cloned into Yep352 vector using *PstI* and *SacI* resulting in the construct **Yep352-F2** (7.9 kb). This construct was fused with the 5'-part of the gene (3290 bp) from pCR-Topo-F1 using *PstI* and *XhoI* and resulting in **Yep352-yll048** (12 kb). The vector Yep352 contains the *URA* marker for selection in yeast. The expression of the gene is under control of the *YLL048* promotor.

4.1.8 Plasmids containing different constructs of the α -factor

In order to express a minigene in yeast, the DNA of the peptide pheromone α -factor was ordered as single stranded DNA oligomers with sense and antisense sequence. After hybridization of the oligomers to double stranded DNA, the insert was ligated to pCR-XL-Topo by TA-cloning and transformed to *E. coli*. Different truncated forms of the α -factor were cloned following the same cloning strategy described in details for **pCR-Topo-mod4** coding for the mature α -factor. Oligomers coding for the amino acid sequence: MWHWLQLKPGQPMY were ordered as sense and anti-sense primers with an additional A-overhang at the 3'-end. Oligomers were mixed (30 ng/ μ l), denatured for 1 min at 94°C, and annealed for 30 min at 50°C. The hybridized DNA (120 ng) was mixed with 10 ng pCR-XL-Topo-vector and incubated with 1 μ l topoisomerase at RT, after 5 min 1 μ l stop solution was added, and the sample was centrifuged. An aliquot of 2 μ l was mixed with 50 μ l electrocompetent DH5 α provided with the TA-cloning kit. Electroporation was carried out at 1.8 kV and after regenerating the cells for 1 h at 37°C in LB medium, they were plated out on kanamycin containing agar plates (50 μ g/ml). Clones were checked with *Eco*RI digestion. The orientation of the insert DNA was checked by PCR using the primers TopoHin (annealing upstream of the MCS) and insert-alpha primer, and alternatively, TopoRück (annealing downstream of the MCS) and insert-alpha primer. In case of sense orientation (same reading orientation of insert and vector) a PCR fragment of the size of 400 bp was obtained by using TopoHin and Insert-primer. In case of anti-sense orientation a PCR fragment of the size of 1400 bp was amplified by TopoRück and Insert-primer. For cloning into an expression plasmid, clones with the sense orientation were selected. The positive plasmids were sequenced with the M13 forward primer.

The insert DNA was subcloned from the pCR-Topo-mod1 into the p424 yeast expression vector using *Spe*I and *Xho*I, *Bam*HI and *Cla*I, and *Spe*I and *Cla*I respectively. The expression of the α -factor is under the control of the constitutive ADH-promotor. The selection marker for yeast is *TRP*.

Methods

Tab.6: List of α -factor constructs as amino acid sequence

Plasmid	Insert (amino acids)	Restriction
pCR-Topo-mod1	MNATLAKREAEAWHWLQLKPGQPMY	
p424-mod1	MNATLAKREAEAWHWLQLKPGQPMY	<i>SpeI</i> and <i>XhoI</i>
		<i>BamHI</i> and <i>Clal</i>
		<i>SpeI</i> and <i>Clal</i>
pCR-Topo-mod2	MKREAEAWHWLQLKPGQPMY	
p424-mod2	MKREAEAWHWLQLKPGQPMY	<i>SpeI</i> and <i>XhoI</i>
		<i>BamHI</i> and <i>Clal</i>
		<i>SpeI</i> and <i>Clal</i>
pCR-Topo-mod3	MWHWLQLKPGQPMYKRNAT	
p424-mod3	MWHWLQLKPGQPMYKRNAT	<i>SpeI</i> and <i>XhoI</i>
		<i>BamHI</i> and <i>Clal</i>
		<i>SpeI</i> and <i>Clal</i>
pCR-Topo-mod4	MWHWLQLKPGQPMY	
p424-mod3	MWHWLQLKPGQPMY	<i>SpeI</i> and <i>XhoI</i>
		<i>BamHI</i> and <i>Clal</i>
		<i>SpeI</i> and <i>Clal</i>

4.2 Yeast methods

4.2.1 Yeast media and growth conditions

Yeast peptone dextrose medium (YPD) was composed of 5 g yeast extract and 10 g peptone per 1 L and after autoclaving 100 ml of 20% glucose was added.

Lactate medium contained 3 g yeast extract, 0.5 g glucose, 0.5 g CaCl₂, 0.5 g NaCl, 0.6 g MgCl₂, 1 g KH₂PO₄, 1 g NH₄Cl, 22 ml 90% lactic acid, 7.5 g NaOH per 1 L and the pH was adjusted to 5.5 with NaOH.

Minimal medium was composed of 6.7 g yeast nitrogen base and 5 g (NH₄)₂SO₄ per 1 L. After autoclaving 100 ml of 20% glucose and 50 ml amino acid mix (20x) were added. The medium was further supplemented by 10 ml auxotrophic components as leucine, histidine, uracile, tryptophane depending on the plasmid expressed in the yeast. The selection markers were prepared as stock solutions in water with 192 mg uracil, 192 mg tryptophane, 288 mg leucine, or 192 mg histidine, respectively per 50 ml. The amino acid mix consisted of 112 mg adenine, 384 mg arginine, 384 mg methionine, 144 mg tyrosine, 576 mg isoleucine, 480 mg phenylalanine, 576 mg valine, and 576 mg threonine per 500 ml.

All yeast strains were grown routinely at 30°C, unless indicated otherwise.

4.2.2 Competent yeast cells

Competent yeast cells were prepared according to the protocol of Schiestl and Gietz (1989). Shortly, cells were inoculated from a fresh overnight culture in 50 ml YPD medium to an OD₆₀₀ of 0.2. They were grown at 30°C with vigorous agitation until the OD₆₀₀ of 0.8-1 was achieved. Cells were harvested by centrifugation (500 x g, 5 min, RT), washed once in 20 ml sterile water and resuspended in 1 ml sterile 100 mM LiAc, 10 mM Tris-HCl pH 8.0, 1 mM EDTA. For *P. pastoris* instead of LiAc LiCl was used. The samples were transferred into a sterile eppendorf tube and centrifuged 500 x g, 5 min. The pellet was resuspended in 100 µl LiAc-buffer.

4.2.3 Transformation of yeast cells

Single stranded carrier salmon testis DNA was dissolved at a concentration of 2 µg/µl in TE-buffer on a stir plate overnight at 4°C and aliquots were stored at -20°C. Before use, the carrier DNA was denatured by incubation at 95°C for 5 min and chilled immediately on ice.

The competent cells (50µl) were vortexed, centrifuged at 20,000 x g for 30 s and the supernatant was removed. The cell pellet was sequentially resuspended in 240 µl PEG (50%

Methods

w/v), 36 μ l 1 M LiAc, 25 μ l carrier DNA (2 μ g/ μ l) and 50 μ l plasmid DNA (0.1-10 μ g) by vigorous vortexing. The transformation suspension was incubated at 30°C for 30 min. For heat shock cells were placed at 42°C for 20 min and inverted every 5 min. The cells were sedimented at 20,000 x g for 30 s and the supernatant was discarded. To transform plasmid DNA, the pellet was carefully resuspended in 100 μ l sterile water and incubated at RT for 5 min. No more than 20 μ l of the transformation mix was plated onto selective agar plates and incubated at 30°C for 2-3 days. Recombination into the chromosome was achieved by transformation of a PCR fragment and subsequent regeneration of the cells in 2-3 ml YPD medium for 90 min. The cells were centrifuged at 20,000 x g for 5 min, suspended in 50 μ l medium and spread onto selective medium plates. To check for positive transformants, colony PCRs were performed with fresh colonies. A single colony was picked, transferred to an eppendorf tube, resuspended in 10 mM Tris-HCl pH 8, and incubated with 1% lyticase for 15 min at 30°C. This suspension (1 μ l) was used as template for PCR.

4.2.4 Preparation of genomic DNA of yeast

A culture (5 ml) of the wild type *S. cerevisiae* strain W303-1A was grown overnight at 30°C on YPD medium to an OD₆₀₀ of 1-2. The cells were harvested at 500 x g, 5 min at 4°C and the pellet was resuspended in 500 μ l 0.9 M sorbitol, 0.1 M Tris-HCl pH 8, 10 mM EDTA containing 10 mM fresh DTT. 20 units lyticase per OD₆₀₀ of cells were added and the suspension was incubated for 1 h at 30°C with gentle shaking (200 rpm). After sedimentation of the spheroplasts at 500 x g for 5 min, the pellet was resuspended in 500 μ l 50 mM Tris-HCl pH 8, 20 mM EDTA. Cells were lysed by addition of 50 μ l 10% SDS. After mixing the suspension by careful inverting, the sample was incubated for 20 min at 65°C. After the addition of 200 μ l 5 M KAc pH 5, the sample was placed on ice for 30 min. Subsequently, the cell debris was removed by centrifugation at 20,000 x g for 5 min. The DNA in the supernatant was precipitated with 1 ml 100% ethanol. A short centrifugation of 10 sec at 20,000 x g sedimented the genomic DNA, which was resuspended in 300 μ l 100 mM Tris-HCl pH 8 and incubated for 15 min at 65°C. Contamination with RNA was removed by incubating the samples with 5 μ l RNase (10 mg/ml) for 1 h at 37°C. Finally, the genomic DNA was precipitated with 500 μ l isopropanol and centrifuged at 20,000 x g for 20 sec. The DNA pellet was washed with 70% ethanol and resuspended in 50 μ l 100 mM Tris-HCl, pH 8, 10 mM EDTA.

Tab.7: List of yeast strains used

Name	Background strain	Mutations
W303-1A	<i>MATa ura3-52 leu2-3, 122 his3-11 trp1-1 ade2-1 can1-100</i>	
$\Delta yll048$	W303-1A	$\Delta yll048::HIS$
Cadus6259	<i>MATa ura3-52 leu2-3, 122 his3-11,15 trp1-Δ1 lys2-1</i>	<i>far1-1 tbt1-1 bar1::hisG fus-His3 ste14::trp1::lys3</i>
$\Delta mdl1$	W303-1A	$\Delta mdl1::HIS$

4.3 RNA methods

4.3.1 Random-primed labelling of DNA-fragments

The messenger RNA (mRNA) level of the gene of interest was detected using a gene-specific radiolabelled DNA probe. *YLL048* mRNA was detected by a DNA probe corresponding to nt +145 through nt +868 of ORF *YLL048*. This sequence is not conserved in the ABC superfamily. To obtain the probe, the plasmid pCR-Topo-F1 was digested with *Nde*I and the resulting 723 bp fragment was purified from agarose gel. Radioactive labelling of DNA fragments was performed using the Megaprime DNA Labelling System. About 20-50 ng of agarose gel extracted DNA were mixed with 5 μ l of randomized primer mix in a total volume of 28 μ l and denatured for 10 min at 95°C. After cooling the sample on ice, the sample was briefly centrifuged and mixed with 10 μ l labelling buffer, 10 μ l [α -³²P] dCTP (6000 Ci/mmol) and 2 units Klenow enzyme in a total volume of 40 μ l. The labelling reaction was performed for 3 h at 37°C. The labelled DNA fragment was separated from free nucleotides by gelfiltration using Sephadex G-50 columns equilibrated with TE-buffer pH 8. The amount of radioactivity was determined for the eluted fractions. For hybridization, normally a DNA probe with a specific activity of 10⁶ cpm per ml was used.

4.3.2 Isolation of total RNA

All solutions used for RNA preparation and Northern blot were autoclaved (121°C, 20 min) twice to inactivate RNAses. Total RNA was isolated from logarithmically growing cells by the hot phenol method as described by (Schmitt *et al.*, 1990). A fresh yeast culture (10 ml) of OD₆₀₀ 1 was harvested and resuspended in 400 μ l 50 mM Na-acetate, pH 5.3, 10 mM EDTA. The suspension was mixed with 40 μ l 10% SDS and vortexed vigorously. An equal volume of phenol preequilibrated with Na-acetate and preheated at 65°C was added, vortexed and incubated at

Methods

65°C for 4 min. The suspension was immediately chilled in a dry ice/ethanol bath until phenol crystals appeared. To separate the aqueous from the phenol phase, the suspension was centrifuged at 20,000 x g for 5 min. The aqueous upper phase was collected and extracted with an equal volume of phenol/chloroform for 5 min at RT. The RNA was precipitated with 1/10 volume of 3 M Na-acetate pH 5.3 and 2.5 volumes ethanol. After incubation at -20°C for 30 min, the RNA was pelleted at 20,000 x g for 15 min. The pellet was washed once with 80% ethanol, dried and resuspended in 20 µl sterile water and stored at -80°C.

4.3.3 Northern blot

Total RNA (20 µg) was mixed with 11.8 µl DMSO, 2.4 µl 0.1 M phosphate-buffer (Na₂HPO₄/NaH₂PO₄, pH 6.8) and 40% deionized glyoxal and incubated for 1 h at 50°C. After cooling the mixture in ice water, 6.3 µl glyoxal loading buffer (50% glyoxal, 10 mM phosphate-buffer pH 6.8, 0.4% bromphenolblue, 0.25% xylene cyanol FF) was added prior to loading on a 1% agarose gel prepared with 10 mM phosphate-buffer pH 6.8. Electrophoresis was performed at 60 V for 4 h and the running buffer was recycled every 30 min to avoid changes in the pH during the run. RNA was transferred from the gel onto a Nylon membrane (Hybond N+) by capillary transfer overnight with 20x SSC buffer (175.3 g NaCl, 88.2 g Na-citrate in 1 L H₂O, pH 7.0) and UV-crosslinked in a Stratagene crosslinker. The membrane was washed with 1x SSC, 1% SDS and rinsed with sterile water. To check the efficiency of the transfer, the RNA was stained with 0.02% methylene blue in 0.3 M Na-acetate pH 5.5 for 5-10 min. After removal of excess stain with 5-10% ethanol, the stained rRNA bands could be visualized on the membrane.

The membrane was prehybridized in 10 ml 10x Denhardt's buffer (50x Denhardt's: 5 g Ficoll 400, 5 g polyvinylpyrrolidone, 5 g BSA fraction V in 500 ml water, 0.45 µm filter sterilized, stored at -20°C), 2x SSC, 1% SDS, 20 µg/ml salmon sperm DNA for 3-6 h at 65°C. The labelled probe was added to the prehybridization solution after heat-denaturation. After an o/n incubation at 65°C the membrane was washed 3 times for 15 min with 2x SSC, 1% SDS and 3 times for 15 min with 1x SSC, 1% SDS, at 65°C, and exposed to an X-ray film at -80°C or to a phosphoimager screen at RT for the indicated time.

4.4 Cell biology of yeast

4.4.1 Preparation of crude cell extract

The crude extract from yeast cells was prepared according to (Knop *et al.*, 1999). Yeast cells were inoculated from a fresh o/n culture in 10 ml YPD medium to an OD₆₀₀ of 0.2 and were

grown at 30°C with vigorous agitation to an OD₆₀₀ of 0.8-1.0. 5-10 OD₆₀₀ equivalents were harvested and resuspended in 1 ml cold water. The cell suspension was mixed with 150 µl 1.85 M NaOH, 7.5% β-mercaptoethanol and placed on ice for 10 min. 150 µl 50% TCA (w/v) was added and the sample was incubated for 10 min on ice. The precipitated protein was collected by centrifugation (5 min at 20,000 x g, 4°C). The supernatant was removed, and all residual traces of TCA were aspirated off. The pellet was resuspended in 55 µl sample buffer and neutralized with 5 µl 1 M Tris not adjusted to pH. Proteins were denatured for 10 min at 65°C. After centrifugation aliquots corresponding to 0.5 OD₆₀₀ of cells were analysed for protein content by SDS-PAGE. TCA-precipitated proteins required a longer blotting transfer time than non-treated proteins.

4.4.2 Preparation of total membranes

Yeast cells were inoculated from a fresh overnight culture in 50 ml YPD medium to OD₆₀₀ 0.2. They were grown at 30°C until early logarithmic phase (OD₆₀₀ of 1-1.5). The cells were harvested and resuspended in 1 ml cold water. The cell suspension was mixed with 200 µl TE-buffer (100 mM Tris pH 8, 10 mM EDTA) and 1 mM PMSF. Cell disruption was performed mechanically by vigorous vortexing the cell suspension with glass beads. Every sample was alternately vortexed for 30 s and placed on ice for 8 times. After gravity sedimentation of the glass beads the supernatant was collected. Nuclei and cell debris were removed by centrifugation at 500 x g for 5 min. The supernatant was sedimented for 30 min at 20,000 x g in an eppendorf centrifuge. The pellet contained crude membranes of yeast cells.

4.4.3 Cultivation of yeast cells for mitochondria preparation

A preculture of the wild type *S. cerevisiae* strain W303-1A was grown o/n at 30°C on lactate medium. The main culture (500 ml) was inoculated to an OD₆₀₀ of 0.2 in lactate medium and grown at 30°C with vigorous agitation until the early logarithmic phase (OD₆₀₀ of 1-1.5) was achieved. Transformed yeast cells (e.g. $\Delta md11$, p426-md11) were grown for 24 h as a preculture at 25°C in drop out medium. The main culture was cultivated at 25°C until an OD₆₀₀ of 1 was reached. Cells were harvested by centrifugation (5 min at 3,000 x g).

4.4.4 Preparation of spheroplasts

The cell pellet was washed once with distilled water, and resuspended in 30 ml 0.1 M Tris-sulphate, pH 9.4, 10 mM DTT, and incubated for 10 min at 30°C to break the disulfide

bonds in the cell wall. After centrifugation (5 min at 3,000 x g) the cell pellet was suspended in 8 to 20 ml 1.2 M sorbitol, 20 mM phosphate buffer, pH 7.4. To determine the cell density, an aliquot was taken, diluted 1:100 in water and the OD₆₀₀ was determined. The starting OD₆₀₀ should not exceed 50. The cell wall was digested by 20 units of lyticase per OD₆₀₀ of cells at 30°C with gentle shaking for 1 to 2 h. Conversion to spheroplasts was checked by measuring the OD₆₀₀ of a 1:100 (in water) diluted suspension. Spheroplasts are osmotic labile, therefore 1:100 dilution in water should result in drop of the OD₆₀₀ to less than 10% of the initial value. Spheroplasts were harvested by centrifugation (1,000 x g, 5 min, 4°C) and washed carefully in 8 ml 1.2 M sorbitol-buffer. After resuspending the pellet in 3-10 ml ice-cold 1.2 M sorbitol, 40 mM HEPES pH 7.4, 1 mM PMSF and equal volume water, the spheroplasts were lysed by homogenization with 40 strokes in a tight-fitting douncer at 4°C. The homogenate was centrifuged at 4,000 rpm for 10 min at 4°C to remove any non-lysed spheroplasts and cell debris.

4.4.5 Preparation of mitochondria

The mitochondria were isolated by differential centrifugation according to (Daum *et al.*, 1982). The spheroplasts were prepared as described above. After lysis of the spheroplasts the supernatant was centrifuged at 9,200 rpm for 12 min in a sorvall SS34 rotor (Beckmann). The pellet was carefully resuspended in 1-8 ml 0.6 M sorbitol, 20 mM HEPES pH 7.4 and centrifuged at 4,000 rpm for 5 min. The supernatant was pelleted at 9,200 rpm for 12 min. The crude mitochondria pellet was resuspended in 500 µl 0.6 M sorbitol, 20 mM HEPES pH 7.4, aliquoted, frozen in liquid nitrogen and stored at -80°C.

To purify yeast mitochondria devoid of microsomal contaminations, a purification procedure using a sucrose density gradient was applied (Meisinger *et al.*, 2000). The crude mitochondria purified as described above were loaded onto a step sucrose gradient composed of 1.5 ml of 60% (w/v), 4 ml of 32%, 1.5 ml of 23%, and 1.5 ml of 15% sucrose in 20 mM HEPES, pH 7.2. After centrifugation at 134,000 x g in a SW41 swing-out rotor for 1 h at 4°C, the purified mitochondria were recovered from the 32% / 60% sucrose interface.

4.4.6 Generation of mitoplasts by osmotic swelling

Mitoplasts are mitochondria from which the outer membrane has been removed by osmotic shock (Gasser *et al.*, 1982; Fritz *et al.*, 2001). Crude mitochondria were diluted with 5 volumes of 20 mM HEPES, pH 7.4 to a final concentration of 0.1 M sorbitol. The suspension was stirred gently for 20 min at 4°C. The submitochondrial membranes were loaded on a sucrose step gradient [30%, 34%, 40%, 44%, 50% (w/v) sucrose in 20 mM HEPES, pH 7.2] and centrifuged at 134,000 x g in a SW 28 rotor for at least 12 h. The outer membrane was enriched

at the top of the gradient, whereas the inner membrane vesicles were collected from fractions corresponding to 35-45% sucrose. 500 μ l fractions were collected and the refractive index was determined. The samples were TCA-precipitated (final concentration 5%) and analysed by SDS-PAGE and immunostaining. Alternatively, the inner membrane fractions were 3 fold diluted in 20 mM HEPES-buffer, pH 7.2 and sedimented for 20 min at 20,000 rpm in a SS34 rotor. The pellet was used for reconstitution.

4.4.7 Digitonin fractionation of mitochondria and proteinase K digestion

Mitochondria were fractionated with digitonin as described (Hartl *et al.*, 1986; Klanner *et al.*, 2001; Fritz *et al.*, 2001) with slight modifications. Shortly, mitochondria (100 μ g) in a concentration of 5 mg/ml were resuspended in SEMK buffer (250 mM sucrose, 10 mM MOPS-KOH pH 7.2, 80 mM KCl, 1 mM EDTA) supplemented with varying concentrations of digitonin in the presence and absence of proteinase K (100 μ g/ml) and incubated for 5 min at 4°C. For control, mitochondria were completely solubilized by adding 0.17% (v/v) Triton X-100. Solubilization of mitochondrial membranes was stopped by diluting the sample five-fold with ice-cold SEMK. Protease digestion was continued for additional 30 min on ice before it was inhibited by addition of 1 mM PMSF. The samples were TCA-precipitated (5%) and analysed by SDS-PAGE and immunostaining.

4.4.8 Preparation of microsomes

To obtain microsomes from yeast cells, spheroplasts were prepared and lysed as described above. The supernatant of lysed spheroplasts was mixed with a 72% sucrose solution to obtain a suspension of 50% final sucrose concentration. The suspension was overlaid with 10 ml 42% sucrose and 10 ml 24% sucrose and centrifuged at 104,000 x g for at least 4 h in a SW-28 rotor. The microsomes were harvested from the 24% / 42% sucrose interphase and diluted with 2 volumes of 20 mM HEPES, 100 mM NaCl, pH 7.5. The suspension was centrifuged at 227,000 x g in Ti50 rotor for 45 min. The pellet was resuspended in 500 μ l 20 mM HEPES, 100 mM NaCl, pH 7.5, aliquots were frozen in liquid nitrogen and stored at -80°C.

4.4.9 Preparation of vacuoles

The procedure for isolation of vacuoles was performed as described (Roberts *et al.*, 1991; Zinser and Daum, 1995). The spheroplasts were prepared by lyticase treatment as described previously, but in order to avoid disruption of the fragile vacuolar membrane, a more careful lysis

Methods

of spheroplasts was applied. The pellet of spheroplasts was resuspended in 6-10 volumes of 10 mM 2-(N-morpholino)ethanesulfonic acid (MES)/Tris, pH 6.9, 0.1 mM MgCl₂ and 12% Ficoll 400 and homogenized 10 times with a loose-fitting douncer at 4°C. The lysate was centrifuged at 2,200 x g for 10 min at 4°C. For the Ficoll flotation experiment, the lysed spheroplasts were overlaid with an equal volume of 10 mM MES/Tris, pH 6.9, 0.1 mM MgCl₂ and 12% Ficoll 400 and centrifuged at 60,000 x g for 30 min in a SW-28 rotor. A white turbid fraction containing the vacuoles was collected from the top of the Ficoll gradient and homogenized with a loose-fitting douncer in 10 mM MES/Tris, pH 6.9, 0.1 mM MgCl₂ and 12% Ficoll 400. The suspension was overlaid with an equal volume of 10 mM MES/Tris pH 6.9, 0.5 mM MgCl₂ and 8% Ficoll 400 and centrifuged at 60,000 x g for 30 min in a SW-41 rotor. Again the white turbid suspension on top of the Ficoll gradient was harvested and diluted in 10 mM MES/Tris pH 6.9, 5 mM MgCl₂, 25 mM KCl. The suspension was homogenized with a loose-fitting douncer and centrifuged for 1 h at 37,000 x g in a Ti50 rotor. The pellet was resuspended in a small volume of 10 mM MES/Tris pH 6.9, 5 mM MgCl₂, 25 mM KCl containing 5% glycerol. Aliquots of the vacuole vesicles were frozen in liquid nitrogen and stored at - 80°C.

4.4.10 Marker enzyme for vacuole

The enrichment of vacuole fractions in sucrose gradients was checked using α -mannosidase as vacuolar marker. Fractions were preincubated for 10 min at 37°C in 100 mM Tris-HCl, pH 6.8, 0.2% Triton X-100 and the reaction was started with 7.2 mM p-nitrophenyl- α -D-mannoside. The reaction was allowed to proceed for 2 h at 37°C and was stopped by addition of 250 mM Na₂CO₃. The α -mannosidase activity was followed by measuring the decrease in the absorption at 405 nm.

4.4.11 Subcellular fractionation

Spheroplasts were prepared as described above with slight modifications (Zinser and Daum, 1995). The cell pellet was resuspended in 0.1 M Tris-sulphate, pH 9.4, 10 mM DTT, and incubated for 10 min at 30°C. After centrifugation (5 min at 3,000 x g) the cell pellet was suspended in 1.4 M sorbitol, 50 mM phosphate buffer, pH 7.5 to 50 OD₆₀₀/ml and incubated with 20 units lyticase per OD₆₀₀ of cells at 30°C with gentle shaking for 1 to 2 h. Spheroplasts were harvested by centrifugation (1,000 x g, 5 min, 4°C) and suspended in lysis buffer (0.8 M sorbitol, 10 mM MOPS pH 7.5) with 1 mM PMSF to 100 OD₆₀₀/ml. After douncing 40 times with a tight fitting douncer, the suspension was centrifuged for 10 min at 500 x g and the supernatant was

loaded on a sucrose step gradient (18, 24, 30, 36, 42, 48, 54, 60% (w/v)) (according to R. Egner, personal communication). After centrifugation for at least 3 h at 30,000 rpm in a SW-41 rotor, 1 ml fractions were collected. The refractory index, the activity of marker enzymes, the protein concentration as well as peptide uptake activity were determined of each fraction. Aliquots of the fractions were analysed by Western blot analysis. According to the different sedimentation properties, it was possible to distinguish light microsomes containing smooth ER and heavy microsomes containing rough ER decorated with ribosomes. In order to remove ribosomes from the rER, microsomes were suspended in 0.8 M sorbitol, 10 mM MOPS, 10 mM EDTA pH 7.5. Since the adherence of ribosome to the ER is dependent on divalent cations, the EDTA treatment released ribosomes from the ER. The microsomes were applied to a sucrose step gradient (see above) and centrifuged at least 3 h at 30,000 rpm in a SW-41 rotor. Stripped microsomes underwent a density shift, and were recovered from 20-25% (w/v) sucrose gradient.

4.4.12 Preparation of transport-competent cells

Semi-permeabilized cells were prepared as described by (Baker *et al.*, 1988) and used in peptide uptake assays. *S. cerevisiae* strain W303-1A was grown at 30°C in YPD medium to an OD₆₀₀ of 1. The cells were harvested by centrifugation (1,000 x g, 5 min, 24°C) and resuspended at 50 OD₆₀₀ units per ml in 0.1 M Tris-sulphate, pH 9.4 including 10 mM DTT. Spheroplasting was performed as described previously, but with slight modifications. Shortly, lyticase treated spheroplasts were harvested at 1,000 x g, 5 min, 24°C and resuspended at 5 OD₆₀₀/ml in spheroplasting medium (0.75x YP, 0.7 M sorbitol, 1% glucose). To regenerate the spheroplasts and resume their metabolism, they were incubated with gentle shaking for 20 min at 30°C. The suspension was harvested at 1,000 x g, 5 min at 4°C and resuspended at 300 OD₆₀₀ per ml in ice-cold lysis buffer (400 mM sorbitol, 20 mM HEPES, pH 6.8, 150 mM KOAc, 2 mM MgOAc and 0.5 mM EGTA). Aliquots (200µl) were carefully frozen in the vapours above liquid nitrogen for 45 min. The frozen tubes were transferred to a -80°C freezer. No loss in transport activity was detected after 2 months of storage.

4.5 Biochemical methods

4.5.1 SDS-PAGE (polyacrylamide gel electrophoresis)

The stacking gel buffer is composed of 0.5 M Tris-HCl, pH 6.8 and 0.4% SDS. The running gel buffer contains 1.5 M Tris-HCl, pH 8.8 and 0.4% SDS. The acrylamide solution

Methods

consists of 30% acrylamide and 0.8% N,N'-methylenebisacrylamide. Stock aliquots of 10% ammoniumperoxodisulphate (APS) are prepared in water and stored at -20°C.

The 8 disk gel block was assembled. For the running gel the ingredients were mixed according to table 8. The polymerization reaction was started by addition of N, N, N', N'-tetramethylethylenediamine (TEMED) and APS. Quickly, the mixture was poured into the disk gel block and overlaid with isobutanol. After polymerization of the running gel (1 h), the isopropanol was removed, washed with water, and the stacking gel solutions were prepared according to table 8. The polymerization reaction was started by addition of TEMED and APS. The mixture was poured into the gel block and the combs were immediately put inside the stacking gel.

Before electrophoresis the proteins were denatured in 3x sample buffer (150 mM Tris pH 6.8, 6% SDS, 30% glycerol, 0.3% bromphenolblue and freshly added 40 mM DTT). Soluble proteins were incubated 5 min at 95°C, membrane proteins were incubated 10 min at 65°C. The SDS electrophoresis was performed at 180 V for 2-3 h in running buffer (25 mM Tris, 192 mM glycine, 0.1% SDS, pH ~8.3).

Tab.8: Composition of stacking and running gel according to Laemmli (1970)

	stacking gel	running gel		
	5%	7.5%	10%	12%
acrylamid	6.8 ml	18 ml	24 ml	29 ml
stacking buffer	5 ml			
running buffer		18 ml	18 ml	18 ml
H ₂ O	28 ml	36 ml	30 ml	25 ml
APS	320 µl	470 µl	470 µl	470 µl
TEMED	32 µl	40 µl	40 µl	40 µl

4.5.2 Western blotting

To transfer proteins from the gel onto nitrocellulose, the gel was placed on several Whatmann papers soaked in blotting buffer (25 mM Tris, 192 mM glycine, 20 % methanol, pH 8.2) and covered with a nitrocellulose membrane followed by several Whatmann papers soaked in blotting buffer. The sandwich was transferred to a semidry blotting apparatus (BioRAD) with the nitrocellulose membrane facing the anode. The electroblotting was performed at constant current (100 mA) per gel. Alternatively, the sandwich was placed into a tank blot apparatus (BioRAD) filled with blotting buffer. Proteins were transferred o/n at a constant voltage of 18 V.

To determine the efficiency of the transfer, the membrane was stained with Ponceau Red (0.1% Ponceau Red S, 5 % acetic acid) for 5 min, and washed with water until defined bands were visible. For immunodetection the membrane was blocked with blocking buffer (TBS-T: 10 mM Tris-HCl pH 8.0, 150 mM NaCl, 0.1% (v/v) Triton X-100, including 7% (w/v) skim milk powder and 0.1% (w/v) NaN₃) for at least 30 min at RT or o/n at 4°C. When either the α -strep-tag or α -biotin was used, the membrane was blocked in 3% BSA in TBS-T. The membrane was incubated at RT for 1 h with the primary antibody diluted in blocking buffer, respectively. After washing 5 times for 5 min with TBS-T the protein bands were visualized using horseradish peroxidase conjugated second antibodies (1:10,000). The protein was detected via the Enhanced ChemiLuminescence (ECL) system according to the manufactures instructions. The luminescence signal was recorded on Hyperfilm chemiluminescence film.

Tab.9: List of antibodies and recommended dilutions

antibody	source	dilution (Western)	Reference
α -Mdl1	rabbit	1:500	Research Genetic Inc, Huntsville
α -Sec61	rabbit	1:10,000	Schekman
α -Kar2	rabbit	1:10,000	Schekman
α -porin	rabbit	1:1,000	Lill
α -pre-pro alpha factor	rabbit	1:500	Schekman
α -biotin	goat	1:10,000	
α -strep-tag	mouse	1:2,000	IBA
α -myc	mouse	1:500	HIS-Diagnostic
α -goat, mouse, rabbit		1:10,000	Amersham Pharmacia

4.5.3 Stripping of immunoblots

To re-use Western blots, membranes were stripped with a stripping buffer (60 mM Tris-HCl, pH 6.7, 2% SDS (w/v), 100 mM β -mercaptoethanol) for 20 min at 50°C in a water bath and washed afterwards with TBS, 0.1% Triton X-100 before extensive blocking (at least 1 h) and incubation with the next antibody.

4.5.4 Generation of Mdl1p-specific antiserum

For generation of Mdl1-specific antisera, the synthetic 15mer peptide KGGVIDLDNSVAVER (corresponding to the last C-terminal amino acids) was sent to Research Genetic Inc, Huntsville and used for generation of antibodies in rabbits.

4.5.5 Solubilization of membrane proteins from mitochondria

Detergents are amphiphilic molecules which disrupt the bilayer of the membrane. An important property of a detergent is its critical micelle concentration (CMC). Below its CMC, a detergent is soluble in water in monomeric form, but, at concentrations above the CMC, organized structures are formed, termed micelles. Proteins are solubilized in detergent micelles, with the hydrophobic membrane-penetrant part of the protein coated by the hydrophobic part of the detergent. Tab.10 summarizes the detergents used in the thesis. As Triton X-100 is a heterogeneous mixture of long-chain polyoxyethylene polymers, information about properties differ in literature.

Tab.10: Detergent and some of their properties

detergent	Monomer M_G	CMC [mM]	Aggregation number
Decyl- β -D-maltoside	483	1.6	---
Octyl- β -D-glycopyranoside	292	25	84
Triton X-100	1625	0.3	140
Digitonin	1229	0.7	60

Mitochondria (1 mg) were thawed on ice and centrifuged at 20,000 x g, 5 min, 4°C. The membrane pellet was resuspended in 100 μ l solubilization buffer (20 mM HEPES, pH 7.4, 150 mM NaCl, 2 mM KCl, 20% glycerol, 2 mM MgCl₂, 0.5 mM MnCl₂) containing the appropriate concentration of detergent e.g. decylmaltoside (1.4%) or digitonin (2%) and was solubilized for 30 min on ice. Non-solubilized material was removed by centrifugation at 100,000 x g, 30 min and 4°C. The supernatant was used for chromatography, reconstitution or azido-ATP crosslinking.

4.5.6 Enrichment of Mdl1p from solubilized mitochondria by gelfiltration

All chromatographic procedures with membrane proteins were performed in detergent buffer (0.114% DM or 0.5% digitonin, 20 mM HEPES, pH 7.4, 150 mM NaCl, 2 mM KCl, 20% glycerol, 2 mM MgCl₂, 0.5 mM MnCl₂). Proteins derived from solubilized mitochondria were separated by gelfiltration using a Superose 6 PC3.2/30 column (Amersham Pharmacia)

equilibrated with detergent buffer. All fractions were analysed via SDS-PAGE and immunostaining with α -Mdl1. Mdl1p containing fractions were pooled and used for reconstitution.

4.5.7 Affinity-isolation of Mdl1p from solubilized mitochondria

4.5.7.1 ATP-agarose

ATP-agarose (C-8, N-6 or ribose coupled) or reactive RED 120 was washed 3 times with distilled water and once with detergent buffer (0.114% DM or 0.5% digitonin, 20 mM HEPES, pH 7.4, 150 mM NaCl). ATP-agarose was then incubated in batch with detergent solubilized mitochondrial proteins supplemented with 2 mM MgCl₂ with constant agitation for 1 h at 4°C. The ATP-agarose was washed with detergent buffer, and the protein was eluted with 5 mM ATP in detergent buffer in case of ATP-agarose or by a salt gradient from 150 to 900 mM NaCl in the presence of 5 mM ATP in case of Red-agarose.

4.5.7.2 Metal affinity chromatography

For immobilized metal affinity chromatography (IMAC), solubilized His₆-tagged constructs of the Mdl1p were applied to Ni-NTA-beads. Before use, the Ni-NTA-beads were stripped with 10 mM EDTA, washed 10 times in distilled water (180 x g, 30 sec), incubated with 10 mM NiCl₂ for 5 min, washed 10 times in distilled water and preequilibrated with detergent buffer (0.114% DM or 1% Triton X-100, 20 mM HEPES, pH 7.4, 150 mM NaCl). Binding of the protein was performed in batch with constant agitation for 1 h at 4°C. Washing was performed with 20 mM imidazole steps from 20 mM to 80 mM in detergent buffer and protein was eluted using a imidazole gradient of 80 to 250 mM.

4.5.7.3 Streptactin chromatography

To purify the streptII-tagged constructs of Mdl1p, a streptactin resin was used. Before use, beads were regenerated with 5 mM hydroxyazophenyl benzoic acid (HABA) and extensively washed with 10 mM HEPES, pH 7.2, 150 mM NaCl, 1 mM EDTA. Afterwards, the resin was equilibrated with detergent buffer (0.114% DM, 10 mM HEPES, pH 7.2, 150 mM NaCl). Binding to the resin was performed in batch with constant agitation for 1 h at 4°C. Washing steps were performed with detergent buffer and protein was eluted with detergent buffer supplemented with 2.5 mM desthiobiotin.

4.5.8 Reconstitution into preformed liposomes

For liposome preparation, a lipid mixture of 75% phosphatidylcholine, 20% phosphatidylethanolamine and 5% cardiolipin was dissolved in chloroform. If indicated, a different composition of lipids was used. The chloroform was removed under a stream of nitrogen, and lipids were dried in vacuum. The lipid film was rehydrated in phosphate buffer pH 8 to a final lipid concentration of 8 mg/ml. Liposomes were extruded 11 times through a 200 nm pore-size polycarbonate filter using a LipoFast-Extruder followed by four freeze and thaw cycles. Preformed liposomes were stored at -80°C . If indicated, liposomes were destabilized by preincubation with 1.6% octylglycoside for 3 h before use.

For reconstitution, preformed, unilamellar liposomes were thawed for 10-30 min on ice and collected by centrifugation ($100,000 \times g$, 30 min, 4°C). The liposome pellet was mixed with solubilized membrane protein fraction derived directly from solubilization of mitochondria or from partially purified Mdl1p by gel filtration or affinity chromatography. Solubilized membrane proteins were incubated with liposomes for 1 h on ice and detergent was removed by successive addition of biobeads SM-2. Before use, the biobeads were washed once with methanol and 10 times with distilled water and preequilibrated with solubilization buffer without detergent. After incubation of the reconstitution mixture with 100 mg biobeads for 20 min at 4°C , the suspension was centrifuged ($200 \times g$, 2 min, 4°C) and the supernatant was incubated with a new batch of biobeads. The exchange of biobeads was repeated four times. Proteoliposomes were collected by centrifugation at $100,000 \times g$ for 1 h at 4°C .

4.5.9 Azido-ATP photolabelling of Mdl1p

Crosslinking experiments with 8-azido-ATP were performed with solubilized as well as reconstituted Mdl1p. The samples were preincubated in the presence and absence of nucleotide triphosphates (1.5 mM) for 5 min on ice in solubilization buffer (20 mM HEPES pH 7.4, 150 mM NaCl, 5 mM MgCl_2 , 1 mM MnCl_2 , 15% glycerol, 1% digitonin). For control, proteoliposomes were completely solubilized by addition of 1% Triton X-100. Azido- $[\alpha\text{-}^{32}\text{P}]\text{-ATP}$ was added to a final concentration of 2 μM and incubated on ice for 5 min. Samples were irradiated by UV (254 nm) for 5 min (Xenotest GmbH, 50/60 Hz), and diluted 5 times in solubilization buffer. The photocrosslinked protein was incubated with $\alpha\text{-Mdl1}$ (1:100) for 2 h at 4°C and the immunocomplexes were recovered overnight with 60 μl preequilibrated protein A-sepharose. The beads were washed 3 times with solubilization buffer containing 0.1% digitonin. Finally, the beads were resuspended in loading buffer (1 mM DTT), incubated for 10 min at 65°C and separated by 12% SDS-PAGE. The gel was dried and exposed to a Kodak Biomax film for 2 weeks.

4.5.10 Peptide labelling with NaI¹²⁵

Peptides were iodinated using the chloramine T-method (Hunter and Greenwood, 1964). Chloramine T solution (1 mg/ml) and sodiumdisulfite (1 mg/ml) were freshly prepared in 10 mM Na₂HPO₄/NaH₂PO₄, pH 7.4, 150 mM NaCl, 5 mM KCl. The reaction was routinely performed with 1.5 nmol peptide in a total volume of 50 µl and 1 µl (100 µCi) Na¹²⁵I. The reaction was started by addition of 10 µl chloramine T. After 5 min incubation at RT the reaction was stopped by addition of 20 µl Na₂S₂O₅ (sodiumdisulfite) and further diluted with 100 µl phosphate buffer. Free iodine was removed by ion exchange chromatography using Dowex 1 x 8 material. Anion exchange material (10 mg) was equilibrated in phosphate buffer containing 0.2% dialyzed BSA and was washed 2 times with phosphate buffer without BSA. The Dowex suspension (220 µl) was added to the radiolabelled reaction mix, vortexed and incubated for 5 min at RT. The suspension was applied to an empty spin column and centrifuged for 2 min at 200 x g. The flow-through contained the radiolabelled peptide in a concentration of 5 µM.

4.5.11 Peptide transport assay

The peptide transport reaction was started by addition of 50 pmol (10µl) radiolabelled peptide to 150 µl vesicles in transport buffer (20 mM HEPES, pH 7.2, 150 mM NaCl, 5 mM MgCl₂). If indicated, 3 mM ATP or ADP, non-hydrolysable ATP analogue (AMP-PNP) or 100 fold excess of competitor peptide was added. The reaction was performed for 3 min at 30°C and stopped by addition of excess of unlabelled peptide in 500 µl ice-cold transport buffer. The reaction was incubated 5 min on ice, centrifuged at 20,000 x g for 8 min and the pellet was washed twice with transport buffer. The radioactivity of the pellet was directly quantified by γ -counting.

For transport studies with microsomes peptides with a glycosylation site (NXS, NXT) were used. After the transport assay, microsomes were lysed by resuspending the pellet in 1 ml lysis buffer (1% (w/v) NP-40, 20 mM HEPES, pH 7.2, 150 mM NaCl, 5 mM KCl). After centrifugation the supernatant was loaded on 100 µl preequilibrated concanavalin A-sepharose. After 2 h at 4°C, the sepharose suspension was centrifuged (200 x g, 5 min, 4°C) and washed two times with lysis buffer. Glycosylated peptide was eluted by 1 ml 200 mM α -methylmannoside prepared in lysis buffer for 1 h at RT. After centrifugation the eluted fractions were quantified by γ -counting.

4.5.12 Purification of His₆-tagged NBDs

The cell pellet was resuspended in PBS (10 mM Na₂HPO₄/NaH₂PO₄, pH 7.6, 150 mM NaCl, 5 mM KCl) with 20 mM imidazole, 1 mM PMSF, 1% lysozyme, and 5-10 units benzonase and disrupted by French press treatment at 1000 p.s.i. After centrifugation for 1 h at 100,000 x g the supernatant was applied to a Ni-IDA column. Before use, the column was loaded with 100 mM NiCl₂ and extensively preequilibrated in PBS pH 7.6 with 20 mM imidazole. The column was washed with step gradients of 80 mM and 100 mM imidazole in PBS pH 7.4 and the protein was eluted with 250 mM imidazole. The fractions containing the NBD were pooled, concentrated using a centricon 10, and applied to a superdex 200 HR 11/15 gelfiltration column (Amersham Pharmacia) equilibrated in 20 mM Tris pH 8, 100 mM NaCl. The NBD eluted with an apparent molecular weight of 33 kDa corresponding to the size of the monomer. Fractions were concentrated to 30 mg/ml in a centricon 10 and stored in the presence of 5 mM ATP at 4°C.

4.5.13 Azido-ATP photolabelling of the Mdl1p-NBD

After preincubation of the purified NBD (0.3 μM) with different concentrations of nucleotide triphosphates for 5 min on ice in binding buffer (20 mM Tris pH 8, 100 mM NaCl, 5 mM MgCl₂, 1 mM MnCl₂), 8-azido-[α-³²P]-ATP was added to a final concentration of 0.5 μM and incubated on ice for 5 min. Samples were irradiated by UV (254 nm) for 5 min (Xenotest GmbH, 50/60 Hz), directly resuspended in SDS loading buffer (10 mM DTT) and separated by 15% SDS-PAGE. The gel was dried and exposed to Kodak Biomax film overnight. Alternatively, photocrosslinking with biotin-8-azido-ATP was performed by incubating the NBD (0.3 μM) with 30 μM biotin-8-azido-ATP for 5 min on ice in the presence and absence of unlabelled nucleotides (10 mM) in the binding buffer. The samples were irradiated by UV (254nm) for 5 min. After SDS-PAGE the protein was transferred to a nitrocellulose membrane according to standard procedures. The blot was blocked with 3% BSA for 1 h, followed by incubation with anti-biotin antibody (1:10,000) for 1 h. After washing biotinylated protein bands were detected by peroxidase coupled anti-goat antibody (1:10,000) using the ECL system.

4.5.14 ATPase assay

ATPase activities were measured by the Malachite green assay as described previously (Morbach *et al.*, 1993). The ATPase assay was performed in 20 mM Tris-HCl pH 8, 100 mM NaCl at 30°C with 30 μM NBD, unless specified differently. The reaction was started by addition of ATP and MgCl₂ to final concentrations of 2 and 10 mM, respectively.

4.5.15 Dimerization Assays

Ortho-vanadate stock solution (100 mM stock) was prepared from Na_3VO_4 in distilled water and was adjusted to pH 8 with HCl. After boiling for 2 min, the pH was again adjusted to 8. These steps were repeated until the pH did not change anymore. This stock solution was stored at -20°C . Before use, vanadate was again boiled to break polymeric species. At concentrations below 200 μM , monomeric vanadate is the predominant species in solution (Urbatsch *et al.*, 1995b).

BeCl_2 was prepared as a 10 mM stock solution in distilled water, NaF was prepared as a 500 mM stock solution. Before use, beryllium fluoride solution was mixed in a ratio of 1:100 of BeCl_2 and NaF. Purified wild type NBD (30 μM) was incubated with different concentrations of BeF_x or ortho-vanadate in the presence or absence of ATP for 5 min at 30°C in binding buffer. The sample was applied to a Superdex 75 HR 30/10 gel filtration column in 20 mM Tris-HCl pH 8, 100 mM NaCl, 5 mM MgCl_2 at 4°C and a flow rate of 45 $\mu\text{l}/\text{min}$. The same procedure was applied for purified mutant NBDs (E599Q; D598A; H631R) (30 μM) at different concentrations of ATP.

4.5.16 Determination of the ATP/ADP composition of the dimer

The wild type NBD was incubated with 625 μM ATP supplemented with 0.125 μM of either $[\alpha\text{-}^{32}\text{P}]\text{-ATP}$ or $[\gamma\text{-}^{32}\text{P}]\text{-ATP}$ (4500 Ci/mmol) under trapping conditions and analysed by gel filtration. The fractions were quantified for ATP concentration by β -counting and for protein concentration by the BCA kit. The mutant NBD (E599Q) (30 μM) was incubated for 5 min on ice with ATP supplemented with tracer amounts of $[\alpha\text{-}^{32}\text{P}]\text{-ATP}$ or $[\gamma\text{-}^{32}\text{P}]\text{-ATP}$ and analysed by gel filtration. The nucleotide composition of the dimer was analysed by thin layer chromatography (TLC). The fraction containing the dimer was incubated with 15 mM EDTA for 30 min and precipitated with trichloric acid (10 %) for 30 min at 4°C . After centrifugation at 20,000 $\times g$ for 5 min, the samples were neutralized with 0.5 M KHCO_3 pH 8.3 and applied onto polyethylenimine cellulose plates in 2 M formiat, 250 mM LiCl. To determine the positions of the radioactive species, $[\alpha\text{-}^{32}\text{P}]\text{-ATP}$ and $[\gamma\text{-}^{32}\text{P}]\text{-ATP}$ were incubated with hexokinase, apyrase and NBD.

4.5.17 Thiol-specific labelling of NBDs for FRET

Thiol-reactive reagents like maleimides are used to modify a protein at its cysteines. Maleimide coupled Texas Red (Ex 582 nm, Em 600 nm) was dissolved in methanol and Oregon Green (Ex 490 nm, Em 515 nm) in DMF and used in a 5 to 10x molar excess to label the NBDs (30 μM). The labelling reaction was performed in 50 mM Tris-HCl pH 7.5, 100 mM NaCl for 1- 4

Methods

h on ice in the dark. The reaction was stopped with a 10x excess of glutathione (GSH) and incubated for 1 h on ice. GSH quenched the reaction of thiol-reactive probes, forming highly soluble adducts that are easily removed by dialysis or gelfiltration. After centrifugation (5 min, 20,000 x g) the reaction mix was applied to a 5 ml desalting HiTrap column (Amersham Pharmacia) in 50 mM Tris-HCl pH 7.5, 100 mM NaCl to separate the labelled protein from the dye. The labelled NBDs were checked for dimerization in gelfiltration (Superdex 75 HR 30/10).

5 Results

5.1 Characterisation of the ABC transporter Mdl1p

Although it is widely agreed that ABC transporters undergo a series of conformational changes in response to ATP binding and hydrolysis at the NBDs and to substrate binding, transport and release at the TMDs, only little information is available about the structure of the intermediate states during transport process. We addressed the question by which mechanism ATP hydrolysis powers the translocation of substrate mediated by Mdl1p. Recently, Mdl1p has been identified as a peptide ABC transporter of the inner mitochondrial membrane of *S. cerevisiae* (Young *et al.*, 2001). It is proposed that this half-size transporter acts as a homodimer in its minimal composition. Much of the mechanism how the motor domains of ABC transporters work and cooperate can be learned from the characterisation of isolated NBDs. Therefore, the Mdl1p-NBD was purified and investigated *in vitro*. Different intermediate states of the NBD were studied during ATPase cycle in detail.

5.1.1 Heterologous expression and purification of wild type and mutant Mdl1p-NBDs

The C-terminal domain of the ABC transporter Mdl1p corresponding to the NBD (amino acids 427 to 695) was cloned into the pET28b vector under the control of a T7 promoter and expressed in *E. coli* BL21(DE3). The recombinant plasmid pET-NBD includes the expression cassette with an N-terminal His₆-tag, a thrombin cleavage site and a T7-tag encoded by the vector (Fig.7).

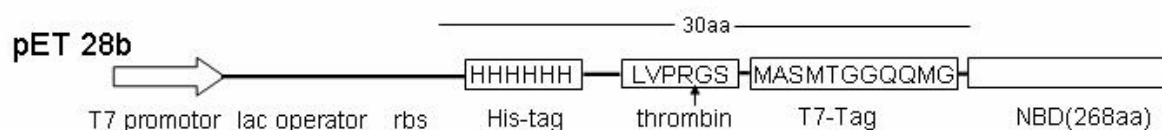
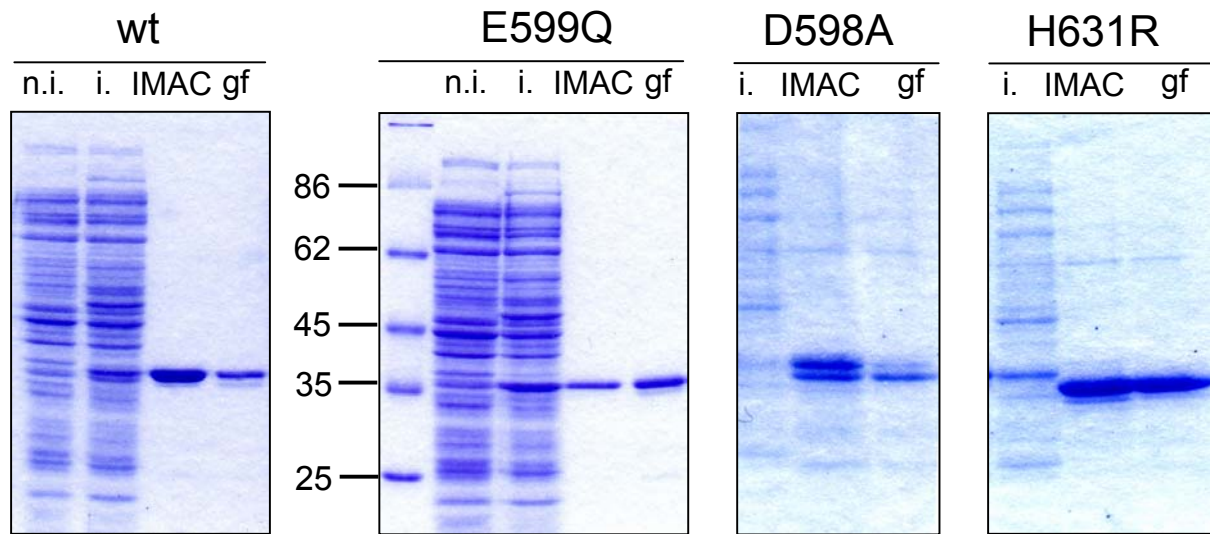
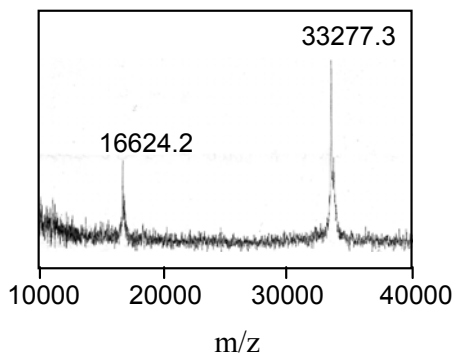


Fig.7: Expression cassette of NBD.

The NBD gene was cloned into the pET28b vector under the control of IPTG-inducible promoter. The construct was fused with an N-terminal His₆-tag, a thrombin cleavage site and a T7-tag encoded by the vector.

A**B****Fig.8: Purification of wild type and mutant Mdl1p-NBDs.**

A: Coomassie-stained 15% SDS-PAGE of crude extract of non-induced BL21(DE3) cells transformed with pET-NBD (n.i.), cells after 3 h induction with 0.2 mM IPTG (i), affinity-purified NBD after elution with 250 mM imidazole (IMAC) and gelfiltration using superdex 200 (g.f.).

B: MALDI-TOF of purified wild type NBD.

To gain insight into the ATP hydrolysis cycle, several mutants of Mdl1p-NBD were created according to mutations in different ABC transporters which affect ATPase activity. The mutations (E552Q; E1197Q) in the NBDs of P-glycoprotein were reported to be highly impaired in ATPase activity (Urbatsch *et al.*, 2000a). An equivalent mutation of the conserved glutamate (E599Q) of Mdl1p-NBD was introduced by site-directed PCR mutagenesis. This glutamate functions as a catalytic base downstream of the Walker B motif. Another mutation concerns the conserved aspartate (D598) of the Walker B motif. The exchange of aspartate to alanine in Mdl1p was reported to abolish peptide export of the ABC transporter (Young *et al.*, 2001). The

conserved histidine (H631R) in the switch region was changed to arginine according to the mutation of HisP (H211R). This mutant was reported neither to hydrolyse ATP nor to energize the transport of substrate by the whole HisQMP₂ complex (Nikaido *et al.*, 1997). All mutant NBD genes were cloned into the pET28b vector producing recombinant NBDs with an N-terminal His₆-tag.

All constructs were overexpressed in *E. coli* BL21(DE3) and purified by immobilized metal affinity chromatography (IMAC) followed by gel filtration. The wild type protein as well as the E599Q mutant were purified to homogeneity as shown by SDS-PAGE and MALDI-TOF-MS (Fig.8). The purified proteins of the two other mutants contained minor contaminations. The yield of the purification was approximately 50 mg protein per 1 L culture and the proteins could be concentrated up to 30 mg/ml.

5.1.2 Activity of wild type Mdl1p-NBD

The activity of the isolated wild type NBD was investigated with respect to ATP and ADP binding using 8-azido-[α -³²P]-ATP photocrosslinking. 8-Azido-[α -³²P]-ATP was crosslinked to the NBDs and could be specifically competed by increasing the concentration of unlabelled nucleoside tri/diphosphates. The IC₅₀ of the wild type NBD was 2 μ M for MgATP and 64 μ M for MgADP (Fig. 9). The absence of Mg²⁺ strongly reduced the affinity for nucleotides of NBDs (data not shown). The affinity of MgCTP, MgGTP, and MgUTP was approximately 30 fold lower as compared to MgATP (Fig.10).

The wild type NBD showed at a concentration of 30 μ M an ATPase activity with a turnover number of 0.5 ATP per minute at 30°C and a K_m value of 0.2 mM ATP (Fig.11). The isolated NBD did not show cooperativity in ATPase activity as determined by a Hill-coefficient of 1.2. ATPase activity was observed to be non-linearly dependent on protein concentration, suggesting that the active form is not monomer (data not shown). ATPase activity of the NBD was inhibited to 50% by 2.4 mM BeF_x (data not shown).

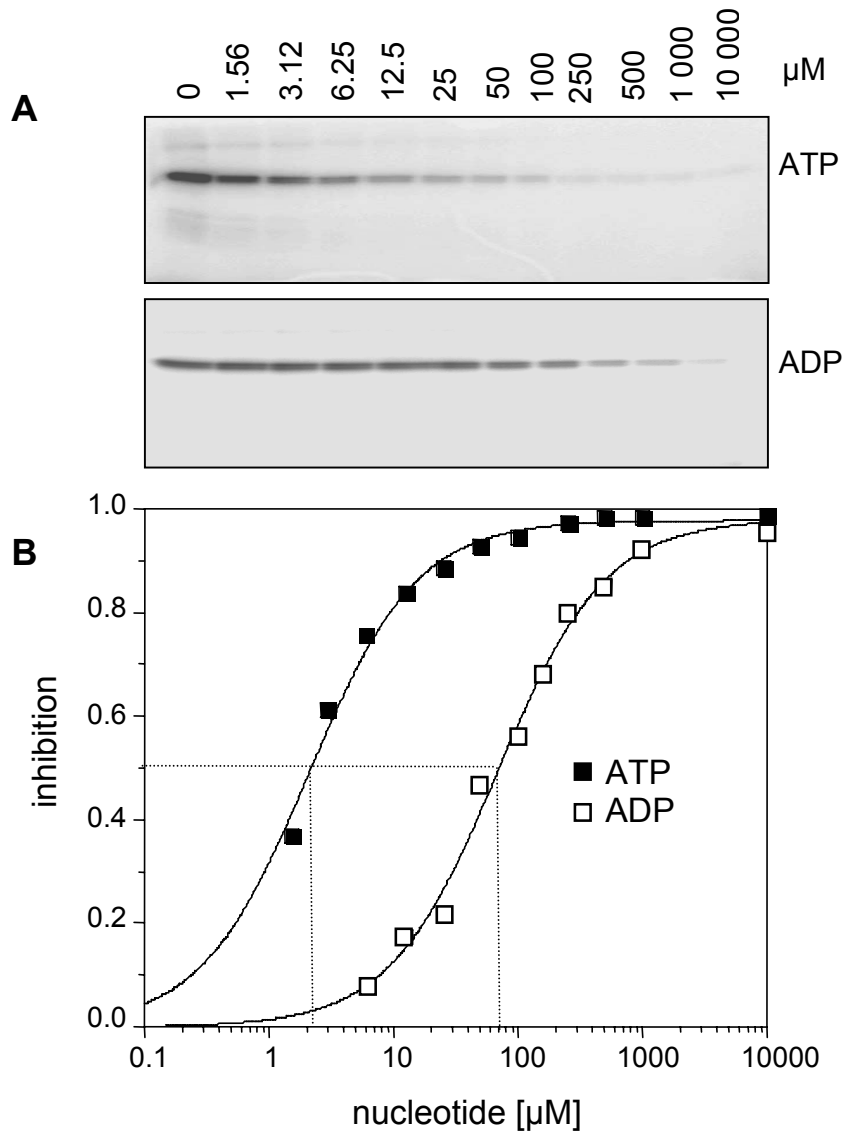


Fig.9: 8-Azido-[$\alpha^{32}\text{P}$]-ATP photocrosslinking of purified wild type NBD.

A: The NBD (300 nM) was incubated with different concentrations of unlabelled adenosine di/triphosphates (0 to 10 mM) on ice for 5 min, crosslinked with 0.5 μM 8-azido-[$\alpha^{32}\text{P}$]-ATP and separated by 15% SDS-PAGE.

B: The signals of the autoradiography were quantified by a phosphoimager obtaining an IC_{50} for MgATP of 2 μM and for MgADP of 64 μM .

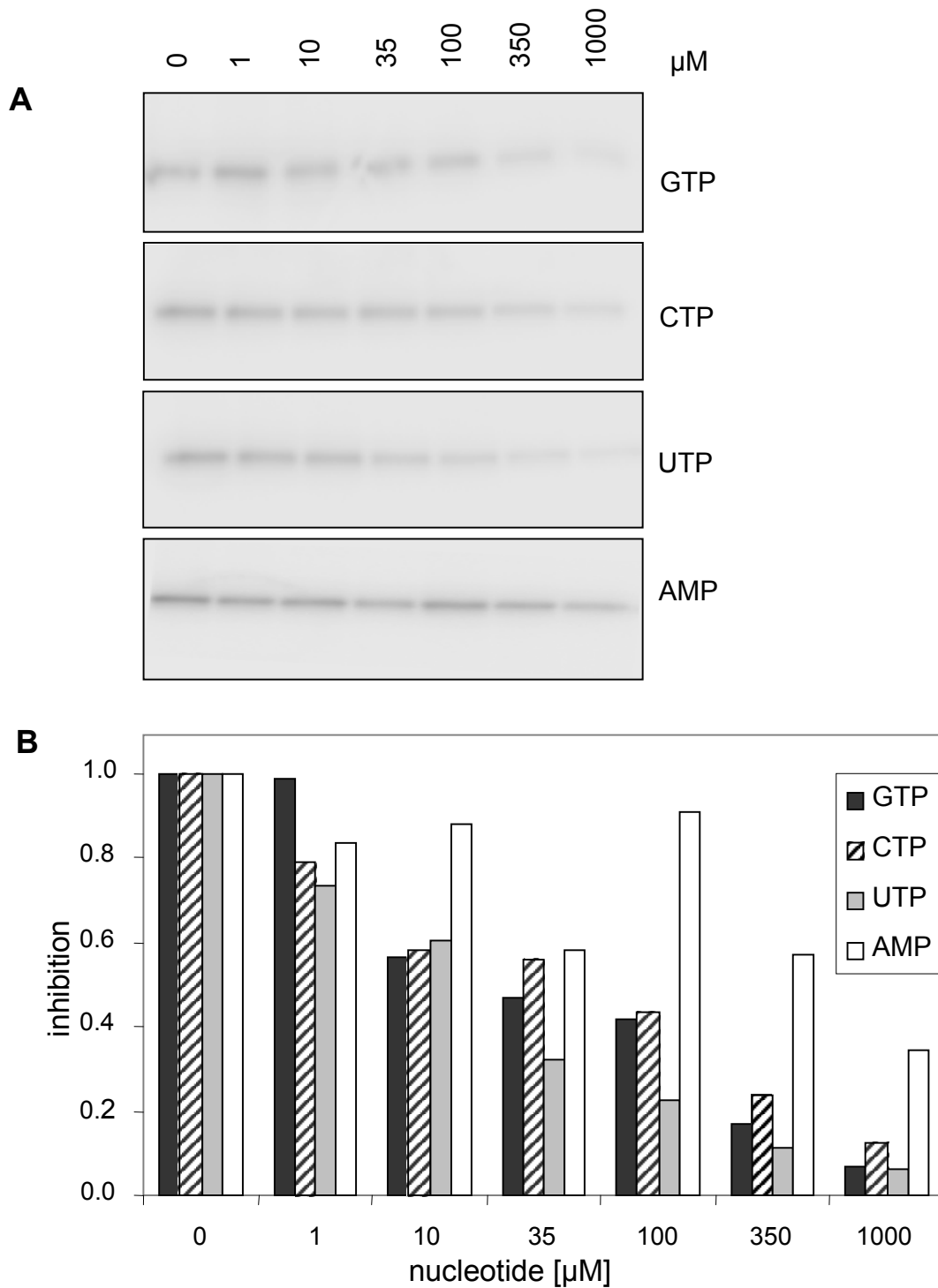


Fig.10: 8-Azido- $[\alpha^{32}\text{P}]$ -ATP photocrosslinking of purified wild type NBD in the presence of NTPs.

A: NBD (300 nM) was incubated with various concentrations (0 to 1 mM) of different nucleotides on ice for 5 min, crosslinked with 0.5 μM 8-azido- $[\alpha^{32}\text{P}]$ -ATP and separated by 15% SDS-PAGE.

B: The signals of the autoradiography were quantified (Phosphoimager). All nucleotides were bound by the NBDs obtaining an IC_{50} of about 35 μM . AMP could not compete binding of 8-azido-ATP.

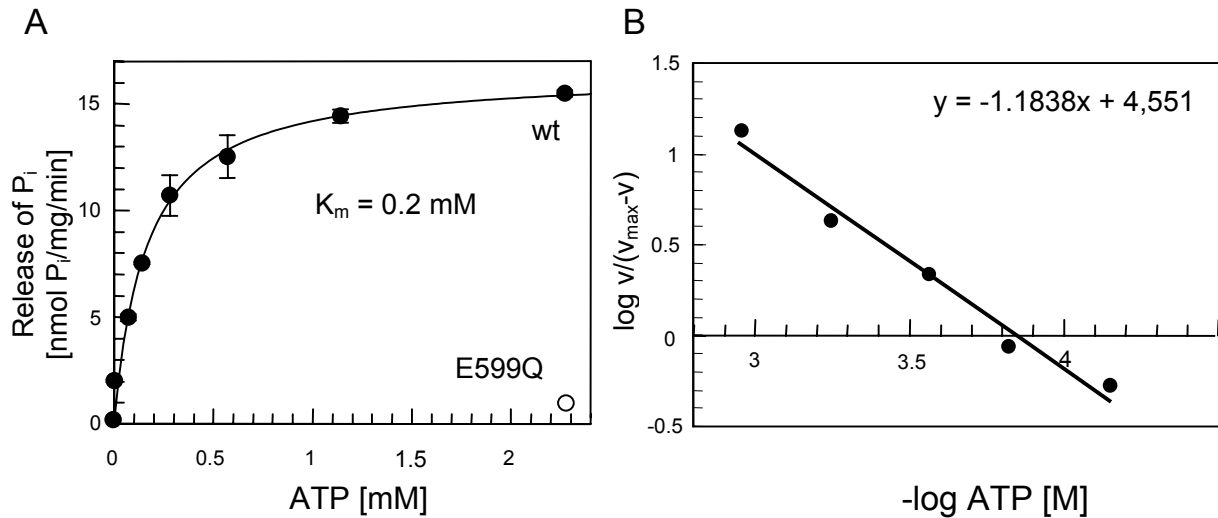


Fig.11: ATPase activity of wild type and E599Q NBDs.

A: ATPase activity of the NBDs (30 μM) was assayed at 30°C in presence of various concentrations of ATP (0 to 2.5 mM). The wt NBD showed an activity with a turnover of 0.5 ATP per min and a K_m value of 0.2 mM. The E599Q mutant exhibited no measurable activity at ATP levels higher than 2.5 mM.

B: The wt NBD showed no cooperativity in ATPase activity with a Hill-coefficient of 1.2 (Hill-plot).

5.1.3 The active form of NBD is a dimer

It is postulated that the interaction of both NBDs plays a central role in the catalytic cycle of ABC transporters (Nikaido, 2002). So far, gelfiltration experiments with isolated NBDs (e.g. HisP and P-gp) did not demonstrate ATP-dependent dimerization, independent of the presence of nucleotides or non-hydrolysable analogues like AMP-PNP (Nikaido *et al.*, 1997; Kerr, 2002). The wild type Mdl1p-NBD appeared as a monomer in gelfiltration studies independent of the presence of different nucleotides. In order to trap nucleotide binding proteins in a conformation during ATP hydrolysis, ATPase inhibitors like ortho-vanadate (V_i) or beryllium fluoride (BeF_x) can be used. ATPase inhibitors are valuable tools for investigations of the catalytic mechanism of ATPase enzymes. Ortho-vanadate and BeF_x act as analogues of inorganic phosphate. The inhibitory complex mimics the transition state during ATP hydrolysis in which ADP is still bound and phosphate is already released (Goodno, 1982; Urbatsch *et al.*, 1995b; Shibuya *et al.*, 2002).

The Mdl1p-NBD was investigated by trapping with ortho-vanadate or BeF_x under two different conditions. Non-hydrolysis condition means in the absence of Mg^{2+} and at 4°C and hydrolysis condition means in the presence of MgATP and at 30°C. Interestingly, after preincubation of the NBD with the ATPase inhibitor ortho-vanadate under hydrolysis conditions, a stable dimer corresponding to a molecular weight of 66 kDa was observed (Fig.12). The dimer was stable during gelfiltration, which took 40 min, even in the absence of ATP and inhibitor in the

mobile phase. The appearance of the ATP induced-dimer, which was stabilized by BeF_x , was dependent on the concentration of the inhibitor (Fig.13). Importantly, preincubation of NBD in the presence of ATPase inhibitors with either MgADP or MgAMP-PNP at 30°C or MgATP at 4°C did not induce dimerization of the NBD. Omitting Mg^{2+} from the reaction strongly reduced the formation of dimers. These experiments demonstrated that ATP binding and subsequent ATP hydrolysis are essential for the formation of dimers.

In order to test the stability of the formed dimer, the dimer fraction was immediately reinjected to a subsequent gelfiltration. It was observed that a peak at the position of the monomer appeared while the signal of the dimer peak decreased, demonstrating that trapping of the dimer state by BeF_x is not irreversible (data not shown).

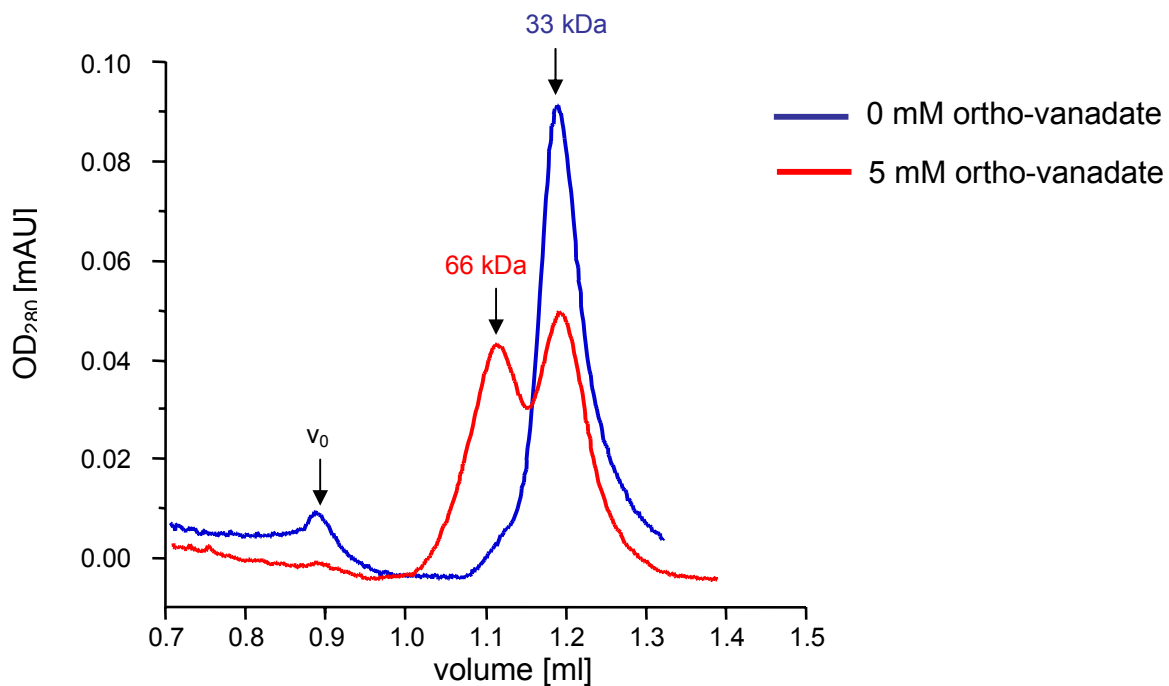


Fig.12: ATP-induced dimerization of the NBD stabilized by ortho-vanadate.

Wild type NBD (30 μM) elutes as monomer from the gelfiltration column independent of the presence of nucleotides (blue line). After preincubation of the NBD with 5 mM ortho-vanadate in the presence of 1 mM MgATP for 5 min at 30°C, a stable dimer was observed by gelfiltration Superdex 75 (red line). The column was calibrated with carboanhydrase (33 kDa) and BSA (66 kDa) with an elution volume of 1.2 ml. The void volume (V_0) was determined by dextrane blue.

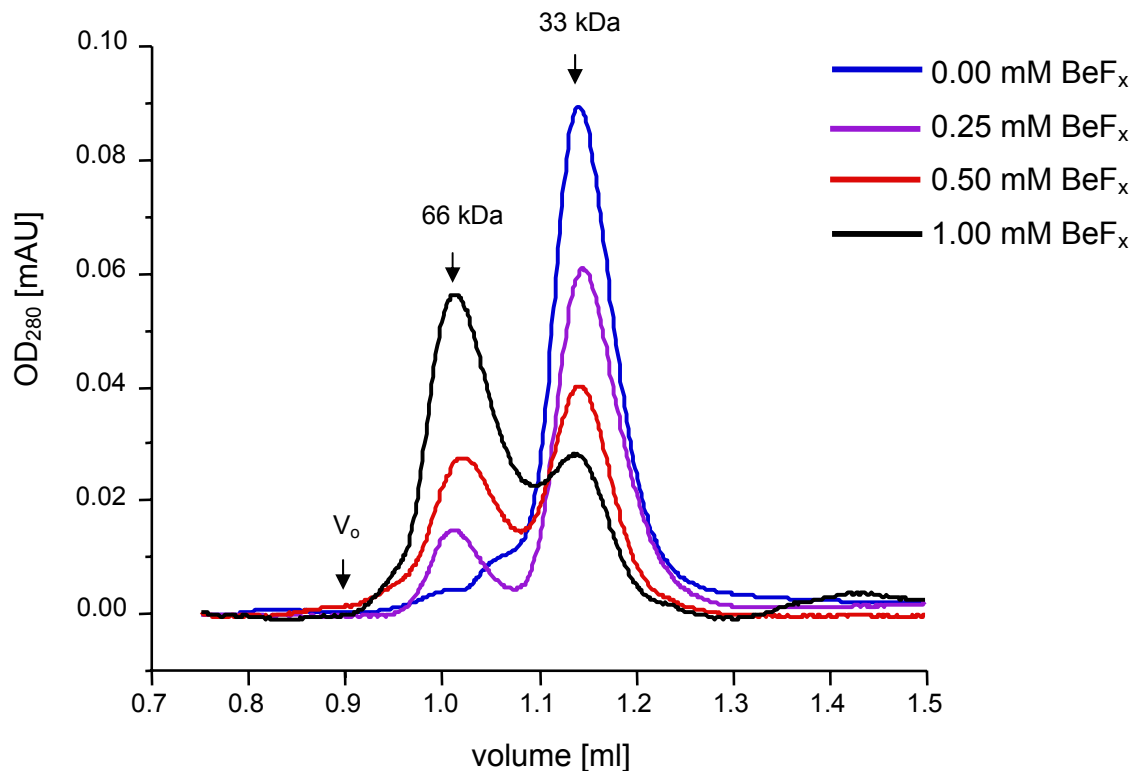


Fig.13: ATP-induced dimerization of the NBD depends on the concentration of BeF_x.

After preincubation of wt NBD (30 μ M) with various concentrations of BeF_x (0 to 1 mM) in the presence of 1 mM MgATP for 5 min at 30°C, a BeF_x-dependent dimer was observed by gel filtration (Superdex 75).

5.1.4 Analysis of mutant NBDs

The ability of the mutants D598A, E599Q and H631R of Mdl1p to bind ATP was analysed by 8-azido-biotin-ATP photocrosslinking experiments. As shown in Fig. 14 mutant NBDs bound ATP to the same extent as the wild type. As expected, all mutants were inactive in ATP hydrolysis as shown in standard ATPase assays measuring P_i release (Fig.11). It was reported that removal of the charge in catalytic base downstream of the Walker B motif (E552Q/E1197Q) of P-gp produced an ABC transporter with severely impaired transport activity and no substrate stimulated ATPase activity (Urbatsch *et al.*, 2000a). It was also reported that an equivalent mutation of the archaeal NBDs from MJ0796 and MJ1296 (E171Q/E179Q) resulted in an ATPase deficient NBD. Interestingly, ATP binding was sufficient to induce a stable dimer of these mutant archaeal NBDs (Moody *et al.*, 2002).

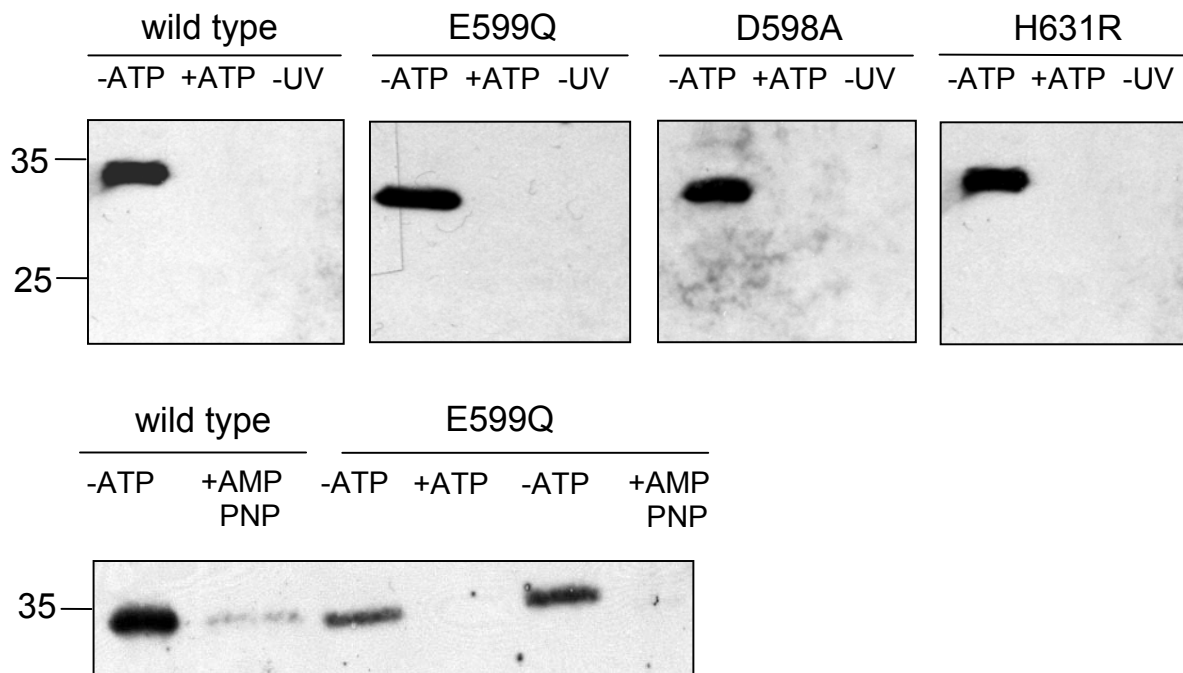


Fig.14: 8-Azido-biotin-ATP photocrosslinking of purified NBD mutants.

The NBDs (300 nM) were incubated with 30 μ M 8- N_3 -biotin-ATP in the absence or presence of 10 mM MgATP or MgAMP-PNP, separated by 15% SDS-PAGE and immunostained with α -biotin. For control, incubation with the antibody was performed without proceeding crosslinking by UV (-UV).

To assay the ability of the NBD mutants to form nucleotide-dependent dimers, experiments were performed in which the mutants were incubated with MgATP or MgADP (Fig.14). Gelfiltration experiments showed that only the E599Q mutant formed an ATP-induced dimer after preincubation with MgATP on ice. Dimerization of the E599Q mutant was dependent on the ATP concentration (Fig.15). The E599Q dimer was stable during gelfiltration even in the absence of nucleotides in the mobile phase. This indicates that the dimer dissociated very slowly. The concentration of 500 μ M ATP was sufficient to shift the monomer NBD completely to the dimer. In contrast to ATP, ADP did not induce dimerization. Moreover, the addition of ADP inhibited ATP-dependent dimer formation. These results are in line with the data obtained for the mutant E171Q NBD from MJ0796 and E179Q NBD from MJ1296 (Moody *et al.*, 2002). In contrast to data obtained from the archaeal NBDs the presence of Mg^{2+} did not impair dimer formation of the Mdl1p-NBD. Different Mg^{2+} concentrations did not influence the dimerization of the E599Q Mdl1p-NBD. Interestingly, MgAMP-PNP or ATP γ S did neither induce dimerization with the wild type Mdl1p-NBD nor with the E599Q NBD. Similar results were obtained from the archaeal mutants. Binding of AMP-PNP to the mutant and wild type Mdl1p-NBD was, however, not impaired as demonstrated by 8-azido-ATP-biotin-photocrosslinking experiments (Fig.14).

The H631R mutant showed in the absence of nucleotides predominantly a dimer, which was independent of ATP (data not shown). Because of the tendency of the D598A mutant to

Results

precipitate, 50% of the protein was detected in the void volume. The remaining non-aggregated protein showed an ATP-independent dimer. It was reported that purification of HisP with a corresponding mutation in the Walker B motif was not successful as well due to precipitation of the protein during purification (Nikaido and Ames, 1999).

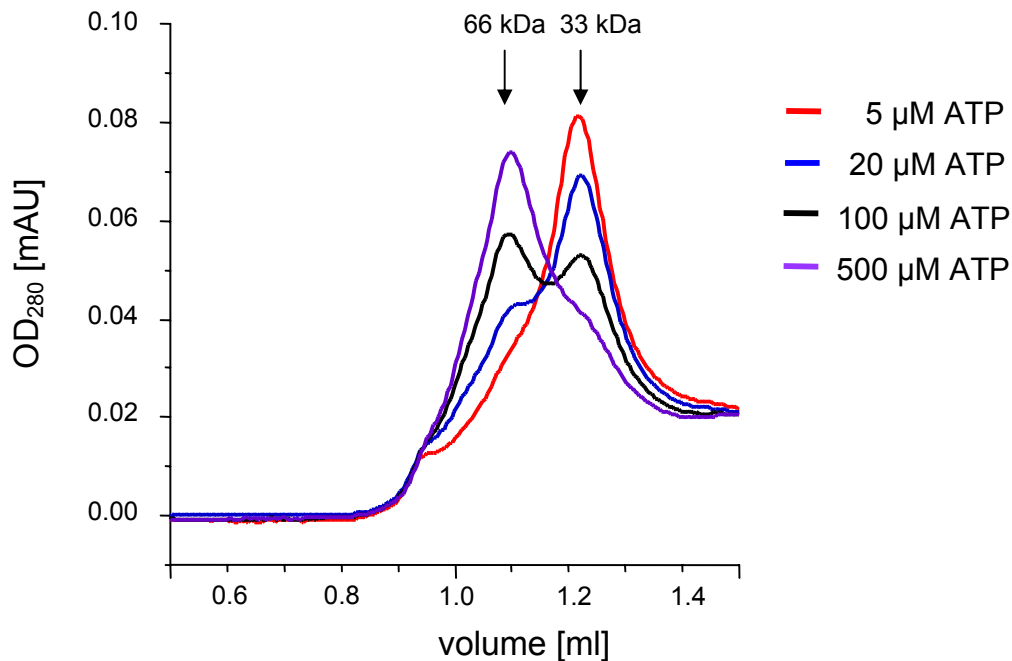


Fig.15: Dimerization of E599Q mutant NBD is dependent on ATP concentration.

After preincubation of the E599Q mutant (30 μM) with increasing concentrations of ATP (0 to 500 μM) for 10 min on ice, an ATP-dependent dimerization was observed by gel filtration (Superdex 75).

5.1.5 Nucleotide composition of the dimer

To analyse the ATP/ADP composition of the nucleotide-induced dimer, wild type NBD was incubated with tracer concentration of [α ³²P]-ATP under hydrolysis conditions in the presence of BeF_x and applied to gel filtration. Radioactive nucleotides exclusively co-eluted with the NBD dimer, whereas no radioactivity was observed in fractions corresponding to the monomer (Fig.16,A). The concentration of [α ³²P]-ATP bound per NBD dimer was determined and a stoichiometry of two nucleotides per dimer was obtained (Fig.16,C). The same experiment was repeated in the presence of [γ ³²P]-ATP. Strikingly, only a minor amount of radioactivity was co-eluted with the dimer compared to the radioactivity obtained from [α ³²P]-ATP trapping experiment. This result clearly demonstrates that both ATP molecules have been hydrolysed by the dimer and inorganic phosphate has been released from the complex. TLC analysis of nucleotides extracted from the dimer confirmed these data (Fig.16,D).

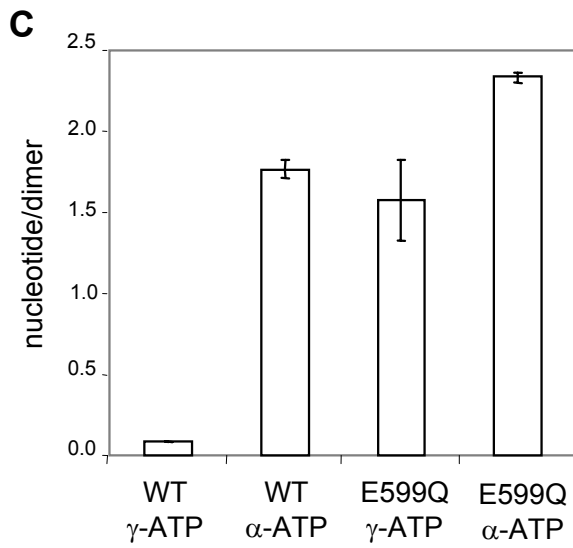
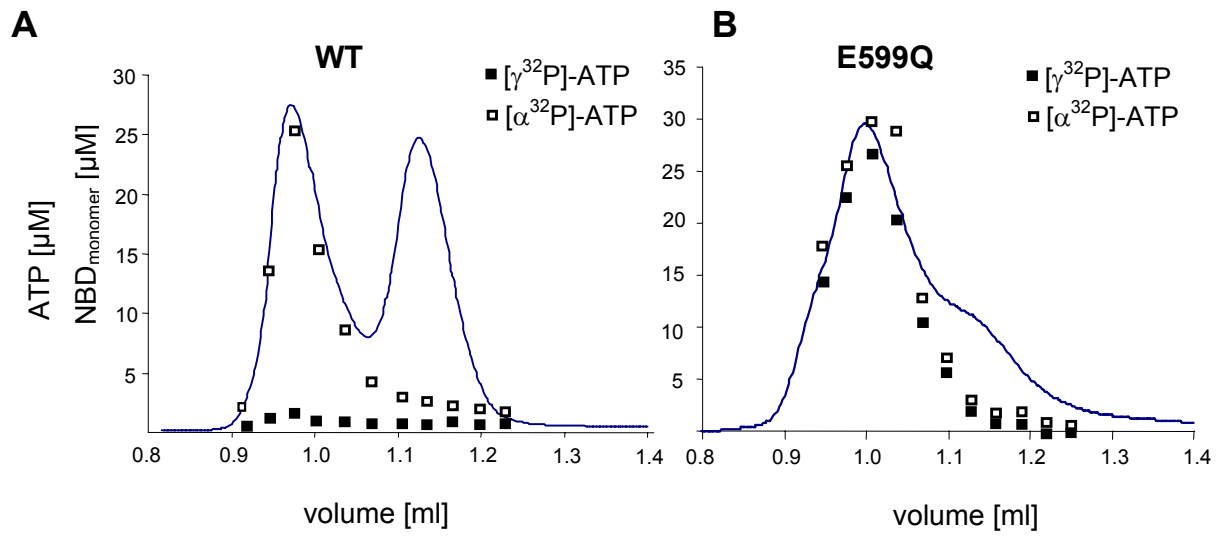
After incubation of the E599Q mutant either with [$\alpha^{32}\text{P}$]-ATP or [$\gamma^{32}\text{P}$]-ATP, radioactivity was exclusively associated with the dimer. Again, no radioactivity was observed in fractions corresponding to the monomer. The mutant dimer always contained two nucleotide molecules. When the experiment was performed under non-hydrolysis condition (absence of Mg^{2+} and on ice) the amount of [$\alpha^{32}\text{P}$]-ATP and [$\gamma^{32}\text{P}$]-ATP bound per dimer was equal, and a stoichiometry of two ATP molecules bound per dimer was obtained (Fig.16,B). This suggested that either ATP was not hydrolysed or that ATP was hydrolysed to ADP but the [$\gamma^{32}\text{P}$]_i was still associated with the complex. To distinguish between the two possibilities, TLC analysis was performed. TLC analysis demonstrated that ATP hydrolysis did not occur under this condition and obviously two ATP molecules were incorporated in the dimer (Fig.16,D).

Incubation of the E599Q mutant under conditions which promote hydrolysis showed slow formation of ADP (Fig.16,D). After preincubation with MgATP for several hours at 30°C the analysis of E599Q dimer by gelfiltration and TLC showed that one ATP was hydrolysed, and a stable ATP/ADP ratio of 1 was achieved (data not shown, personal communication M. Hofacker). Prolongation of the incubation time did not result in two ADP molecules bound in the dimer. This suggests that the mutant dimer is not stable after hydrolysis of the second nucleotide. Prolonged incubation time resulted in an increased formation of monomer which did not contain any nucleotide.

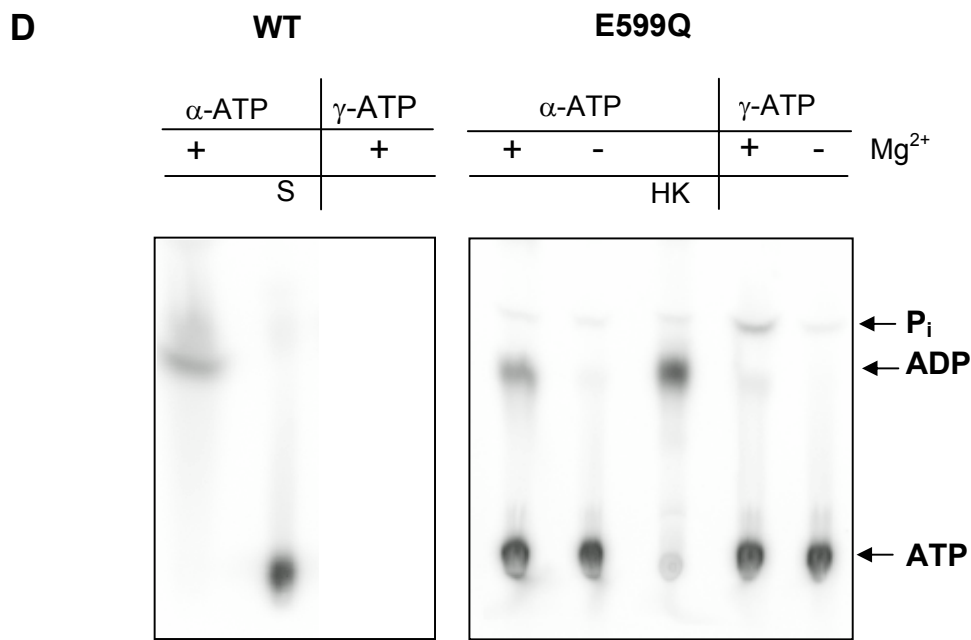
After formation of the ATP-containing dimer no nucleotides could be incorporated into the dimer from the medium (Fig.16,E).

As already mentioned, incubation of the E599Q mutant with non-hydrolysable ATP analogues did not induce a dimer formation. But incubation of the mutant at 30°C with equimolar ratio of unlabelled MgATP and MgATP $\gamma^{35}\text{S}$ resulted in incorporation of radioactivity into the dimer. It was determined that one ATP $\gamma^{35}\text{S}$ molecule was incorporated into a dimer. Surprisingly, incubation of the wild type NBD with equimolar ratio of unlabelled MgATP and MgATP $\gamma^{35}\text{S}$ under hydrolysis conditions in the presence of BeF_x did not result in incorporation of radioactivity, suggesting that for stabilization of the wild type dimer by the ATPase inhibitor both nucleotides have to be hydrolysed.

Results



[mol/mol]	wt	E599Q
γ -ATP	0.074	1.69 +/- 0.5
α -ATP	1.76 +/- 0.06	2.48 +/- 0.3



E

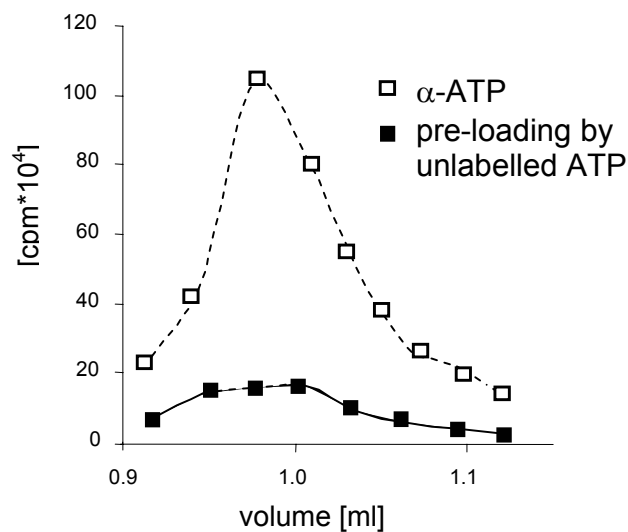


Fig.16: Determination of the nucleotide composition of trapped NBD dimers.

A: Wt NBD (30 μ M) was incubated with MgATP (625 μ M) supplemented with either [α ³²P]-ATP or [γ ³²P]-ATP (0.125 μ M) under **hydrolysis** conditions in the presence of 500 μ M BeF_x and analysed by gelfiltration. The fractions were analysed by β -counting.

B: Mutant E599Q NBD (30 μ M) was incubated with ATP (625 μ M) supplemented with [α ³²P]-ATP or [γ ³²P]-ATP (0.125 μ M) under **non-hydrolysis** conditions and was analysed by gelfiltration and β -counting.

C: Evaluation of the gelfiltration data of panel. A and B. The stoichiometry of bound radioactive nucleotide (mol) per dimer (mol) of BeF_x trapped wt dimer and of ATP-induced E599Q dimer under non-hydrolysis conditions was summarized. In the wt NBD 2 ADP molecules were obtained in the dimer. In the E599Q mutant 2 ATP molecules were preserved in the dimer under non-hydrolysis condition.

D: Wt NBD was incubated with [α ³²P]-ATP or [γ ³²P]-ATP under trapping conditions in the presence of 500 μ M BeF_x and analysed by gelfiltration. After precipitation of protein nucleotides were analysed by TLC. Exclusively ADP was found in the wt dimer. Mutant E599Q NBD was incubated with radiolabelled [α ³²P]-ATP or [γ ³²P]-ATP under non-

Results

hydrolysis and hydrolysis conditions and was analysed as described above. In the absence of Mg^{2+} exclusively ATP molecules were incorporated into the mutant dimer. After preincubation of the mutant at 30°C for 15 min in the presence of Mg^{2+} , ADP together with ATP was observed in the dimer.

S: standard, non treated ATP; HK: ATP preincubated with hexokinase

E: The stability of the E599Q dimer was investigated by preloading the dimer with unlabelled ATP (625 μ M) for 10 min on ice and subsequent incubation with [α - 32 P]-ATP (0.125 μ M) for additional 10 min. The analysis by gelfiltration and β -counting showed that no incorporation of radioactivity into the dimer was observed.

5.1.6 ATP hydrolysis cycle of Mdl1p-NBD

Based on the results obtained from the characterisation of different NBD dimers the following reaction cycle of ATPase hydrolysis for the Mdl1p-NBD can be proposed (Fig.17). ATP binding to both NBDs induces formation of the dimer. After hydrolysis of both ATP molecules to ADP, the dimeric complex dissociates and ADP is released. Our data from both the BeF_x trapped wild type NBD and the E599Q mutant suggest that during ATP hydrolysis at least three different states can be trapped. In one state, both nucleotides are bound as triphosphates as shown for the mutant dimer under non-hydrolysis condition. In the subsequent state, one ATP together with one ADP molecule is trapped in the mutant dimer at the same time after prolonged incubation at hydrolysis conditions. After slow hydrolysis of the second ATP the mutant dimer dissociates. For the wild type dimer a BeF_x trapped dimer state is obtained in which two ADP molecules are incorporated at the same time.

As an asymmetrically loaded state of ATP/ADP dimer for the E599Q mutant was obtained, this experiment strongly indicates that hydrolysis of the ATP molecules is sequential and that hydrolysis of the second ATP results in dissociation of the dimer.

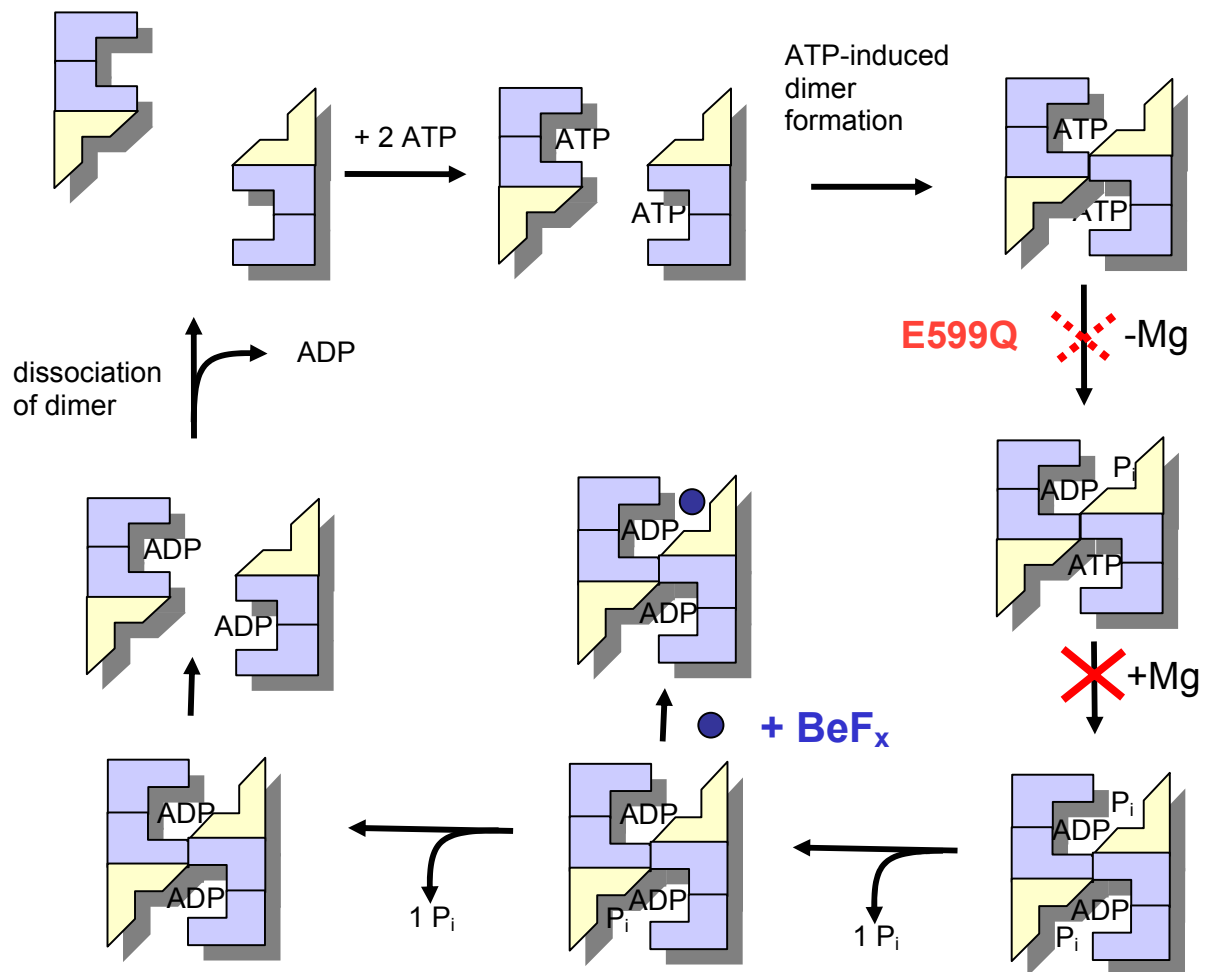


Fig.17: ATPase cycle proposed for Mdl1p-NBD (for details see text).

5.1.7 Expression and purification of full-length Mdl1p

As we obtained very detailed information about the interaction of isolated NBDs during the ATPase cycle, we set out to characterise the inter-domain communication of the full-length ABC transporter Mdl1p. So far, Mdl1p has been identified as a peptide export pump of the inner mitochondrial membrane of *S. cerevisiae*, but no detailed information is provided for the transport mechanism and substrate spectrum of this peptide transporter. To address these questions, the approach was undertaken to overexpress this membrane protein in *S. cerevisiae* or *E. coli*. Purification of Mdl1p would enable us to investigate the transport function *in vitro* after reconstitution of Mdl1p into lipid vesicles.

For purification Mdl1p was isolated from W303-1A mitochondria. The strain was grown on lactate medium at 30°C to mid-logarithmic phase (OD₆₀₀ about 1). As a control, mitochondria were also isolated from the Δ *mdl1* strain. Fig.18 shows a Western blot analysis of wild type mitochondria. A specific band of 62 kDa, which is not expressed in the Δ *mdl1* strain, was detected by the polyclonal α -Mdl1, which is directed against the C-terminal 15 amino acids.

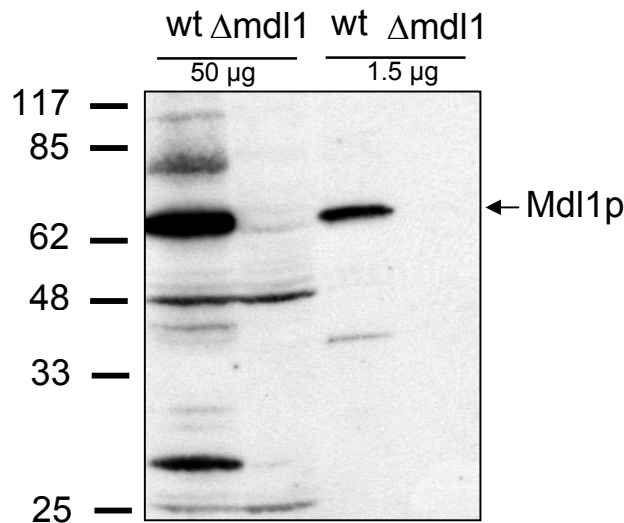


Fig.18: Mitochondria isolated from W303-1A strain and Δ *mdl1* strain. 50 μ g or 1.5 μ g protein of mitochondria was loaded onto a 12% SDS-PAGE and immunostained with α -Mdl1.

As ABC transporters bind nucleotides, it is very convenient to purify Mdl1p by this kind of affinity chromatography. Mitochondria from wild type cells were solubilized with 1.4% decylmaltoside (30 mM) and applied to an ATP-agarose resin (Fig.19). The solubilization efficiency of Mdl1p by DM was only 50%. As a result, Mdl1p could not be purified by this approach since solubilized Mdl1p was unable to bind to different types of ATP-agarose such as C8-, N6- and ribose-coupled ATP.

Alternatively, reactive Red-agarose was used for affinity purification. Most of the detergent solubilized Mdl1p could be bound to the resin, but not specifically eluted either by 5 mM ATP or by NaCl gradient of 300 to 900 mM. It was shown that Mdl1p was absorbed unspecifically to the resin (Fig.20). It is possible that the decrease of the detergent concentration to 0.114% DM (2.4 mM), which is close by the CMC (1.6 mM), in the washing buffer caused precipitation of Mdl1p at the resin.

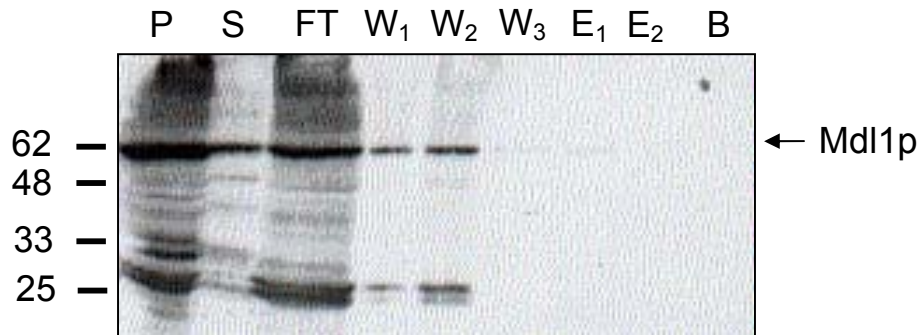


Fig.19: Purification of Mdl1p by ATP-agarose.

Mitochondria were solubilized by 30 mM DM for 30 min on ice, after ultracentrifugation applied to ATP-agarose, washed with detergent buffer (2.4 mM DM) and eluted with 5 mM MgATP. Beads were incubated with loading buffer for 10 min at 65°C. The fractions were analysed by SDS-PAGE and immunoblotting using α -Mdl1.

P: pellet after solubilization, S: solubilized mitochondria, FT: flow through, W_n : wash steps, E_n : elution with 5 mM MgATP, B: ATP-agarose beads

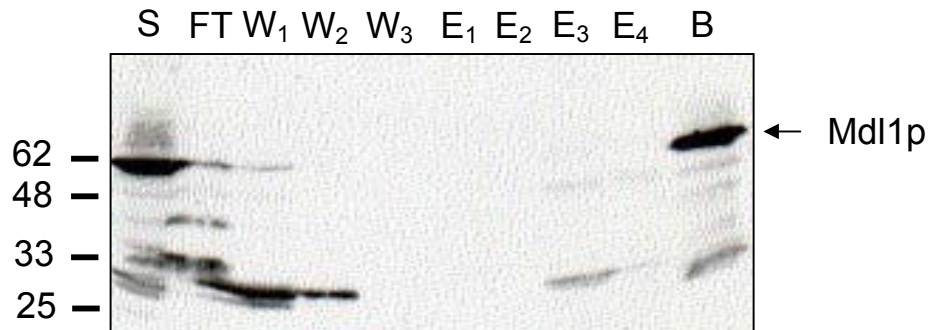


Fig.20: Purification of Mdl1p by reactive Red-agarose.

The samples were treated as described by Fig.19.

S: solubilized mitochondria, FT: flow through, W_n : wash steps, E_n : elution with 5 mM MgATP and NaCl gradient (300-900 mM), B: Red-agarose beads

5.1.8 Reconstitution of Mdl1p

Based on the reconstitution protocol established for the TAP complex (Gorbulev *et al.*, 2001), Mdl1p solubilized from mitochondria was partially enriched by gelfiltration column Superose 6 PC 3.2/30 (Fig.21,A). The obtained fractions were analysed by immunoblotting (Fig.21,B). Solubilized Mdl1p did not aggregate since no Mdl1p was found in the void volumen of the column. Fractions containing Mdl1p were incubated with liposomes (23% cholesterol, 10 % phosphatidic acid, 67% phosphatidylcholine) and reconstitution was performed by rapid removal of detergent by biobeads. By this approach, the proteoliposomes did not incorporate Mdl1p and did not show radioactive peptide uptake.

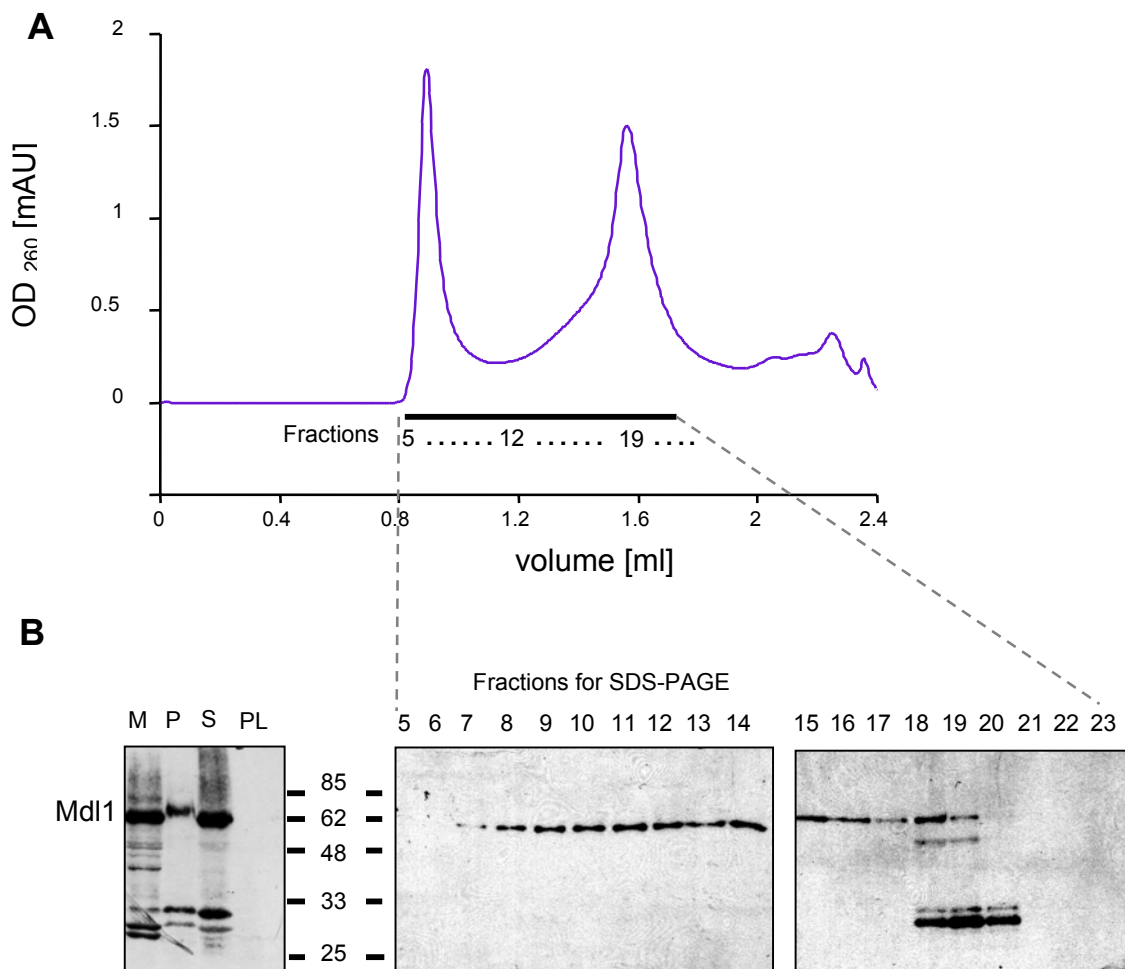


Fig.21: Reconstitution of Mdl1p enriched by gelfiltration.

A: 100 µg mitochondria (10 µg/µl) were solubilized with 30 mM DM for 30 min on ice, centrifuged 20.000 x g for 15 min and applied to a gelfiltration column (Superose 6 PC 3.2/30) containing 2.4 mM DM in the mobile phase. Fractionation was started at 460 µl with a fractionation size of 60 µl.

B: Elution fractions were analysed by SDS-PAGE and immunostaining with α-Mdl1. Fractions containing Mdl1p (9-16) were incubated with preformed liposomes (23% cholesterol, 10% phosphatidic acid, 67% phosphatidylcholine) and reconstituted by rapid removal of detergent with biobeads.

M: mitochondria P: pellet after solubilization S: solubilized mitochondria (load on the column) PL: proteoliposomes

In order to apply higher concentrations of Mdl1p during the reconstitution procedure, DM - solubilized mitochondria were directly incubated with rhodamine-labelled (0.4%) liposomes of the composition described above and reconstituted by rapid removal of detergent using biobeads. The proteoliposomes were floated in a sucrose gradient from 20 to 50% (w/v). According to their density, sealed proteoliposomes migrated in the sucrose gradient from the bottom to 20-25% sucrose monitored by the absorbance of rhodamine-labelled lipids (Fig.22). Liposomes without incorporated proteins floated to the top of the sucrose gradient. A strong absorbance derived from rhodamine-labelled lipids was observed at the top of the gradient. As shown by Western blot analysis the proteoliposomes enriched at 25-30% sucrose contained incorporated Mdl1p.

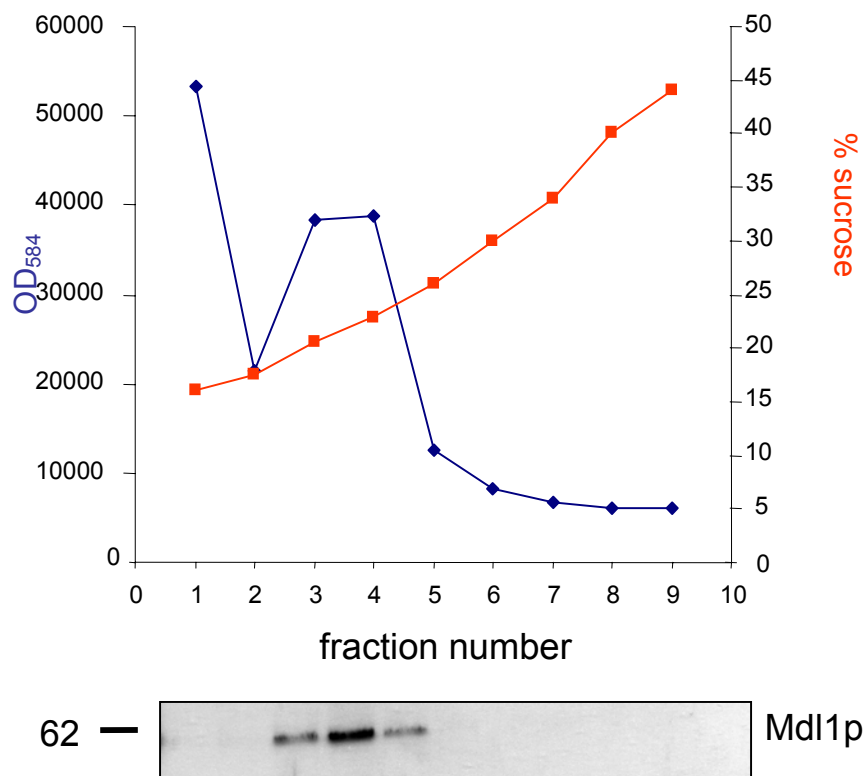


Fig.22: Reconstitution of Mdl1p from solubilized mitochondria.

DM-solubilized mitochondria were incubated with rhodamine-labelled liposomes and reconstituted by rapid removal of detergent with biobeads. Proteoliposomes were floated in a sucrose gradient (134.000 x g, 12 h) from 20 to 50% and fractions were checked by absorbance 584 nm (for rhodamine), refractory index, SDS-PAGE and immunostaining with Mdl1p antisera.

The proteoliposomes were tested for radioactive peptide uptake using the peptides R9LQK or R10T. However, no transport activity could be detected. One explanation could be that other proteins like porins, which could release imported peptides, were incorporated in the liposomes as well (Mannella, 1992).

Results

Furthermore, it is also conceivable that the lipid composition of 23% cholesterol, 10% phosphatidic acid, and 67% phosphatidylcholine was not suitable for the activity of a yeast mitochondrial protein like Mdl1p. Cholesterol has been reported to be inhibitory on the transport of reconstituted ATP/ADP carrier from mitochondria (Heimpel *et al.*, 2001). In further experiments cardiolipin (CL), a characteristic phospholipid of the inner mitochondrial membrane in eukaryotic cells, was used. The lipid composition was changed to 75% phosphatidylcholine, 20% phosphatidylethanolamine and 5% cardiolipin.

To obtain proteoliposomes without porins, mitoplasts were generated from mitochondria by osmotic swelling (Fig.23). Mitoplasts are mitochondria from which the outer membrane has been removed. The generated mitoplasts were applied to a sucrose gradient of 30 to 50% (w/v). Fractions with highly enriched Mdl1p corresponding to the inner membrane were harvested from the 36.5% to 37.5% sucrose interphase. A high concentration of Mdl1p in these fractions could be observed by the Western blot analysis. The enriched inner membranes were used for reconstitution into liposomes which were destabilized by preincubation with 1.6% (55 mM) octylglucoside for 3 h before use. Detergent-mediated destabilization of liposomes was reported to enhance incorporation of membrane proteins. After reconstitution and removal of detergents by biobeads the proteoliposomes were floated in a sucrose gradient from 10% to 40%. After sucrose gradient centrifugation a high amount of Mdl1p was detected in the proteoliposomes by SDS-PAGE and immunostaining. However, the proteoliposomes were not active in transport activity using the peptides R9LQK and R10T. Western blot analysis showed the presence of porins, demonstrating that inner membrane preparation was still contaminated by proteins of the outer mitochondrial membrane. The existence of contact sites between outer and inner membrane makes it very difficult to separate both membranes. The presence of porins, through which solutes of the size of 6 kDa can diffuse, might be the reason for release of imported peptides back to the medium. It is also conceivable that the peptides used are not a suitable substrate for Mdl1p.

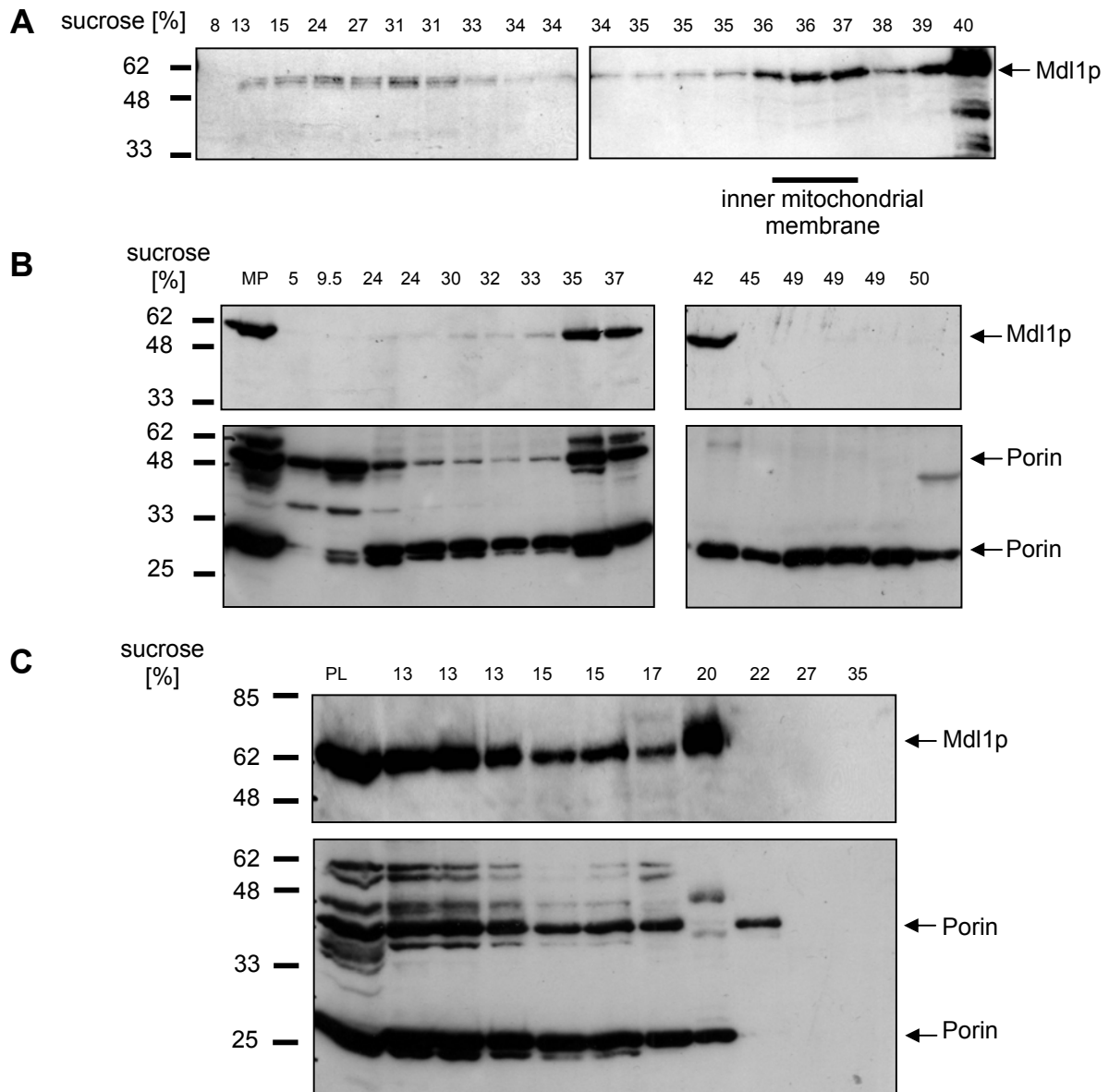


Fig.23: Mitoplasts preparation and reconstitution of Mdl1p from mitoplasts.

A: Mitoplasts were generated from mitochondria (1 mg) by osmotic swelling diluting the mitochondria in 5-fold volume for 30 min on ice. The suspension was applied to a sucrose gradient of 30 to 50% (134.000 x g, 12 h). 500 µl fractions were checked by refractory index, and subsequently TCA-precipitated, analysed by SDS-PAGE and immunoblotting with α -Mdl1.

B: Inner membranes were prepared as described above and isolated from the sucrose fractions corresponding to 35 to 42%. Fractions were checked by refractory index, SDS-PAGE and immunostaining with Mdl1p and porin antisera. MP: mitoplasts

C: Inner membranes were 10-times diluted to decrease the sucrose concentration and centrifuged (227.000 x g, 45 min). The pellet was solubilized (30 mM DM) for 30 min on ice, centrifuged (15 min, 22.000 x g) and the supernatant was incubated with preformed and octylglycoside-destabilized (55 mM) liposomes (75% phosphatidylcholine, 20% phosphatidylethanolamine, 5% cardiolipin) and reconstituted by rapid removal of detergent with biobeads. Proteoliposomes were floated in a sucrose gradient from 40 to 10% (134.000 x g, 12 h). Fractions were checked by refractory index, SDS-PAGE and immunostaining with Mdl1 and porin antisera. PL: proteoliposomes

5.1.9 Specific ATP binding of Mdl1p

In order to exclude that solubilization and subsequent reconstitution inactivate Mdl1p, ATP binding of wild type Mdl1p was investigated by 8-azido- $[\alpha^{32}\text{P}]$ -ATP photocrosslinking and subsequent immunoprecipitation (Fig.24). 8-Azido- $[\alpha^{32}\text{P}]$ -ATP was crosslinked to both DM-solubilized and reconstituted Mdl1p. The binding was competed by an excess of unlabelled nucleotides. To obtain signals of ATP binding based on Mdl1p, specificity was achieved by immunoprecipitation of ATP-crosslinked protein with α -Mdl1. Solubilized mitochondria derived from $\Delta md11$ strain did not show an ATP-crosslinking signal.

In order to investigate the orientation of reconstituted Mdl1p, proteoliposomes were crosslinked either directly or after solubilization by Triton X-100. Both signals showed the same intensity, suggesting that Mdl1p is predominantly reconstituted with its NBDs facing the outside of the liposomes. But it cannot be excluded that ATP molecules could diffuse through porins into the liposomes causing crosslinking.

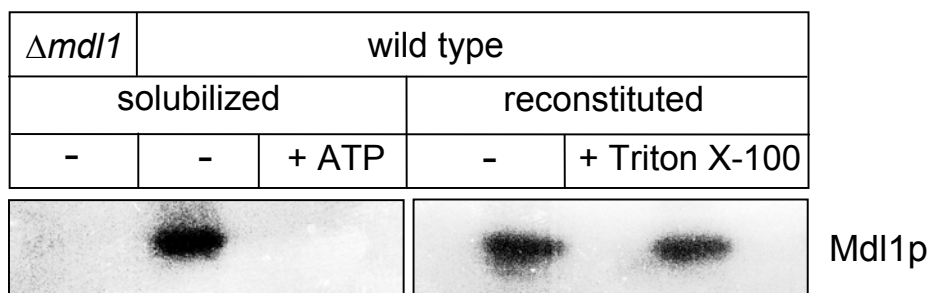


Fig.24: Photocrosslinking of Mdl1p.

DM-solubilized or reconstituted Mdl1p was incubated with 8-azido- $[\alpha^{32}\text{P}]$ -ATP (2 μM) in the presence or absence of 1.5 mM MgATP for 5 min on ice and photocrosslinked with UV (254 nm) for 5 min. Proteoliposomes solubilized by Triton X-100 (1%) were used as control. The samples were 5-times diluted in solubilization buffer and immunoprecipitated with α -Mdl1 (1:100) and protein A sepharose. After SDS-PAGE the gel was dried and analysed by autoradiography (2 weeks exposure at -80°C).

In summary, Mdl1p from wild type mitochondria was successfully reconstituted into proteoliposomes. The lipid composition of liposomes was adapted to a reconstitution of a mitochondrial membrane protein. The reconstitution procedure did not impair the ATP binding activity of Mdl1p. However, positive peptide transport activity could not be obtained. One possible explanation could be a contamination of the proteoliposomes by porins of the outer membrane. Therefore, the next approach was to introduce an affinity tag to Mdl1p in order to facilitate purification and subsequent reconstitution.

5.1.10 Expression, purification and activity of recombinant Mdl1p

In order to express higher amounts of Mdl1p in yeast, the *MDL1* gene was cloned into the high copy plasmid p426 under the control of the strong and constitutive GPD promotor. The *MDL1* gene deleted in its N-terminal mitochondrial targeting sequence was cloned into the same expression vector. To facilitate purification, plasmid-encoded Mdl1p was fused with a StrepII-tag at its C-terminus. The $\Delta mdl1$ strain was transformed with the recombinant plasmid and positive transformants were selected on drop out media for uracil and checked by colony-PCR (Fig.25). Yeast cells were grown at 30°C in minimal media and mitochondria were isolated. Western blot analysis showed considerable degradation of overexpressed Mdl1p and no protein band of the proper size was detected (Fig.25,A). In order to avoid degradation, the growth temperature was decreased to 25°C. As shown in Fig.25,B a 10-50 fold overexpression of Mdl1p was achieved from plasmid-encoded gene compared to the chromosomal gene.

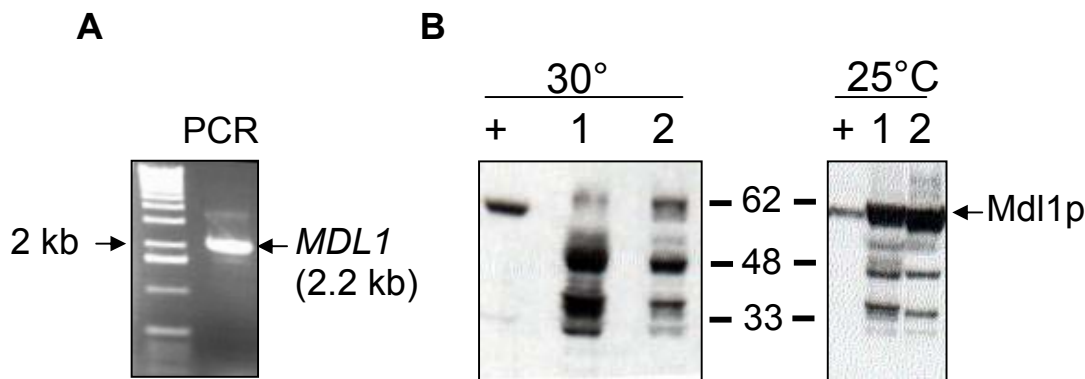


Fig.25: Transformation and homologous expression of Mdl1p.

A: Colony-PCR was performed with $\Delta mdl1$ strain transformed with p426-mdl1-StrepII. Fresh colonies selected on drop out agar plates (without uracil) were lysed by lyticase and used as template for *MDL1* specific PCR with the primers formdl1fl and revmdl1 (see 4.1.5 for PCR conditions).

B: Yeast cells were grown in minimal media at 30°C and at 25°C, respectively. 10 μ g mitochondria of wt cells (+), p426-mdl1-StrepII (1) and p426- Δ mt-mdl1-StrepII (2) were analysed by 12% SDS-PAGE and immunostained with α -Mdl1.

After overexpression of the recombinant Mdl1p in yeast, mitochondria were detergent solubilized by 30 mM DM (1.4%). Again, the solubilization efficiency was only 50%. The supernatant was applied to Streptactin-beads and washed with detergent buffer (1.6 mM DM). A part of detergent solubilized Mdl1p was obtained in the flow through and first wash step. Mdl1p which bound to Streptactin-beads could not be specifically eluted by 2.5 mM desthiobiotin, suggesting that Mdl1p was adsorbed unspecifically to the resin (Fig.26). One explanation for this observation could be that the decrease of the detergent concentration to 1.6 mM DM in the washing buffer caused precipitation of Mdl1p. To ensure the integrity of the tag, the blot was

Results

incubated with a polyclonal α -Strep-tag. The Western blot analysis showed that a polyclonal antibody is not suitable to detect Strep-tagged proteins from yeast extracts because of its high cross-reactivity.

Next, the functionality of Strep-tagged Mdl1p was investigated with respect to ATP binding using 8-azido- $[\alpha^{32}\text{P}]$ -ATP photocrosslinking experiments as shown before. 8-Azido- $[\alpha^{32}\text{P}]$ -ATP was crosslinked to solubilized Mdl1p and could be specifically competed by an excess of unlabelled nucleotide. The ATP-crosslinking of the overexpressed Mdl1p was much more efficient than of the wild-type due to the higher expression levels (data not shown).

In conclusion, the homologous overexpression of Mdl1p was achieved, the protein was active with respect to ATP binding, but purification based on the introduced Strep-tag at the C-terminus could not be established.

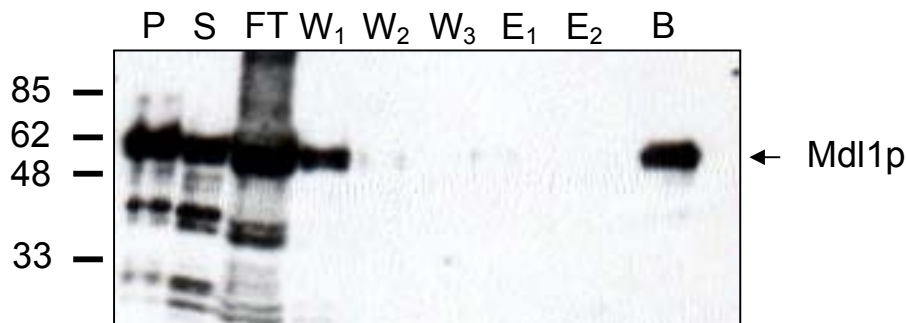


Fig.26: Purification of Mdl1p encoded by p426-mdl1-StrepII.

Yeast cells transformed by p426-mdl1-StrepII were grown at 25°C. Isolated mitochondria were detergent solubilized (30 mM DM) and after ultracentrifugation applied to Streptactin-beads. After washing with detergent buffer (1.6 mM DM), protein was eluted with 2.5 mM desthiobiotin. Beads were incubated with loading buffer for 10 min at 65°C. The fractions were analysed by 12% SDS-PAGE and immunostaining by α -Mdl1.

P: pellet after solubilization, S: solubilized mitochondria, FT: flow through, W_n: wash steps, E_n: elution steps, B: beads

5.1.11 Deletion of mitochondrial targeting sequence (MTS)

Mdl1p has been identified as an export pump translocating peptides from the matrix to the intermembrane space of mitochondria (Young *et al.*, 2001). It is very difficult to investigate efflux pumps like Mdl1p because substrates have to be transferred into the mitochondria before starting the experiment. The strategy followed here was to convert the exporter into an importer by changing the subcellular localisation of Mdl1p to another compartment like ER or plasma membrane.

Most mitochondrial proteins like Mdl1p are encoded in the nucleus and posttranslationally imported into the mitochondria. Mitochondrial targeting is often mediated by an N-terminal leader

sequence (Neupert, 1997). The import signal peptide usually consists of 20 to 35 residues at the N-terminus and is highly degenerated in primary sequence, but rich in basic, hydrophobic and hydroxylated residues and generally lacks acidic ones (Fig.27) (Schatz and Dobberstein, 1996). It was suggested that due to the distribution of charged and apolar residues the leader peptide can fold into a defined secondary structure which is essential for import. The N-terminal part of the targeting sequence forms a positively charged amphiphilic α -helix or β -sheet, whereas the C-terminal part probably serves as a recognition site for matrix proteases (von Heijne, 1986). In particular, arginine is enriched in positions -2, -3, -10, -11. Especially, the arginine at -2 seems to be part of a recognition signal for the major matrix protease (MPP) (Gavel and von Heijne, 1990). One of the proposed motifs seems to be conserved in Mdl1p (R-2 group: RXXS), in which the cleavage occurs between the two undefined residues. Therefore, a 59 amino acids truncated version of Mdl1p was created disrupting the RXXS site. For correct translation initiation an additional methionine was introduced at the new defined start position +60.

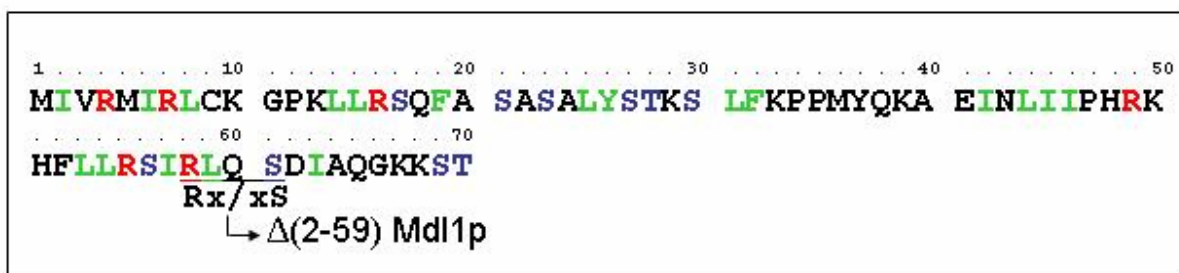


Fig.27: The N-terminal sequence of Mdl1p contains a classical mitochondrial targeting sequence (MTS).

The classical MTS is rich in Arg (red) as positive charged amino acid, Ser (blue) as hydroxylated amino acid, Leu, Phe, Tyr (green) as hydrophobic amino acids. Underlined sequence represents one of the potential recognition sites (Rx/xS) for mitochondrial proteases which cleave the MTS after import of the protein into the matrix.

x: not defined amino acid, /: cleavage site of protease

To investigate whether the truncation of the N-terminal 59 amino acids indeed influences the targeting of Mdl1p, the *MDL1* gene and the truncated version were cloned into the plasmid p426. The $\Delta mdl1$ strain was transformed with the recombinant plasmids, respectively. Mitochondria were prepared from the different yeast strains grown at 25°C. Using the standard isolation method of mitochondria by differential centrifugation (Daum *et al.*, 1982), contamination of mitochondria with ER cannot be excluded. Therefore, mitochondria devoid of microsomal contaminations should be purified by sucrose gradient method (Meisinger *et al.*, 2000). Comparison of the mitochondria prepared by the two different methods showed that the mitochondria isolated by differential centrifugation are only slightly more contaminated with ER

Results

compared to mitochondria purified by sucrose gradient. Contamination with ER membranes was assayed by detection of the ER resident Sec61 protein using Western blot analysis. Surprisingly, the truncated Mdl1p was still targeted exclusively to the mitochondria (Fig.28,A). No difference between the distribution of full-length Mdl1p and truncated Mdl1p was observed. Loading crude mitochondria onto a sucrose gradient and analysis of the fractions by Western blot showed the same protein pattern for full-length as well as truncated Mdl1p (Fig.28,B).

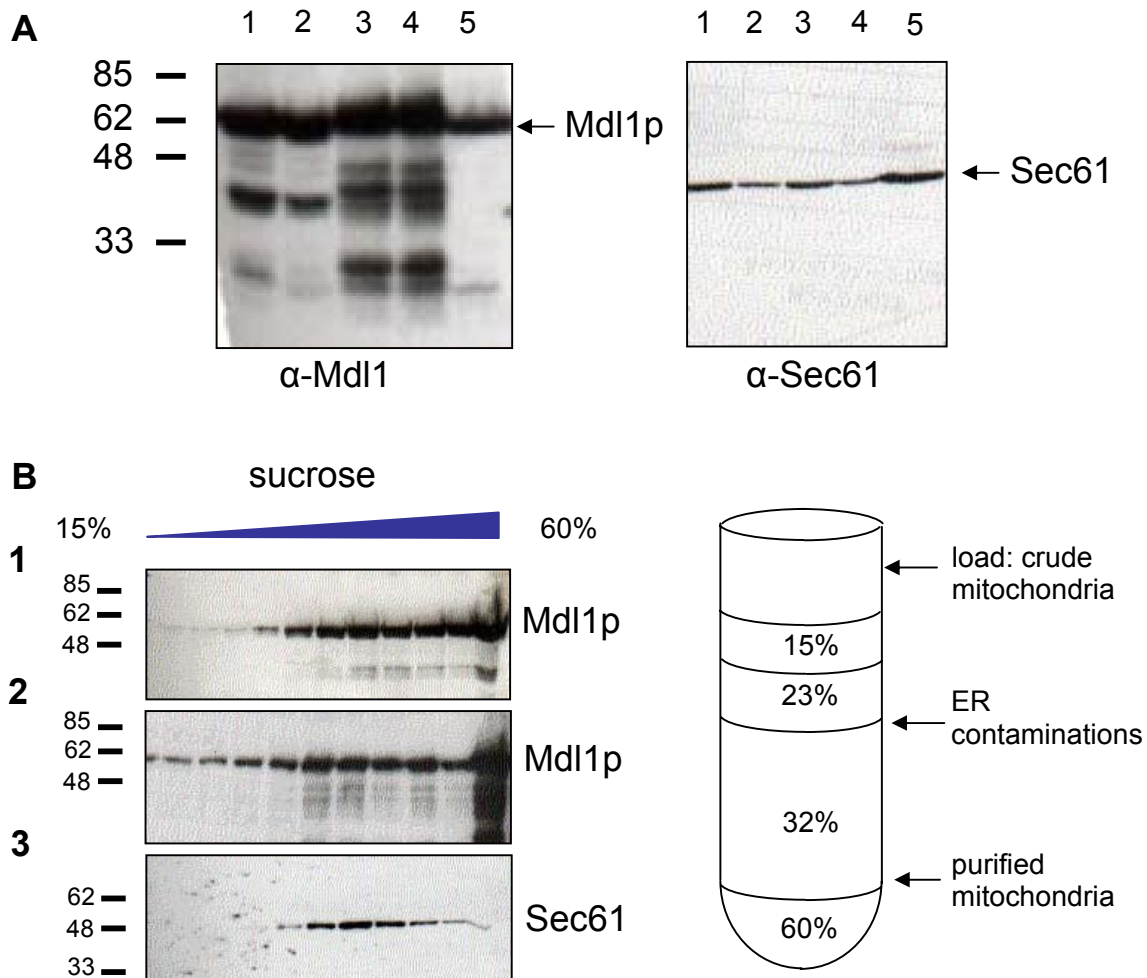


Fig.28: Influence of the deletion of the MTS for Mdl1p targeting.

A: Transformed yeast cells were grown on minimal medium at 25°C. Mitochondria derived from p426-mdl1 transformed cells were isolated either by differential (1) or by sucrose gradient (2) centrifugation. Mitochondria derived from p426- Δ mt-mdl1 were isolated by the two different methods, respectively (3) (4). For control, mitochondria of wt cells were prepared by differential centrifugation (5). The fractions were analysed by 12% SDS-PAGE and immunostaining with α -Mdl1 or α -Sec61.

B: Mitochondria derived from yeast transformed by p426-mdl1 (1) or p426- Δ mt-mdl1 (2, 3) were separated in a sucrose gradient. TCA-precipitated fractions were analysed by 12% SDS-PAGE and immunostaining with α -Mdl1 or α -Sec61.

The subcellular localisation of Mdl1p was further investigated by partial digitonin-mediated solubilization of mitochondria followed by proteinase K digestion (Klanner *et al.*, 2001; Segui-Real *et al.*, 1993). Mitochondria are organelles which are protected by an outer and inner membrane. In the presence of low digitonin concentration, only the outer membrane is solubilized. Therefore, matrix-resident proteins and regions of polytopic membrane proteins (e.g. the epitope for α -Mdl1) are protected from proteinase K digestion. After total detergent solubilization of both membranes the matrix-located proteins are degraded by proteinase K as well.

The proteinase K protection assay showed the same degradation pattern for full-length as well as truncated Mdl1p (Fig.29). This is a strong indication that both proteins are localised in the same organelle and shared the same topology. The epitope of the α -Sec61 is exposed to the cytosol. As a control, the ER resident protein Sec61 was readily degraded in the absence of detergent. If Mdl1p deleted in its classical mitochondrial leader sequence would have been directed to the ER, the epitope would be exposed to the cytosol and would become degraded by proteinase K already in the absence of a detergent.

In summary, the truncation of the N-terminal 59 amino acids did not impair the targeting of Mdl1p to the mitochondria. This suggests that an additional internal targeting sequence is present as shown previously for other inner mitochondrial membrane proteins e.g. ATP/ADP carrier and oxoglutarate carrier (Luciano *et al.*, 2001; Wiedemann *et al.*, 2001; Endres *et al.*, 1999; Kurz *et al.*, 1999; Kubrich *et al.*, 1998; Palmisano *et al.*, 1998). The sequence of the internal signal peptide has not been defined so far. The simultaneous presence of a classical N-terminal sequence and an internal targeting sequence in one protein has not been described, so far.

Results

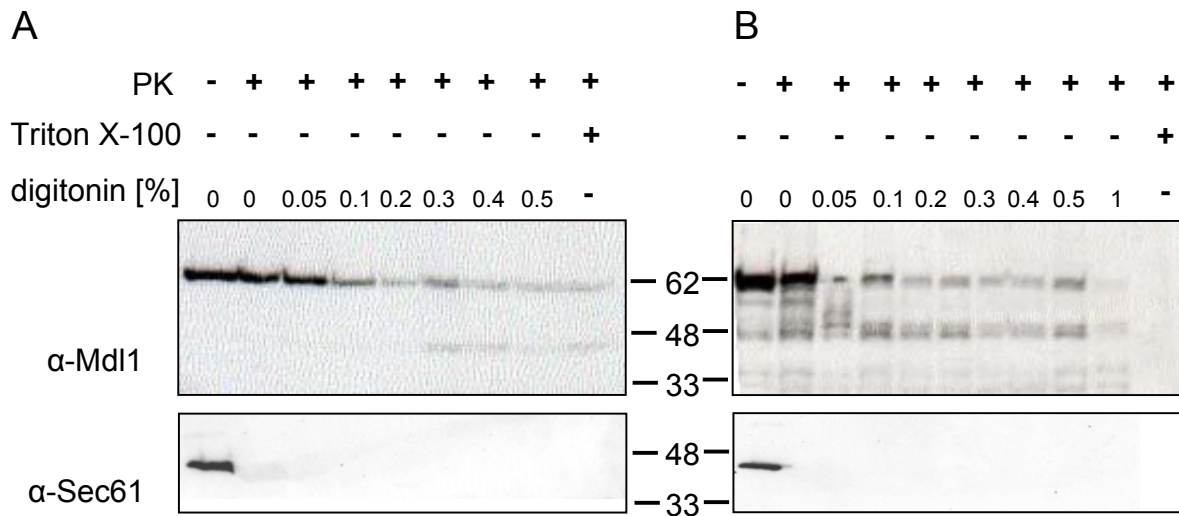


Fig.29: Digitonin-mediated fractionation of mitochondria and proteinase K digestion.

Mitochondria from yeast transformed with p426-mdl1 (A) or p426- Δ mt-mdl1 (B) were incubated in the presence of increasing concentrations of digitonin or Triton X-100 (0.17%) as indicated and the accessibility of Mdl1p to proteinase K (0.1 μ g/ μ l) was examined. TCA-precipitated fractions were analysed by SDS-PAGE and immunostaining with α -Mdl1p and α -Sec61.

5.1.12 Expression and purification of His-tagged Mdl1p

Mdl1p truncated in its N-terminal 59 amino acids was subcloned from pBAD-mdl1-mt into the low copy plasmid pXY113 under the control of the strong inducible GAL promotor. The Mdl1p construct contained an N-terminal hexa-histidine tag. Δ mdl1 strain was transformed with the plasmid and positive transformants were selected on drop out media for uracil and by colony-PCR. The yeast cells were grown at 30°C in minimal medium with glucose (2%) to OD 0.8, washed and resuspended in minimal medium containing galactose (2%). Cells were harvested after 24 h induction.

Mitochondria were detergent-solubilized (1% Triton X-100) and applied to Ni-NTA-beads (Fig.30). The beads were washed with detergent buffer (1% Triton X-100) containing 0, 10, 20, 40 mM imidazole and protein was eluted with 250 mM imidazole. As shown by Western analysis the solubilization by Triton X-100 worked very efficiently. A part of detergent-solubilized Mdl1p was detected in the flow through and first wash step (0 mM imidazole) and a truncated version of Mdl1p was already eluted by 20 and 40 mM imidazole. Mdl1p could be specifically eluted by 250 mM imidazole, but two different populations of Mdl1p were purified: a truncated as well as a full-length Mdl1p. It is conceivable that the truncated version of Mdl1p is generated by N-terminal cleavage by signal peptidases in the mitochondria. The full-length Mdl1p was not processed and

could bind via its N-terminal His-tag to the Ni-NTA resin, whereas the truncated version was processed at its N-terminus losing its His-tag. Therefore, the truncated form eluted already with low concentrations of imidazole. The fact that a part of the truncated version is eluted at 250 mM imidazole might be because the formation of dimers between truncated Mdl1p and His-tagged full-length Mdl1p. This construct might present a promising candidate for purification of Mdl1p from yeast mitochondria.

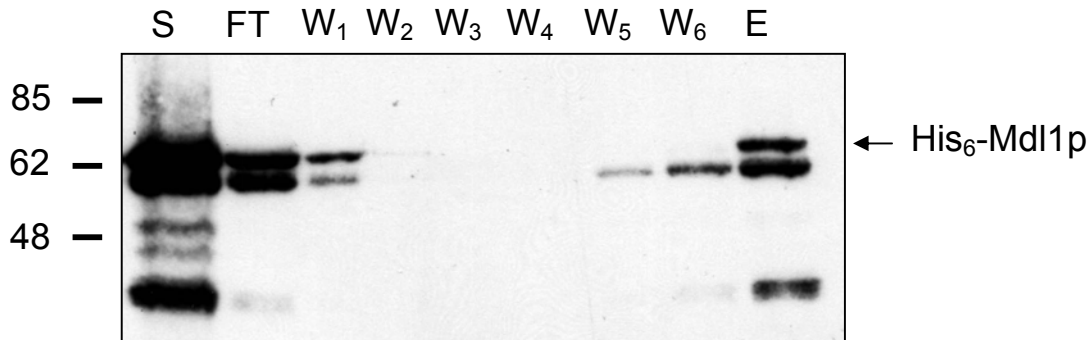


Fig.30: Purification of Mdl1p from mitochondria of pXY113-GAL-mdl1-His₆ transformed yeast.

Transformed yeast cells were cultivated with glucose (2%) in minimal medium (-URA) to OD 0.8 at 30°C, washed and induced with galactose (2%) for 24 h. Mitochondria were detergent solubilized (1% Triton X-100) for 1 h on ice, centrifuged (22.000 x g, 15 min), applied to NTA-beads, washed with detergent buffer containing 0, 10, 20, 40 mM imidazole and eluted with 250 mM imidazole. The fractions were analysed by SDS-PAGE and immunostaining with α -Mdl1.

S: solubilized mitochondria, FT: flow through, W_n: wash steps, W₁₋₃: 0 mM imidazole, W₄: 10 mM imidazole, W₅: 20 mM imidazole, W₆: 40 mM imidazole, E: elution step with 250 mM imidazole

5.1.13 Heterologous expression of Mdl1p in *E. coli*

Several strategies were applied to facilitate overexpression and integration of a membrane protein into the inner membrane of *E. coli*: i) the use of inducible promoters, ii) decrease in growth temperature, iii) use of strains specialized for expression of membrane proteins (Shanklin, 2000) and iv) fusion of the gene to periplasmic signal sequences.

MDL1 which has been deleted in its classical N-terminal targeting sequence was cloned into the pBAD-HisB in frame with an N-terminal His₆-tag encoded by the vector. To regulate the expression of the membrane protein, transcription of *MDL1* was tightly controlled by the arabinose-inducible promoter, whose activity is highly dependent on the concentration of the inducer. To facilitate proper incorporation of membrane protein into the inner membrane the expression was performed in the *E. coli* strain C41. This strain contains increased membrane surface through invagination of the inner membrane and is therefore optimized for expression of membrane proteins (Shanklin, 2000). Inner membrane vesicles were isolated from these cells,

Results

after solubilization with 30 mM DM the supernatant was applied to SDS-PAGE and Western blotting. A strong induction of the Mdl1p was detected (Fig.31). The polytopic membrane protein was correctly targeted to the inner membrane. The affinity purification using the His-tag, however, could not be established. The protein could neither be bound to Ni-NTA-beads nor be detected by α -His-tag (data not shown). It is likely that the N-terminal His-tag was cleaved off by proteases of *E. coli*. As the N-terminus of Mdl1p might be processed in *E. coli*, affinity tags were introduced at the C-terminus in further constructs.

Alternatively, the gene truncated in its N-terminal 59 amino acids was cloned into pASK-IBA2 under the control of the *tet* promoter. The construct was fused N-terminally with the OmpA periplasmic leader sequence and C-terminally with a StrepII-tag. The construct was overexpressed in *E. coli* strain C41 induced by anhydrotetracycline (AHT). After preparation and solubilization of membrane vesicles by 30 mM DM, the non-solubilized material was removed by ultracentrifugation and the supernatant was applied to SDS-PAGE. The Western blot analysis showed for both, induced and uninduced cells, a 62 kDa band corresponding to the size of Mdl1p. Surprisingly, a band appeared at the appropriate size of Mdl1p in uninduced cells. The constitutive expression of the *tet* repressor, which is also encoded on the expression plasmid, should guarantee the repression of the promoter in the absence of the inducer (AHT). Purification approaches by streptactin resin were not successful; the protein could not be eluted by 2.5 mM desthiobiotin.

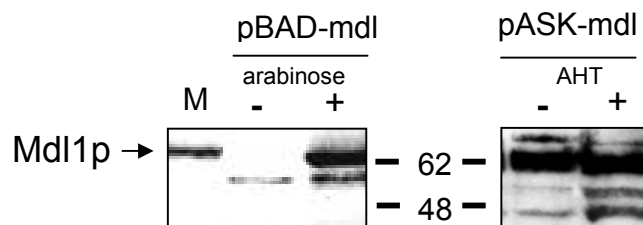


Fig.31: Heterologous expression of different Mdl1p constructs in *E.coli*.

E. coli transformed with pBAD- Δ mt-mdl1 was induced at OD 0.5 with 0.02 % arabinose for 3 h at 30°C.

E. coli transformed with pASK- Δ mt-mdl1 was induced with AHT (200 ng/ml) for 3 h at 30°C. After cell lysis, debris were pelleted by 20.000 x g for 20 min and the supernatant was centrifuged at 100.000 x g for 1 h. The membrane pellet was solubilized with 30 mM DM for 1 h on ice, centrifuged at 20.000 x g for 15 min and the supernatant was analysed by SDS-PAGE and immunostaining with α -Mdl1.

M: yeast mitochondria (pos. control), +: induced, -: non-induced

Alternatively, *MDL1* was cloned into pET22 under the control of T7 promoter resulting in a Mdl1p construct fused N-terminally with the PepB periplasmic leader sequence and C-terminally with His₆-tag. BL21(DE3) cells transformed with pET- Δ mt-mdl1 were induced by IPTG.

Isolated membranes were solubilized with 30 mM DM, ultracentrifuged, and the supernatant was applied to Ni-NTA beads (Fig.32). After washing with step gradients of imidazole (10 - 80 mM) the protein was finally eluted with 250 mM imidazole. This construct might be a promising candidate to be purified from bacterial source.

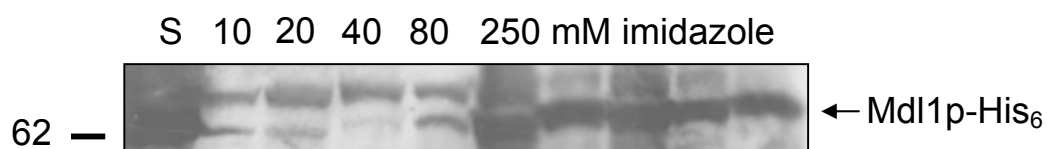


Fig.32: Heterologous expression of Mdl1p in *E. coli* and purification via His-tag.

E. coli cells transformed with pET- Δ mt-mdl1 were induced at OD 0.5 with 0.2 mM IPTG for 3 h at 30°C. After cell lysis debris were removed by 20.000 x g for 20 min and the supernatant was centrifuged by 100.000 x g for 1 h. The membrane pellet was solubilized with 30 mM DM for 1 h on ice, centrifuged at 20.000 x g for 15 min and the supernatant was applied to NTA-beads. The beads were washed with a step gradient of imidazole and finally eluted with 250 mM imidazole. The fractions were analysed by SDS-PAGE and immunostaining with α -Mdl1.

S: solubilized membranes

In conclusion, a screen of different gene constructs was performed in order to establish an overexpression of Mdl1p in *E. coli*. For several gene products a strong induction as well as the correct incorporation of Mdl1p into the inner membrane. Due to N-terminal processing of the gene product in *E. coli*, it was decided to introduce affinity tags exclusively at the C-terminus. Further experiments will focus on the establishment of the purification procedure

5.2 Identification and characterisation of an intracellular peptide transporter of *S. cerevisiae*

In experiments designed either to analyse the intracellular peptide trafficking in the yeast *S. cerevisiae* or to express TAP heterologously (Urlinger *et al.*, 1997), an intrinsic peptide transport system was observed which translocated peptides into microsomes. Based on studies of energy requirement and specific inhibition (e.g. by ortho-vanadate) of the transport, the newly discovered transport activity was suspected to be mediated by an ABC transporter. The genomic yeast data bank was screened for potential ABC transporter gene candidates whose function has not been defined, so far. To identify the open reading frame (ORF) which is responsible for the peptide transport activity, several mutants deleted in putative ABC transporter genes were

created (Urlinger's PhD thesis). The deletion of the ORF *YLL048::HIS3* resulted in a loss of peptide transport function. We set out to characterise this ABC transporter encoded by *YLL048* and to evaluate its physiological role for *S. cerevisiae*.

5.2.1 Characterisation of the ABC transporter encoded by *YLL048*

Microsomes derived from wild type cells (W303-1A) showed a significant uptake of the radiolabelled R9LQK peptide in the presence of ATP at 27°C (Fig.33). The transport activity was competed by a 300-fold excess of unlabelled peptide. The deletion mutant *YLL048::HIS* was completely impaired in peptide transport. Transformation of the deletion mutant ($\Delta yll048$) with the plasmid harbouring the *YLL048* gene fully restored the transport activity. The observation that the transport activity of the transformed deletion mutant was even higher than of the wild type microsomes, was most likely due to the higher expression of gene encoded by the 2 μ plasmid compared to the chromosome.

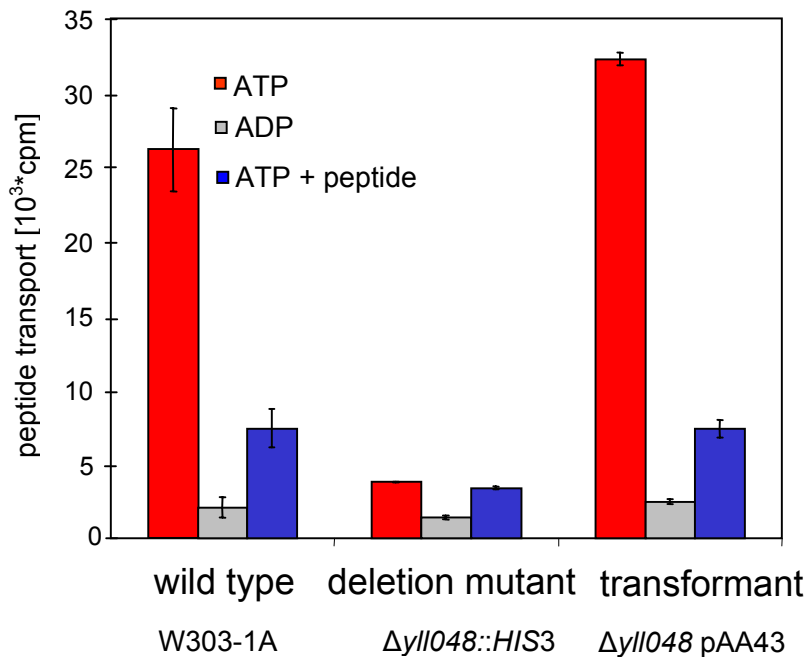


Fig.33: Restoration of ATP-dependent peptide transport of the $\Delta yll048$ strain transformed with plasmid-encoded *YLL048* (pAA48).

Peptide transport of radiolabelled R9LQK (100 nM) was measured in the presence of ATP (2 mM) at 27°C for 3 min into microsomes prepared from wild type, $\Delta yll048$ deletion strain and $\Delta yll048$ deletion strain transformed with pAA43. As a control, the peptide transport rate was measured with ADP or ATP in the presence of a 300-fold excess of unlabelled peptide.

Fig.34 shows the time-dependent peptide transport of radiolabelled R9LQK peptide into microsomes. The transporter was inactive at 4°C in the presence of ATP or at 27°C in the presence of ADP. The ATP-dependent peptide transport was inhibited by a 300-fold molar excess of unlabelled peptide. Presence of apyrase completely abolished the transport activity. To exclude that the transporter was denatured during the assay, transport activity was also determined after 40 min preincubation at 27°C resulting in the same transport rate as without preincubation.

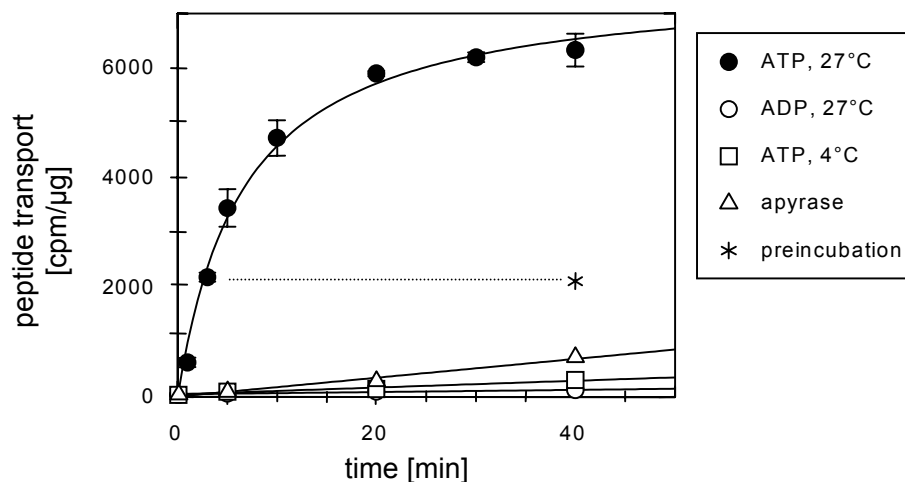


Fig.34: ATP-dependent peptide transport mediated by *YLL048* encoded protein.

Time-dependent peptide transport of radiolabelled R9LQK into wt microsomes was measured in the presence of ATP at 27°C. Transporter was inactive at 4°C in the presence of ATP or at 27°C in the presence of ADP. To exclude that the transporter was denatured during the assay, transport activity was determined after preincubation of 40 min at 27°C (star).

To investigate the energy requirement of the transporter, different nucleotide triphosphates (NTPs) were tested. GTP, UTP, and CTP also energized the transporter albeit to a lower extent compared to ATP (Fig.35).

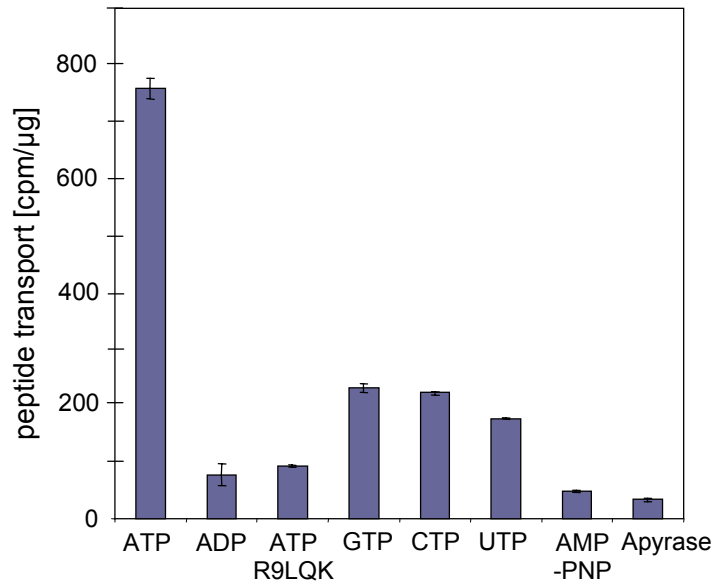


Fig.35: Nucleotide-dependence of the transport activity of YLL048p.

Peptide transport of radiolabelled R9LQK (100 nM) in wt microsomes was measured in the presence of different nucleotides (2 mM) at 27°C for 3 min as well as in the presence of apyrase (1 unit) and AMP-PNP.

5.2.2 Substrate specificity

The substrate specificity of YLL048p was analysed using randomized peptide libraries ranging from 5 to 56 amino acids (Fig.36). A competition of the translocation of reporter peptide R9LQK was observed with a 100-fold molar excess of different peptide libraries. This indicated that YLL048p has a broad substrate specificity. The transporter preferred peptides longer than 7 amino acids. So far, no upper limit for substrate recognition was determined. Randomized nonamer libraries (x_9) containing D-amino acids at different positions (x) competed for peptide translocation as well. Therefore, it can be concluded that D-amino acids were accepted in the substrate binding pocket. D-amino acids at the C-terminal position were slightly disfavoured.

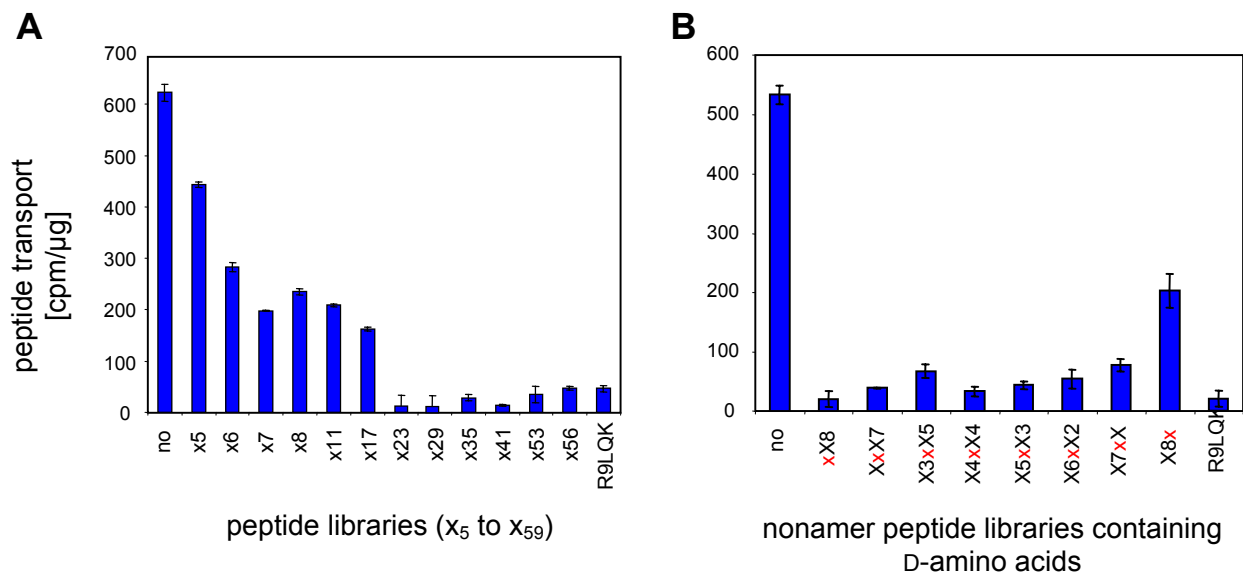


Fig.36: Substrate specificity of the YLL048p.

A: Peptide transport of reporter peptide R9LQK (100 nM) was measured into microsomes at 27°C for 3 min with ATP in the presence of 100-fold molar excess of randomized peptide libraries ranging from 5 to 56 amino acids.

B: Competition of translocation of the reporter peptide R9LQK (100 nM) was measured in the presence of 100-fold molar excess of nonamer peptide libraries which contained a D-amino acid at defined positions.

Red x: position of D-amino acid

Surprisingly, the YLL048p has been described as a bile acid transporter (BAT1p) (Ortiz *et al.*, 1997). Using microsomes, an ATP-dependent [³H]-taurocholate uptake activity was measured which was inhibited by competition with a 375-fold molar excess of unlabelled taurocholate (1.5 mM) (Fig.37). The $\Delta yll048$ strain did not exhibit any bile acid transport activity. Furthermore, it was shown that a 7.5-fold molar excess of peptides already competed for the transport of [³H]-taurocholate and vice versa, the peptides transport activity was reduced by a 375-fold molar excess of taurocholate. Comparing the concentration of both substrates, the transporter YLL048p has a much higher affinity for peptides than for bile acids.

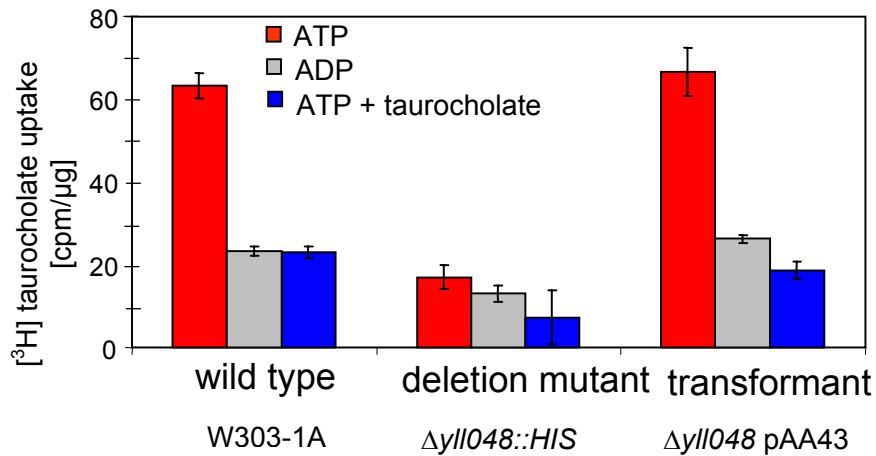
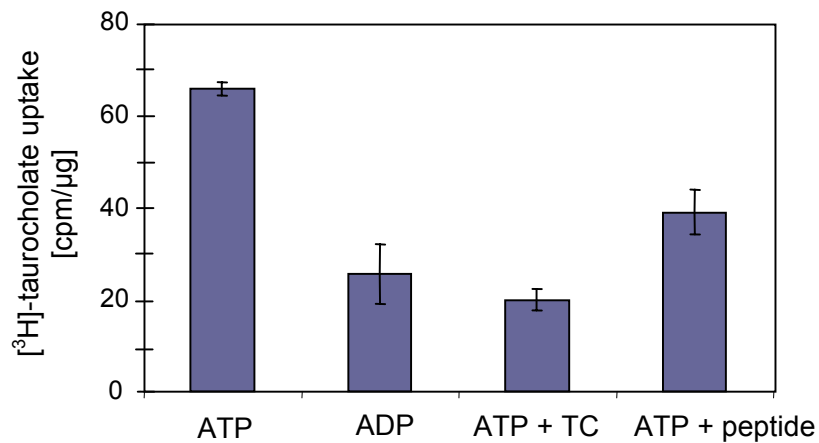
A**B**

Fig.37: ATP-dependent [³H]-taurocholate transport into microsomes.

A: Transport of [³H]-taurocholate (TC) (4 μM) was measured in the presence of ATP (2 mM) at 27°C for 3 min into microsomes prepared from wild type, $\Delta yll048$ deletion strain and $\Delta yll048$ deletion strain transformed with pAA43. For control, the transport rate was measured with ADP or ATP in the presence of a 375-fold excess of unlabelled TC (1.5 mM).

B: Transport of [³H]-TC (4 μM) was measured in the presence of ATP (2 mM) at 27°C for 3 min into microsomes prepared from wild type strain. For control, the transport rate was measured with ADP or ATP in the presence of 1.5 mM unlabelled TC (375-fold molar excess) or in the presence of 30 μM unlabelled peptide (7.5-fold molar excess).

5.2.3 Subcellular localisation of the ABC transporter encoded by *YLL048*

To determine the subcellular localisation of the transporter, peptide transport activity of different organelles separated by sucrose gradient centrifugation was measured (Fig.38). Fractions harvested from 37% to 42% sucrose exhibited a significantly increased ATP-dependent peptide transport activity. These fractions were identified as endoplasmic reticulum

(ER) by immunodetection with antibodies against Kar2p and Sec61p, two marker enzymes of the ER. To exclude that the *YLL048* mediated transport activity is localised in the vacuoles, vacuoles containing fractions were identified by α -mannosidase assay. The vacuoles were detected at the top of the gradient (20% sucrose). This observation is in line with literature where vacuoles are described to float on sucrose gradients because of their association with lipid particles (storage granula) which decrease their density (Zinser and Daum, 1995). Here, we can provide evidence that YLL048p is not predominantly localised in the vacuole membranes or secretory vesicles as proposed by Ortiz *et al.* (Ortiz *et al.*, 1997).

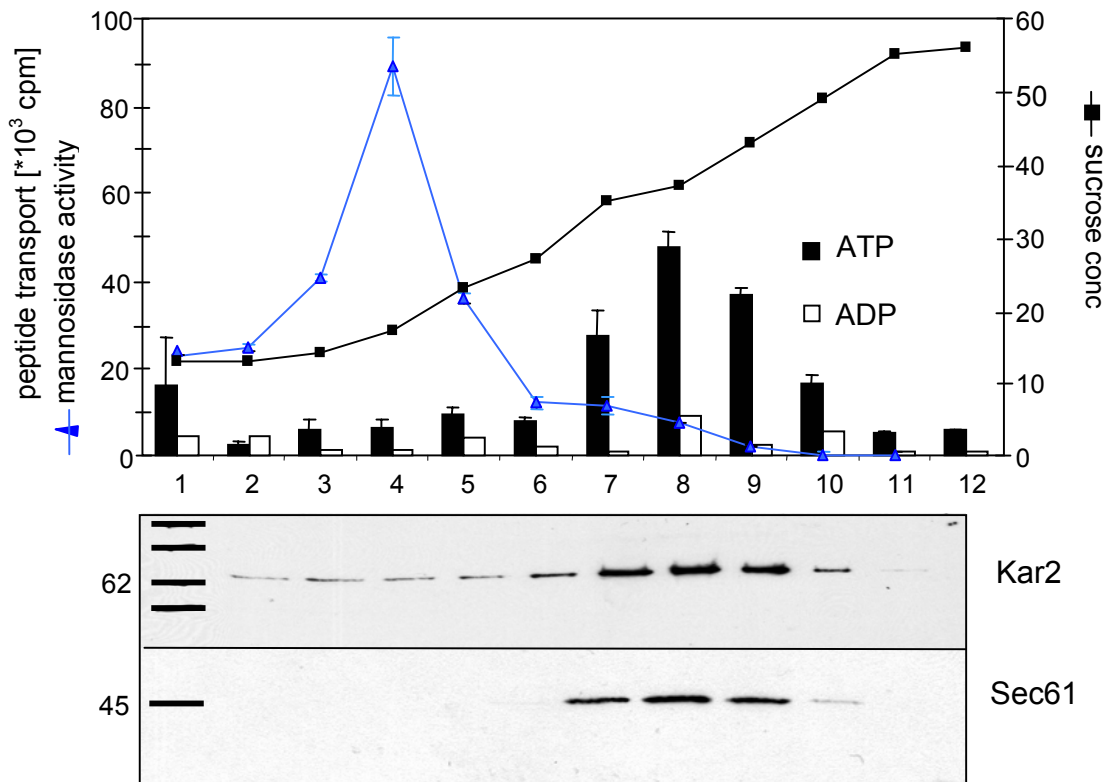


Fig.38. Peptide transport activity is colocalised with microsomal fractions.

ATP-dependent peptide transport activity of the reporter peptide R9LQK (100 nM) was measured into different fractions separated by a sucrose gradient. The localisation of the microsomal fractions in the gradient was determined by SDS-PAGE and immunostaining with two ER marker proteins (Sec61 and Kar2). The localisation of vacuoles was determined by α -mannosidase assay.

In order to confirm the ER localisation of this transporter, the peptide R10T containing the recognition site (NXT/NXS) for glycosylation was used (Fig.39). The ER is the only compartment where N-glycosylation of proteins occurs. Microsomes containing YLL048p were incubated at

Results

27°C for 3 min in the presence of ATP. Only a very little amount of glycosylated peptide could be detected by binding to concavalin A sepharose. One explanation for this observation might be that the yeast glycosylation machinery does not accept peptides, which are not delivered via the Sec61 complex into the ER. It is also possible that the N-glycan attached to the peptide is not recognized by the lectin concavalin A. In order to test the glycosylation in yeast microsomes, an acetylated and amidated tripeptide (Ac-NYT-NH₂) was used, which enters the microsomes by passive diffusion (Wieland *et al.*, 1987) (Fig.40,A). This Ac-NYT-NH₂ consists of the N-linked glycosylation site including a tyrosine which could be efficiently iodinated. As diffusion is a slow process, microsomes were incubated with the radiolabelled Ac-NYT-NH₂ for 30 min at 27°C. Radioactive Ac-NYT-NH₂ could be eluted from concavalin A, demonstrating that an efficient glycosylation of the tripeptide was obtained. Surprisingly, although no efficient glycosylation of the peptide R10T could be observed, the R10T peptide decreased the glycosylation efficiency of the reporter tripeptide (Fig.40,B).

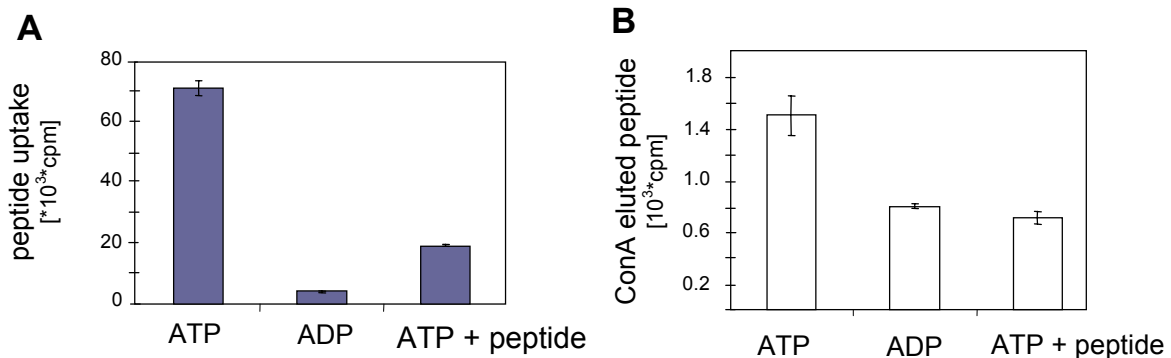


Fig.39: Peptide transport into wild type microsomes.

A: Microsomes were prepared from wild type yeast cells. Transport of radiolabelled R10T peptide (100 nM) containing an internal glycosylation site was measured in the presence of ATP (2 mM) at 27°C for 3 min. The microsome pellets were directly γ -counted.

B: Alternatively, after transport assay microsomes were lysed by NP40 (1%) and incubated with concavalin A sepharose for 1 h. After washing, glycosylated peptide R10T was eluted by β -methyl-mannoside before γ -counting.

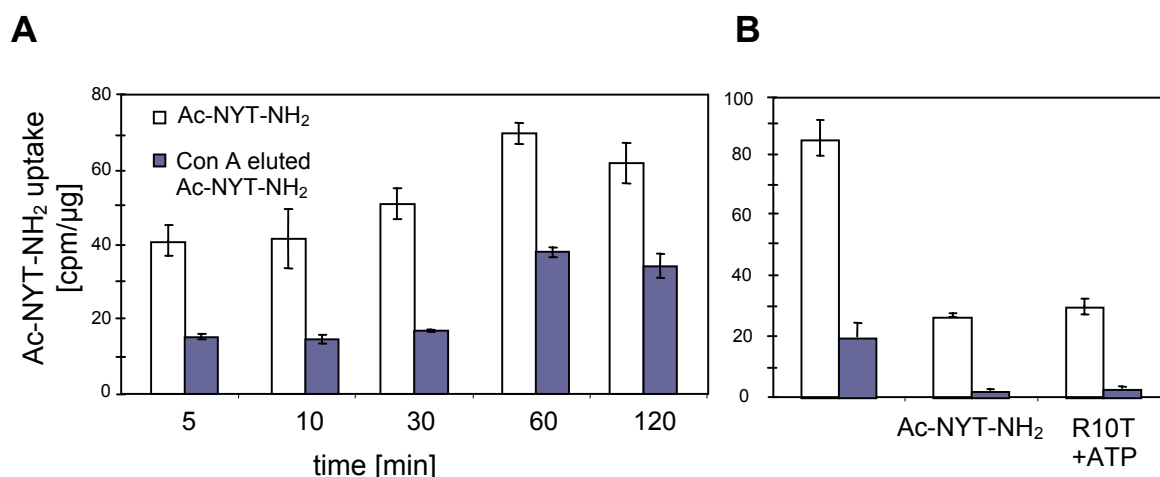


Fig.40: Passive translocation of Ac-NYT-NH₂ into microsomes.

A: Passive translocation of radiolabelled Ac-NYT-NH₂ (100 nM) into microsomes was performed at 27°C for different time points. The microsome pellets were directly γ -counted (open bars). Alternatively, NP40-lysed microsomes were incubated with concavalin A sepharose for 1 h and glycosylated tripeptide was eluted by β -methyl-mannoside and quantified (filled bars).

B: Radiolabelled Ac-NYT-NH₂ (100 nM) was incubated for 30 min at 27°C with microsomes in the presence of 100-fold molar excess of unlabelled Ac-NYT-NH₂ or unlabelled R10T in the presence of 2 mM ATP. The microsome pellets were directly γ -counted (open bars) or glycosylated tripeptide was quantified after microsome lysis and elution from concavalin A sepharose (filled bars).

In summary, we concluded that the ABC transporter YLL048p mediates ATP-dependent peptide transport. The radioactive transport activity is peptide specific because peptide translocation was competed by an excess of unlabelled peptides. In addition, we demonstrated that the same transporter mediates bile acid transport albeit with a decreased affinity compared to peptides. Subcellular fractionation experiments clearly correlated the peptide transport activity with ER membranes. But for unknown reasons, no efficient glycosylation of peptides with an internal glycosylation site could be observed after import. Efficiency of the glycosylation machinery was studied by Ac-NYT-NH₂ which enters the ER lumen by passive diffusion. Surprisingly, the transport of peptides with a glycosylation site reduced the efficiency of the glycosylation of Ac-NYT-NH₂.

The physiological role for a peptide uptake system of the yeast cell is not well understood. Therefore, we set out to investigate different factors which might influence the expression of YLL048.

5.2.4 Physiological function of YLL048p in yeast

The physiological function of the bile acid transporter (Bat1p) proposed by Ortiz *et al.* was the detoxification of the cytosol by translocating bile acids and derivatives into vacuoles

Results

(Ortiz *et al.*, 1997). Kolaczowska and colleagues reported a highly increased toxicity of bile acids toward the *PDR1*, *PDR3* double disruptant mutants together with decreased level of *BAT1* promoter dependent β -galactosidase activity (Kolaczowska *et al.*, 1998). Therefore, Bat1p was described as a new member of the pleiotropic drug resistance (PDR) network. Although classical response elements for the transcription factors Pdr1p and Pdr3p are missing in the *BAT1* promoter, we tested this possibility. By Northern blot analysis mRNA levels of *YLL048* were investigated in strains with *PDR1* and *PDR3* double deletion as well as in gain-of-function *PDR1* and *PDR3* strains (Fig.41). In all strains tested no change of *YLL048* mRNA level could be observed. Neither in the *PDR1*, *PDR3* double deletion strains nor in strains overexpressing the transcription factors a change in *YLL048* mRNA level was obtained. Therefore, a regulation of *YLL048* in the PDR can be excluded.

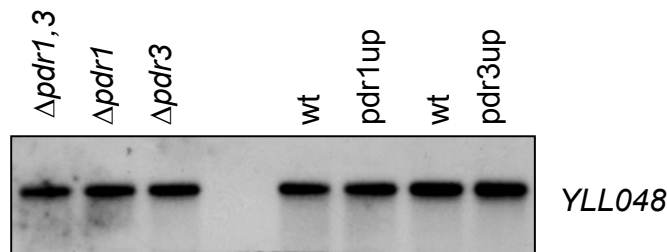


Fig.41: Northern blot analysis of *YLL048* mRNA level.

Total RNA was isolated from logarithmically growing cells by the hot phenol method as described previously (Schmitt *et al.*, 1990) and applied to agarose electrophoresis. RNAs were transferred onto a Nylon membrane (Hybond N+) by capillary transfer. *YLL048* mRNA was detected by hybridization with a 723 bp radioactive probe corresponding to nt +145 to nt +868 of this ORF. mRNA level of *YLL048* was tested of W303-1A, deletion strain of *PDR1* and/or *PDR3* as well as of strains upregulating *PDR1* or *PDR3*.

In order to explain the physiological relevance of peptide transport into microsomes, we speculate that the *YLL048* encoded protein might be part of a novel route of peptide trafficking in yeast involved in the unfolded protein response (UPR) (Higashio and Kohno, 2002). To test the hypothesis, upregulation of *YLL048* expression induced by heat shock was studied (Fig.42,A). Cells grown at room temperature were shifted to 37°C for different time periods. However, the synthesis of *YLL048* mRNA did not change during the chase of 60 min. For positive control, the mRNA level of *PDR15* showed a shift on RNA level in dependence of increased growth temperature (H. Wolfger, PhD thesis).

To test the involvement of *YLL048* in stress response, cells were exposed up to 60 min to stress factors as increased concentration of NaCl, sorbate and sorbitol (Fig.42). Again no shift in the synthesis of *YLL048* mRNA level could be observed under the tested conditions. As negative

control, H₂O₂ was used which induced the lysis of the cells and therefore a decrease in the mRNA level. In summary, an upregulation of *YLL048* in response to stress conditions and heat shock could not be observed on mRNA level.

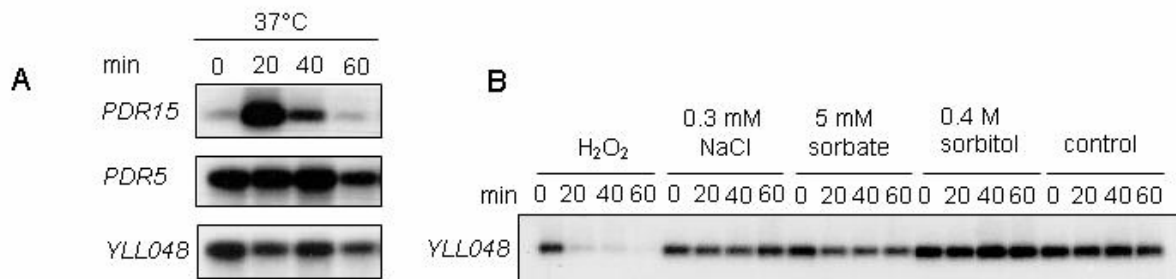


Fig.42: Northern blot analysis of mRNA of *PDR15*, *PDR5*, and *YLL048* after stress.

A: Total RNA was isolated from cells grown at RT which have been exposed to heat shock (37°C) for different time periods.

B: Total RNA was isolated from cells grown for different time periods in the presence of H₂O₂, 0.3 M NaCl, 5 mM sorbate, and 0.4 mM sorbitol

5.3 *In vivo* screen of TAP mutants based on an autocrine stimulation assay in yeast

The mechanism of peptide transport by the TAP complex has been studied in detail (Lankat-Buttgereit, 2002). The transporter is responsible for translocation of peptides from the cytosol into the lumen of the ER. The functional expression of human TAP in the yeast *S. cerevisiae* has been established (Urlinger *et al.*, 1997). The heterologously expressed TAP1 and TAP2 subunits have been reported to be located in the ER membrane as well as the plasma membrane. In order to establish a fast and efficient method to characterise a broad spectrum of TAP mutants and associated factors, which might alter the transport activity, a genetic *in vivo* screen was designed. This assay should be based on TAP-mediated peptide transport monitored by a fast read out system.

However, peptide trafficking in yeast is not well characterised. Several peptide transporters are involved in nutrient uptake. Beside the use of peptides as energy source, peptides play an important role in mating of yeast cells. The process of mating is mediated by peptide pheromones, the α - and **a**-factor. We set out to build up a screening assay based on TAP-mediated secretion of peptide pheromones. To establish such an *in vivo* screen was very convenient because *in vitro* transport assays already demonstrated that the TAP complex recognized the pheromone α -factor as substrate.

5.3.1 Pheromones mediate mating in the yeast

The assay takes advantage of processes involved in mating of two haploid cells, *MAT α* and *MAT**a*** (Cross, 1988). Mating requires the action of extracellular peptide hormones (α - and **a**-factor) that are released from haploid partners of opposite mating type. The α -factor is secreted by *MAT α* cells and binds to a G-protein-coupled receptor on the surface of **a**-mating-type cell and vice versa. The pheromone receptors Ste2 and Ste3 induce a MAP-kinase-dependent signal transduction, which switches the expression of specific genes causing a cell cycle arrest in G1, combined with a change of the cell morphology (Sprague, Jr. *et al.*, 1983; Kuchler *et al.*, 1993; Blumer *et al.*, 1988).

In contrast to the **a**-factor, which is exported by the ABC transporter Ste6, the α -factor is expressed as a larger pre-pro-protein (120 amino acids) including an ER leader sequence and is secreted by the classical secretory pathway (Julius *et al.*, 1983). During the maturation of the α -factor (WHWLQLKPGQPMY) its pre-pro sequence is processed in the ER and Golgi.

5.3.2 TAP-mediated α -factor secretion

To bypass the Sec61-dependent secretory pathway of the α -factor, the mature pheromone was planned to be expressed from a minigene lacking the pre-pro-sequence. Therefore, mature α -factor is predicted to remain in the cytosol. Yeast cells expressing a functional TAP should export the α -factor into the extracellular space, whereas TAP deficient cells are not able to secrete the pheromone. Four different constructs of the α -factor were cloned into the yeast expression vector p426 under the control of the strong, constitutive ADH promoter. The first construct (**MWHWLQLKPGQPMY**) contained the mature α -factor sequence including an N-terminal methionine. The second construct (**MWHWLQLKPGQPMYKRNAT**) consisted of a recognition site for the Kex2 protease (KR) and a glycosylation recognition site (underlined) at its C-terminus. In the third construct (**MKREAEAWHWLQLKPGQPMY**) the mature α -factor was N-terminally fused with its natural recognition site of Kex2 protease (KR) and Ste13 (EA) based on the original sequence of the pro- α -sequence. The fourth construct (**MNATLAKREAEA-**WHWLQLKPGQPM****) contained a glycosylation site as well as the Kex2 protease recognition sites. The Kex2 protease is responsible for cleavage of the pro-sequence in the Golgi apparatus. The reason to introduce glycosylation sites into the peptide was to protect the pheromone from retrograde transport from the ER to the cytosol as described for peptides (Koopmann *et al.*, 2000). The α -factor constructs were designed to be transported to the ER by TAP from where they can follow the classical secretory pathway.

To obtain autocrine stimulation, expression of the α -factor was performed in **a**-mating cells Cadus 6259. After secretion, the α -factor should interact with its Ste2 receptor at the same cell surface resulting in an autocrine stimulus which triggers a MAPK-cascade. Normally, the pheromone stimulation causes a cell cycle arrest. To avoid this arrest, the strain used was deleted in the *FAR1*-gene (McKinney *et al.*, 1993; Peter *et al.*, 1993). In addition, this strain contains a *BAR1* (protease) mutation in order to reduce degradation of the α -factor and a *STE14* mutation to reduce background cascade stimulation in the absence of extracellular pheromone (Manfredi *et al.*, 1996). For screening of stimulated cells, the *HIS3* gene cassette was set under the control of α -factor inducible *FUS1*-promotor, integrated into the genome (Trueheart *et al.*, 1987; Manfredi *et al.*, 1996). Thus, the selection of functional TAP complex was based on a shift from histidine auxotrophy to prototrophy of stimulated cells (Fig.43).

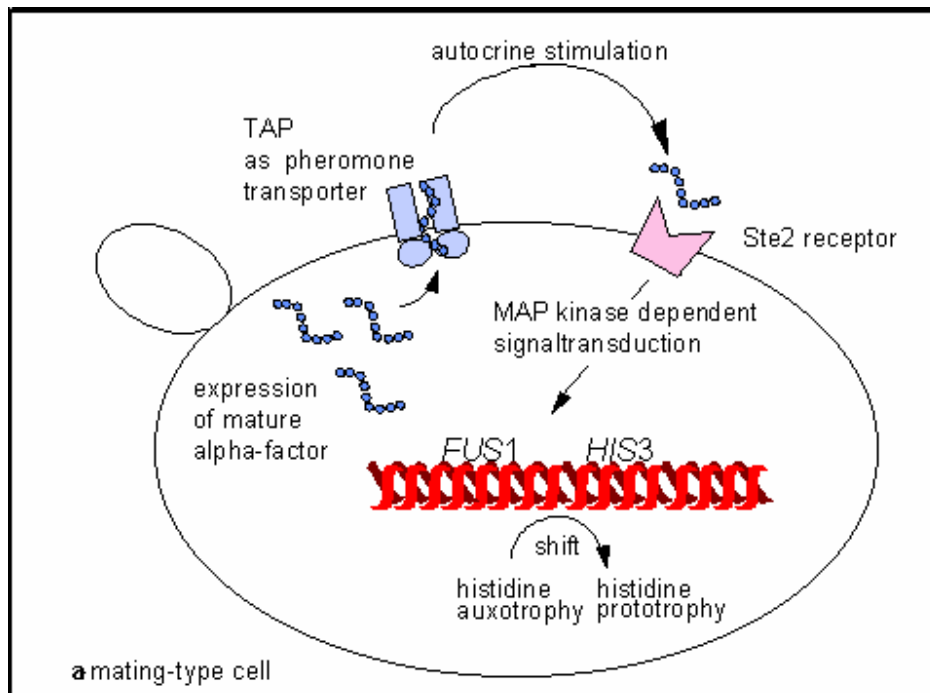


Fig.43: Scheme of the function of the autocrine stimulation assay.

Mature α -factor is expressed in an **a** mating-type cell and becomes exported into the medium by TAP. At the cell surface, the pheromone binds to the Ste2 receptor inducing a signal cascade which results in the activation of the *FUS*-promotor dependent expression of *HIS*-cassette. Thus, the selection of functional TAP complex is based on a shift from histidine auxotrophy to prototrophy of stimulated cells.

5.3.3 Functionality of the autocrine stimulation assay

In order to investigate the functionality of the autocrine stimulation of the strain Cadus 6259, synthetic mature α -factor was added to freshly inoculated yeast cells in the absence of histidine. The α -factor triggered the growth of the cells as measured by the increase of the OD_{600} (0.5-1) after 24 h incubation. The external concentration of the α -factor sufficient to induce the shift from *HIS* auxotrophy to prototrophy was determined to be 112 nM. Cells did not grow in the absence of external pheromone. The sensitivity of cells towards α -factor could be controlled by addition of aminotriazole (AT) (Klopotoski and Wiater, 1965). AT is a competitive inhibitor of *HIS3* gene product (imidazole glycerol phosphate dehydratase). The addition of 1.7 mM AT in combination with 560 nM α -factor inhibits the growth of the cells. The addition of AT to the medium reduces the sensitivity of the cells to the pheromone 10 times.

The Cadus 6259 strain transformed with plasmid-encoded TAP1 (Ura) and TAP2 (Leu) genes in combination with different constructs of α -factor (Trp) did not grow in the absence of

histidine. The presence of the TAP genes and α -factor gene in the yeast cells was confirmed by colony-PCR. However, the expression of the TAP1 and TAP2 subunits could not be detected in the Cadus strain by Western blot analysis (Fig.44,A). The expression of the mature α -factor in yeast cells was investigated using an antibody against the pre-pro- α -factor (Fig.44,B) (kind gift from R. Schekman). The antibody was generated against the precursor form of the α -factor, but was able to recognize the mature α -factor as well.

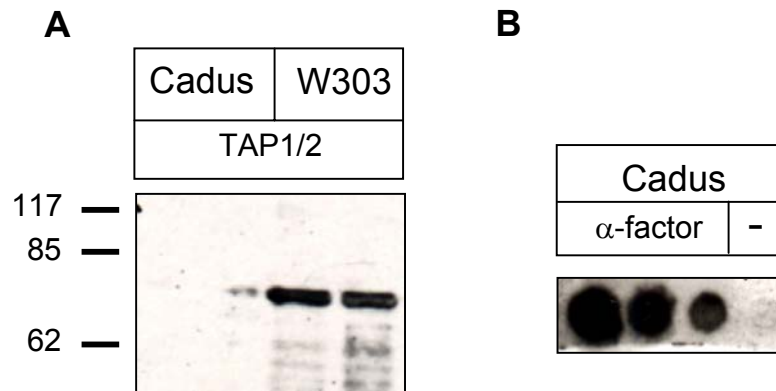


Fig.44: Western blot analysis of TAP expression and western dot blot analysis of α -factor expression in yeast.

A: Microsomes derived from W303-1A strain and Cadus 6259 strain transformed with TAP1 and 2 genes were applied to 12% SDS-PAGE and immunostained with α -TAP1 and TAP2.

B: Cytosolic extract of Cadus strain 6259 transformed with p426- α -factor (mod 4) was TCA-precipitated (5% final conc.). The supernatant was applied to nitrocellulose and immunostained with α -pre-pro-alpha-factor. Different concentrations of the extract were applied to the membrane.

In summary, a selection assay for TAP mutants based TAP-mediated secretion of the α -factor could not be established. The functionality of the signalling pathway of the Cadus strain was demonstrated by addition of synthetic α -factor to the medium. Furthermore, *in vitro* assays clearly demonstrated that the pheromone is recognized by the TAP complex. But for unknown reasons, the expression of the TAP subunits was not detected in the Cadus strain. As previously described we have characterised an intracellular peptide transporter encoded by *YLL048*. *In vitro* transport assays on isolated yeast microsomes showed that the YLL048p transported the α -factor as well (data not shown). But no stimulation to *HIS* prototrophy was obtained in Cadus strain. One reason might be that the expression of α -factor in the cytosol was not efficient. It is possible that the peptide was rapidly degraded in the cytosol before it could be transported to the ER lumen. It is also possible that the truncated α -factor although imported into the ER did not follow the secretory pathway to the cell surface but became either degraded in the ER or exported into the cytosol for degradation.

6 Discussion

6.1 Characterisation of the ATPase cycle of isolated Mdl1p-NBD

ABC transporters undergo a series of conformational changes in response to ATP binding and hydrolysis at the NBDs. These conformational changes are coupled to rearrangements in the TMDs which finally results in the translocation of solutes across the membrane. Observations of strong cooperativity between the two NBDs in ATP hydrolysis of the complete transporter suggested a dimerization of the NBDs during the catalytic cycle (Nikaido *et al.*, 1997; Sharma and Davidson, 2000; Jones and George, 1999). The fact that inactivation of one of the NBDs entirely abolishes the transport activity confirmed the necessity of two functional ATPase subunits in each transport cycle (Urbatsch *et al.*, 1998; Urbatsch *et al.*, 2000a; Urbatsch *et al.*, 2000b). But only recently the reason for the interdependency of the ABC subunits was clarified on molecular level. The catalytic pocket for ATP hydrolysis is produced only by cooperation of two monomers (Nikaido, 2002). Structural (Hopfner *et al.*, 2000; Smith *et al.*, 2002; Locher *et al.*, 2002) and biochemical data (Fetsch and Davidson, 2002; Loo *et al.*, 2002) clarified which residues are involved in ATP binding and subsequent dimerization of the NBDs. Although dimerization has been recognized as an essential intermediate in the ATPase cycle, the mechanism of ATP hydrolysis in both NBDs is still under debate and the nature of structural changes occurring at each step of the ATPase cycle has not been defined.

Recently, an intracellular half-size ABC transporter Mdl1p (multidrug resistance like), localised in the inner mitochondrial membrane of *Saccharomyces cerevisiae*, has been identified (Young *et al.*, 2001). Mdl1p was proposed to act as a homodimer in its minimal composition. We are interested in the mechanism how ATP hydrolysis drives the export of peptides. Therefore, the C-terminal domain (amino acids 427 to 695) corresponding to the NBD of the mitochondrial ABC transporter Mdl1p was overexpressed in *E. coli* and purified to homogeneity. Purified NBD was active with respect to ATP binding and hydrolysis. The Mdl1p-NBD appeared as a monomer in gelfiltration studies independent of the presence of nucleotides as was previously observed for isolated HisP (Nikaido *et al.*, 1997).

Importantly, in the presence of ATPase inhibitors such as ortho-vanadate or BeF_x the isolated Mdl1p-NBD was trapped as a dimer which was stable during gelfiltration. Ortho-vanadate and BeF_x act as analogues of inorganic phosphate and mimick an intermediate state during ATP hydrolysis after phosphate dissociation but before release of ADP (Goodno, 1982; Phan and Reisler, 1992; Urbatsch *et al.*, 1995b). Ortho-vanadate acts as a transition state analogue presumably occupying the γ -phosphate position adjacent to the ADP (Smith and

Discussion

Rayment, 1995), whereas BeF_x is a ground state analogue mimicking the bound MgATP (Maruta *et al.*, 1993; Henry *et al.*, 1993). Each of these stable inhibitory complexes mimics specific states in the ATPase kinetic pathway (Shibuya *et al.*, 2002). As demonstrated on myosin X-ray structures, the inhibited complex trapped by ortho-vanadate reassembles a posthydrolysis state while the complex trapped by BeF_x represents a prehydrolysis state (Fisher *et al.*, 1995).

ADP could not replace ATP in the trapping reaction. Incubation of the NBD with MgATP at 4°C in the presence of BeF_x did not induce dimerization either. These experiments demonstrate that ATP binding and hydrolysis are essential for dimerization. Using [α - ^{32}P]-ATP or [γ - ^{32}P]-ATP the nucleotide composition of BeF_x -trapped states was analysed by β -counting and thin layer chromatography after gelfiltration. Radioactive nucleotides coeluted exclusively with the dimer in the gelfiltration, whereas no radioactivity was observed in fractions corresponding to the monomer. Analysis of the dimer showed exclusively two ADP molecules without P_i bound in the dimer. These data indicate that ATP could not be preserved in the NBD. After hydrolysis of two ATP molecules the dimer is stabilized by exchange of P_i with BeF_x . The half-life of the inhibitory complex was significantly longer than 1 h as no dissociation of the dimer was observed during the gelfiltration (1 h). During this time only inorganic phosphate was released from the dimer.

6.1.1 Analysis of mutants in the ATPase cycle

An ATPase deficient mutant of the Mdl1p-NBD was created by removal of the charge in the catalytic centre downstream of the Walker B motif (E599Q). This exchange was equivalent to the mutation of P-gp (E552Q/E1197Q), which was described to be severely impaired in transport activity and in substrate-stimulated ATPase activity (Urbatsch *et al.*, 2000a). Although the E522Q mutant of P-gp was catalytically inactive in standard ATPase assays (as measured by P_i or ADP release), the ability to form an ortho-vanadate-stimulated transition state (P-gp-ADP- V_i) was retained. Binding of Mg^{2+} to this mutant was not impaired. As ortho-vanadate could be bound to E522Q mutant, it was suggested that the mutant is not inhibited in ATP hydrolysis, but rather in the release of ADP. Therefore, this mutant was described to be incapable to complete a single catalytic turnover (Urbatsch *et al.*, 2000a). The observation that an equivalent mutant of isolated archaeal NBDs from MJ0796 (E171Q) or MJ1267 (E179Q) induced an ATP-dependent dimerization of the NBDs was a key step in visualizing the dimer as a catalytic intermediate (Moody *et al.*, 2002). The mutant (E599Q) of Mdl1p-NBD also formed a stable dimer upon ATP binding. Gelfiltration analysis and thin layer chromatography demonstrated that two nucleotides were incorporated per dimer. The nucleotide composition was determined under non-hydrolysing

conditions, which means in the absence of Mg^{2+} at 4°C, and under hydrolysing conditions, in which the NBD was incubated in the presence of Mg^{2+} at 30°C. Under non-hydrolysing conditions exclusively two ATP molecules were observed in the dimer. Under hydrolysis conditions the dimer contained ATP and ADP along with a very small amount of phosphate. This result indicates that the E599Q mutant is able to hydrolyse at least one ATP although with decreased efficiency compared to the wild type NBD. Two ADP molecules sandwiched in the mutant dimer were not observed simultaneously although the incubation was prolonged to 8 h. This indicated that a dimer with two ADP molecules seems to be unstable, suggesting that at least one ATP molecule is required to hold the dimer together. Probably, incubation of the E599Q mutant in the presence of BeF_x under hydrolysis conditions would result in a transition state with two ADP molecules.

The dimer formation of the archaeal NBDs from MJ0796 (E171Q) and MJ1267 (E179Q) was impaired by Mg^{2+} . In comparison, Mg^{2+} did not effect the formation of Mdl1p-NBD dimers significantly. However, Mg^{2+} influenced the species of nucleotides trapped in the NBDs. As described previously, the presence of Mg^{2+} triggered the hydrolysis of ATP within the dimer.

Based on these results, we can conclude that ATP binding is essential and sufficient for dimerization of the mutant NBD. It was shown that ABC transporters are unable to hydrolyse the ATP-analogues AMP-PNP or $ATP_{\gamma}S$ or at least the hydrolysis efficiency is highly decreased. Surprisingly, incubation of the E599Q mutant of Mdl1p in the presence of AMP-PNP or $ATP_{\gamma}S$ did not induce dimerization. The same observation was made with E171Q mutant from MJ0796 or E179Q from MJ1267 (Moody *et al.*, 2002). The inability of AMP-PNP to promote dimerization might be explained by its poor imitation of ATP. However, binding of AMP-PNP to NBD as tested for E599Q mutant was not impaired. But we could demonstrate that incubation of the E599Q mutant with equimolar ratio of unlabelled ATP and $ATP_{\gamma}^{35}S$ resulted in the incorporation of one $ATP_{\gamma}^{35}S$ molecule bound per dimer, suggesting that the presence of one hydrolysable ATP molecule is essential for dimer formation.

Mutagenesis of aspartate into alanine in the Walker B motif (D598A) of Mdl1p resulted in a mutant which was indeed deficient in hydrolysis of the γ -phosphate anhydride bond although binding of ATP was not impaired. This mutant did not show ATP-induced dimerization. Another invariant residue of NBDs is the histidine 631 of Mdl1p in the switch II region. It was proposed that this histidine is intimately involved in hydrolysis since it forms an H-bond with γ - P_i of ATP via a water molecule (Nikaido and Ames, 1999). A homodimer of HisP (H211R) was inactive in

ATPase activity but retained full activity in complex with wild type HisP. An equivalent mutation in the Mdl1p-NBD (H631R) resulted in an inactive NBD. Gelfiltration analysis of the H631R mutant in the absence of nucleotides showed predominantly a dimer, which was not dependent on ATP.

6.1.2 Model of the ATPase cycle

Based on our data we propose a model, where ATP binding to both NBDs induces formation of the dimer. After hydrolysis of two ATP molecules, the dimeric complex dissociates and ADP molecules are released. The association of the NBDs is a central step of the ATPase cycle, but it remains still controversial how both NBDs cooperate and coordinate ATP hydrolysis. Based on dimeric crystal structures it is proposed that two ATP molecules are bound to a dimer at the same time (Hopfner *et al.*, 2000; Smith *et al.*, 2002). As the two ATP molecules are buried into the interior made up by the dimer interface, no nucleotides are exchangeable as long as the dimer does not dissociate. Preloading of the Mdl1p-NBD with non-radiolabelled ATP followed by incubation with [α - 32 P]-ATP resulted in no incorporation of radioactive nucleotides into the dimer. The same observation was made with P-gp (Urbatsch *et al.*, 1995b).

Both NBDs are required for the functionality of an ABC transporter and both must hydrolyse ATP (Higgins, 2001; Urbatsch *et al.*, 1995a; Urbatsch *et al.*, 1998). But the question remains whether the motor domains work as equivalent modules hydrolysing both ATPs synchronically, sequentially or alternately. A model based on P-gp, LmrA and HisMQP₂ was proposed in which only one NBD hydrolyses one ATP molecule at a time (Senior *et al.*, 1995; van Veen *et al.*, 2000; Higgins, 2001; Jones and George, 2002). In this alternating model two ATP molecules are bound simultaneously. Hydrolysis of ATP occurs at one NBD followed by release of ADP and P_i. Before the ATP at the second NBD can be hydrolysed, the first NBD has to be reloaded by new ATP.

For sterical reasons loading of a new nucleotide into the dimer without dissociation of the subunits is difficult to imagine. Therefore, following the alternating catalytic cycle model, the dissociation of the dimer occurs after every hydrolysis of ATP at each NBD. It is also conceivable that the association of the NBDs, which are fixed to the TMDs, in a full-length transporter is not as tight as in isolated NBDs.

The ATPase model based on isolated NBDs clearly contradicts an alternating modus. Once a dimer is formed, both ATPs are hydrolysed before the dimer dissociates. After loading of the monomers with new ATP molecules a new cycle of hydrolysis can be performed. In a BeF_x-

trapped dimer two ADP molecules were observed for Mdl1p. In contrast, for P-gp ortho-vanadate-induced trapping of nucleotides resulted in 1 mol [$\alpha^{32}\text{P}$]-ADP bound per mol P-gp (Urbatsch *et al.*, 1995b). The same stoichiometry was observed concerning the inhibitory complex stabilized by BeF_x (Sank Aran *et al.*, 1997). For MalFGK₂ trapping of nucleotides by ortho-vanadate demonstrated 0.9 mol nucleotides bound per mol protein (Sharma and Davidson, 2000). In contrast to our data, isolated MalK was insensitive to ortho-vanadate and it was proposed that the TMDs of MalFGK₂ are crucial for conferring sensitivity to the ATPase inhibitor (Hunke *et al.*, 1995).

It is difficult to understand why the stoichiometries concerning Mdl1p-NBD and P-gp or MalFGK₂ differ. P-gp and MalFGK₂ resemble full-length transporters, whereas the investigations with Mdl1p were performed on isolated NBDs in the absence of TMDs and substrate. It is known that isolated NBDs (e.g. HisP, H211R) can show a different behaviour compared to the complex since TMDs might superimpose a regulatory effect on the NBDs (Nikaido and Ames, 1999). Finally, we cannot exclude the possibility that different ABC transporters function in a different modus to hydrolyse ATP. The fact that ABC transporters behave different can be shown by the fact that trapping of P-gp with ortho-vanadate or BeF_x even worked in the presence of ADP (Sankaran *et al.*, 1997). For Mdl1p-NBD, trapping the dimer by ortho-vanadate or BeF_x was strictly dependent on proceeding ATP hydrolysis.

6.2 Characterisation of yeast ABC transporter Mdl1p

The inner membrane of mitochondria and chloroplasts is the only cellular membrane that is not exposed to the cytosol and therefore not accessible to the ubiquitin/proteasome pathway. Therefore, the mitochondria rely on an additional quality control system mediated by ATP-dependent AAA proteases working in concert with Mdl1p, a member of the ABC superfamily. These AAA proteases degrade improperly folded mitochondrial membrane proteins and short-lived regulatory proteins to peptides and amino acids (Arnold and Langer, 2002; Langer *et al.*, 2001). Breakdown products of a molecular mass of 600-2100 dalton are transported to the intermembrane space by Mdl1p.

In general, it is difficult to study exporters like Mdl1p since the substrate binding site and the ATP binding pocket are not directly accessible. To investigate efflux transport, the substrates as well as competitive inhibitors have to be delivered into mitochondrial matrix. Subsequently, the release of labelled substrates into the medium has to be measured. The transport activity of Mdl1p was characterised by quantification of peptides in the intermembrane space. These

peptides are derived from degraded proteins after *in-organello*-synthesis and labelling (Young *et al.*, 2001). Based on this method it is impossible to influence the generated pool of peptides inside the mitochondria. It is also impossible to manipulate the ATP concentration inside the organelle. Using isolated mitochondria it cannot be excluded that after export of the peptides into the intermembrane space, these peptides become further processed by other proteases. So far, the information about the substrate spectrum of Mdl1p is very limited and the transport mechanism how ATP energizes the export of peptides is not understood. To address these questions, we followed the strategy to overexpress this transporter in *S. cerevisiae* or *E. coli*. Purification of Mdl1p and reconstitution into liposomes would facilitate the investigation of transport function *in vitro*. Alternatively, an approach to study the transport activity *in vivo* was performed. For this reason, we tried to convert the export function of Mdl1p into an import activity by disrupting the mitochondrial targeting of Mdl1p. Mdl1p delocalised to the ER membrane might function as a peptide importer comparable to TAP.

6.2.1 Expression and reconstitution of Mdl1p

Homologous overexpression of Mdl1p in yeast has been established. The first step in purification of a membrane protein is the detergent-mediated solubilization. Decylmaltoside (DM) has been used for solubilization as it is a very mild detergent and it was successfully used in the functional reconstitution of TAP (Gorbulev *et al.*, 2001). DM solubilization did not impair ATP binding of Mdl1p, but the solubilization efficiency was only 50%. Much better solubilization (about 90%) was achieved by 1% Triton X-100.

Although first approaches to purify Mdl1p based on affinity chromatography were not successful, reconstitution approaches with Mdl1p partially enriched by gelfiltration were performed. After gelfiltration and subsequent reconstitution into liposomes, no incorporation of Mdl1p could be detected. The fact that the liposomes were not destabilized by detergent before use, could possibly explain the low reconstitution efficiency. DM is known to hardly destabilize liposomes and a stepwise addition of DM to preformed liposomes over a long time scale would probably achieve a more efficient destabilization of liposomes. Therefore, other detergents like octylglucoside were used for destabilization of liposomes in the further experiments. Furthermore, the lipid composition was optimized to retain functionality of a mitochondrial protein. Cholesterol which was reported to be inhibitory on the transport of mitochondrial membrane proteins was exchanged by cardiolipin (Heimpel *et al.*, 2001). In eukaryotes, cardiolipin is a characteristic phospholipid of the inner mitochondrial membrane and it was reported to be essential for the activity of several mitochondrial proteins (Heimpel *et al.*, 2001; Jiang *et al.*,

2000). For the following reconstitution experiments the liposomes were composed of phosphatidylcholine, phosphatidylethanolamine and cardiolipin in a ratio of 75:20:5.

To obtain a higher incorporation of Mdl1p into liposomes, solubilized mitochondria were directly used and reconstituted into preformed liposomes. Mdl1p was successfully incorporated into liposomes as shown by Western blot analysis. Sucrose gradient centrifugation showed that proteoliposomes were sealed and floated in the gradient. Azido-ATP-crosslinking experiments demonstrated that the ATP binding activity of Mdl1p during the reconstitution procedure was not impaired. Proteoliposomes were crosslinked either directly or after solubilization with Triton X-100. Both signals showed the same intensity, suggesting that the NBDs of reconstituted Mdl1p predominantly faced the outside of the vesicles. Although the ATP binding activity was demonstrated, no peptide uptake could be observed into the proteoliposomes. It is possible that reconstitution of other proteins resulted in release of imported peptides. It was shown that porins of the outer membrane were incorporated into the proteoliposomes as well. As porins are water filled channels, they might allow the diffusion of molecules up to a molecular mass of 6 kDa (Mannella, 1992); (Young *et al.*, 2001). Taking the existence of porins in proteoliposomes into account, it cannot be excluded that azido-ATP might have diffused through porins into the liposomes as well.

To avoid reconstitution of porins, proteins of solubilized mitoplasts (mitochondria stripped of the outer membrane) were reconstituted into liposomes. The proteoliposomes which floated in a sucrose gradient contained a high amount of incorporated Mdl1p but were still contaminated by porins. No peptide uptake could be observed. In order to trap the imported peptides inside the vesicles one could include peptide specific antibodies inside the liposomes. It is very unlikely that such immuno-complexes would be released into the medium. Similar strategies were applied to measure TAP-mediated peptide import into the ER. Only peptides which were glycosylated could accumulate in the ER, non-glycosylated peptides were efficiently exported via Sec61 (Koopmann *et al.*, 2000).

Reconstitution experiments with extracts of solubilized mitochondria had the advantage that interaction partners could be co-reconstituted which might be essential for Mdl1p transport activity. So far, it is not proven whether Mdl1p is functional in a minimal composition as a homodimer. The native molecular mass of the Mdl1p complex was determined to be 200 kDa (Young *et al.*, 2001). The accessory proteins of this complex are not defined.

6.2.2 Deletion of the mitochondrial targeting sequence

As it is difficult to study export, we tried to convert Mdl1p into an importer by directing the protein to the ER membrane. Mitochondrial targeting is often mediated through N-terminal leader sequences usually consisting of 20 to 35 residues highly enriched in basic, hydrophobic and hydroxylated amino acids (Neupert, 1997; von Heijne, 1986; Schatz and Dobberstein, 1996). A classical leader sequence of 59 amino acids has been predicted for Mdl1p. Mitochondrial targeting of ABC-me, a close homolog of Mdl1p, was investigated by deletion of amino acids 2-69 (Shirihai *et al.*, 2000). The truncated Δ 2-69 ABC-me-GFP was distributed in the cytosol, indicating that the N-terminus is indeed necessary for mitochondrial localisation. It has to be noticed that the truncated protein ABC-me was not incorporated into any membrane.

A construct of Mdl1p deleted in the amino acids 2-59 was expressed in yeast. To investigate if the deletion of the predicted mitochondrial targeting sequence influences the localisation of the protein, isolation of mitochondria was performed via sucrose gradients. No difference between the distribution of full-length and truncated Mdl1p was observed. This result was confirmed by partial digitonin-mediated solubilization of mitochondria followed by proteinase K digestion. Both methods showed that N-terminally truncated Mdl1p was still localised in the mitochondria and suggested an internal targeting sequence additional to the classical N-terminal one. Such internal targeting sequences have been observed in other inner mitochondrial membrane proteins e.g. ATP/ADP carrier and oxoglutarate carrier (Luciano *et al.*, 2001; Wiedemann *et al.*, 2001; Endres *et al.*, 1999; Kurz *et al.*, 1999; Kubrich *et al.*, 1998; Palmisano *et al.*, 1998). The targeting sequence has not been defined, so far. To characterise the mitochondrial targeting of Mdl1p *in vitro* transcription and translation assays would be the method of choice. In order to obtain targeting of Mdl1p to the ER, it might be convenient to fuse Mdl1p with a classical ER targeting sequence.

6.3 Identification and characterisation of an intracellular peptide transporter of *S. cerevisiae*

The transporter associated with antigen processing (TAP) has been for a long time the only known intracellular peptide ABC transporter which mediates the import of peptides into the lumen of the endoplasmic reticulum (Lankat-Buttgereit and Tampé, 2002). In experiments investigating peptide transport into yeast microsomes, we discovered a new peptide uptake activity. This transport is mediated by ORF *YLL048* since deletion of *YLL048::HIS3* resulted in loss of peptide uptake. The transport activity could be fully restored after transformation of the deletion mutant by plasmid-encoded *YLL048*. The ORF encodes a full-length ABC transporter which showed overlapping substrate spectrum with TAP and the same subcellular localisation. *YLL048p* is so far the first ABC transporter of *S. cerevisiae* mainly localised in the ER.

To clarify the subcellular localisation of the transporter several strategies were followed. First, we tried to generate a specific antibody against the linker region as well as the C-terminus of this ABC transporter. However, no specific antisera were obtained. Secondly, chromosomal tagging was tried in order to introduce an antibody-tag or GFP to *YLL048*. Unfortunately, after homologous recombination the ABC transporter was either not expressed or rapidly degraded. Lacking tools to identify the localisation of *YLL048p*, subcellular fractionation experiments in sucrose gradients were performed and peptide transport activity of all fractions was measured. Fractions corresponding to the ER showed a significantly increased ATP-dependent peptide transport activity. Fractions corresponding to vacuoles were identified by using α -mannosidase as reporter enzyme and did not show any peptide uptake.

In order to confirm the ER localisation of the transporter, glycosylation of NXT recognition sites of the reporter peptide was investigated. However, the transported peptides were very inefficiently glycosylated. One explanation might be that the glycosylation machinery of yeast did not accept peptides as substrates, although the reporter peptide R10T was successfully glycosylated in human and insect cell microsomes after import by TAP. The functionality of the glycosylation machinery of the isolated yeast microsomes was demonstrated using acetylated tripeptide (Ac-NYT-NH₂) (Wieland *et al.*, 1987; Römisch and Schekman, 1992).

Interestingly, *YLL048* was previously described to encode a bile acid transporter (BAT1p) localised in vacuoles and secretory vesicles (Ortiz *et al.*, 1997). In line with published data we demonstrated an ATP-dependent [³H]-taurocholate uptake mediated by *YLL048* into subcellular organelles. The $\Delta yll048$ strain did not exhibit any bile acid transport activity. Furthermore, it was

Discussion

shown that bile acids competed with peptides for transport. The transporter had a higher affinity for peptides than for bile acids. For efficient competition taurocholate had to be used in concentration of 1.5 mM, where this reagent based on its amphiphilic character might already function as detergent disrupting the integrity of the membrane.

The physiological function of YLL048p is still not well understood. The gene product is not essential for cell viability as deletion mutants did not show any phenotype. It is difficult to imagine that YLL048p acts as a taurocholate uptake system because yeast cells do not have any bile acid metabolism. It was discussed that Bat1p might be responsible for vacuolar sequestration of heme-derived catabolites, which could be considered as bile-like molecules in yeast (Ortiz *et al.*, 1997). A highly increased toxicity of bile acids was reported towards the *PDR1*, *PDR3* double disruptant mutants (Kolaczkowski *et al.*, 2002) suggesting Bat1p as a new member of the PDR network. However, we could not observe an influence of the Pdr1p and Pdr3p on the transcription level of *YLL048*.

We have characterised YLL048p as a specific peptide uptake system of yeast ER. The physiological relevance of peptide uptake into the ER is not clarified yet. Here, the possibility was investigated whether YLL048p might be part of a novel route of peptide trafficking in yeast involved in the unfolded protein response (UPR) (Higashio and Kohno, 2002). However, upregulation of *YLL048* transcription induced by heat shock as well as under stress conditions was not observed.

7 ZUSAMMENFASSUNG

Der Transport von Molekülen über Membranen stellt einen vektoriellen Prozess dar, der den Stoffaustausch und die Kommunikation der einzelnen Kompartimente untereinander sowie mit der extrazellulären Umgebung ermöglicht. ABC (ATP-Binding Cassette) Transporter stellen eine der grössten Superfamilie von Membranproteinen dar, die den aktiven Transport von unterschiedlichen Substanzen über biologische Membranen bewerkstelligen. ABC Transporter sind in allen drei Domänen des Lebens vertreten, wo sie eine Vielzahl von zellulären Funktionen ausüben. In Bakterien dienen ABC Transporter häufig der Nahrungsaufnahme. Andere bakterielle Transporter sind an der Resistenzentwicklung beteiligt, indem sie Antibiotika und Toxine aus dem Cytosol exportieren. In Eukaryoten erfüllt diese Proteinfamilie vielfältige Funktionen und neben der Transportaktivität können diese Proteine als Ionenkanäle, Regulatoren von Kanälen oder Rezeptoren arbeiten. Einige Vertreter weisen eine hohe klinische Relevanz auf. Beispielsweise ist die Mutation des ABC Transporters CFTR die molekulare Grundlage für die Entstehung der cystischen Fibrose. Andere Vertreter dieser Proteinfamilie sind an der Entwicklung der Multidrogenresistenz beteiligt, und ihre Überexpression stellt ein ernstzunehmendes Problem bei der Behandlung von Tumoren und AIDS durch Chemotherapie dar. Daher sind die Aufklärung des Transportmechanismus sowie die potentielle Inhibition des Transporters von zentraler Bedeutung.

Alle ABC Transporter weisen den gleichen modularen Aufbau aus vier Untereinheiten auf. Zwei Transmembrandomänen (TMD) durchspannen die Membran mehrfach und bilden die Translokationspore für das Substrat. Die zwei löslichen Nukleotidbindedomänen (NBD) energetisieren den Transportprozess durch ATP Hydrolyse. Die ATP Bindung und Hydrolyse findet an stark konservierten Regionen der NBD statt: der Walker A und Walker B Sequenz sowie dem C-Loop.

Kommunikation und Kooperation der einzelnen Untereinheiten sind von zentraler Bedeutung, um den Transportprozess effizient zu leisten. Ziel dieser Arbeit war die Aufklärung des molekularen Mechanismus, durch den Substrattranslokation an ATP-Hydrolyse gekoppelt wird. Dabei diente mir der Peptidtransport, der durch ABC Transporter in der Hefe ausgeführt wird, als Modellsystem. Die Bäckerhefe stellt aufgrund leichter genetischer Manipulierbarkeit und schneller Produktion von Biomasse einen idealen Modellorganismus dar. Der ABC Transporter TAP (transporter associated with antigen processing) konnte erfolgreich in der Hefe exprimiert werden. Der Transportkomplex ist für

die Translokation antigener Peptide vom Cytosol ins ER verantwortlich und nimmt eine zentrale Funktion bei der Antigenpräsentation ein. Als TAP-homologes Protein wurde Mdl1p (multidrug resistance like) im Genom der Hefe *S. cerevisiae* beschrieben und als Peptidtransporter der inneren Mitochondrienmembran identifiziert.

Ziel dieser Arbeit war die funktionale Charakterisierung von Mdl1p. Die inneren Mitochondrienmembran ist neben der Chloroplastenmembran die einzige zelluläre Membran, die nicht mit dem Cytosol in Kontakt tritt und folglich nicht der Qualitätskontrolle durch das Ubiquitin/Proteasomsystem unterliegt. Daher verfügen Mitochondrien über eine autonome ATP-abhängige Qualitätskontrolle, die durch einen proteolytischen Multienzymkomplex vermittelt wird. Die AAA-Proteasen (ATPase associated with a variety of cellular activities) sind für den Abbau von missgefalteten Proteinen der inneren Mitochondrienmembran verantwortlich. Mdl1p exportiert Peptide, die als Degradationsprodukte von missgefalteten Proteinen in der Matrix entstehen, in den Intermembranraum des Mitochondriums. Mdl1p bildet einen Homodimer, wobei jede Untereinheit aus einer TMD und einer NBD besteht. Der Mechanismus der Peptidtranslokation und deren Energetisierung sind auf molekularer Ebene nicht aufgeklärt und wurden im Rahmen dieser Arbeit untersucht. Um die Arbeitsweise von Mdl1p zu verstehen, wurde Mdl1p in *S. cerevisiae* und *E. coli* exprimiert und anschließend partiell reinigt. Es wurde gezeigt, dass Mdl1p funktional hinsichtlich ATP Bindung war. Um Peptidtransportaktivitäten *in vitro* zu messen, wurde aus Hefemitochondrien partiell gereinigtes Mdl1p in Proteoliposomen rekonstituiert. Es konnte jedoch kein Peptidtransport nachgewiesen werden. Weiterführende Experimente sollen die Substratspezifität des Transporters im rekonstituierten System ermitteln. Um die Aktivität des Transporters *in vivo* zu untersuchen, wurde die Strategie verfolgt, durch Deletion der klassischen N-terminalen Signalsequenz Mdl1p ins ER zu dirigieren. Durch diese Modifikation sollte eine Mdl1p Mutante generiert werden, die als Importer fungiert und so eine leichtere Messung der Peptidtransportaktivität ermöglicht. Überraschenderweise wurde beobachtet, dass die um 59 Aminosäuren N-terminal verkürzte Variante ebenfalls ins Mitochondrium dirigiert wird. Diese Beobachtung lässt die Vermutung zu, dass zusätzlich zu der klassischen N-terminalen Präsequenz eine redundante interne Signalsequenz vorliegt, wie sie z.B. für die Zielsteuerung des mitochondrialen ADP/ATP carriers beschrieben wurde.

Aufgrund seines modulartigen Aufbaus konnte der ABC Transporter Mdl1p in seine N-terminale TMD und C-terminale NBD unterteilt werden. Die lösliche NBD wurde in *E. coli* überexprimiert und über einen Affinitätstag zur Homogenität gereinigt. Dabei wurde eine

Ausbeute von 50 mg Protein pro 1 L Zellkultur erzielt, und das Protein konnte auf 30 mg/ml konzentriert werden. Die Aktivität des Proteins wurde bezüglich ATP Bindung und Hydrolyse demonstriert. Die ATPase Aktivität folgte einer Michaelis-Menten Kinetik mit einer maximalen Wechselzahl von 0.5 ATP/min und einem K_m -Wert von 0.2 mM. Hinsichtlich der ATPase Aktivität zeigte die isolierte NBD keine Kooperativität, jedoch war die ATPase Aktivität nicht linear von der Proteinkonzentrations abhängig. Diese Beobachtung liess auf einen nicht monomeren Zwischenzustand im ATPase Zyklus schliessen. Es ist beschrieben, dass andere isolierte NBDs wie z.B. HisP und MalK ebenfalls keine Kooperativität in der ATPase Aktivität zeigen. Eine kooperative ATPase Aktivität konnte jedoch in den ABC Transportkomplex wie HisQMP₂ und MalFGK₂ nachgewiesen werden. Gelfiltrationsexperimente, wie sie an isolierten NBDs wie z.B HisP oder MalK durchgeführt wurden, haben keinen Dimer nachweisen können. Zum ersten Mal ist es uns gelungen, einen dimeren Zwischenzustand der Wildtyp-NBD unter dem Einfluss von ATPase Inhibitoren wie ortho-Vanadat oder Berylliumfluorid in der Gelfiltration zu beobachten. Ortho-Vanadat und BeF_x stellen Analoga des anorganischen Phosphates dar. Sie stabilisieren einen Enzymzustand während der ATP Hydrolyse, in dem das ADP Molekül in der Bindungstasche erhalten bleibt, während das Phosphat bereits dissoziiert ist. Eine Stöchiometriebestimmung hat ergeben, dass der Dimer symmetrisch mit zwei Nukleotiden beladen war. Beide Nukleotide lagen in hydrolysiertes Form vor.

Mutation des konservierten Glutamats stromabwärts des Walker B Motivs führte zu einer ATPase inaktiven NBD (E599). Diese Mutante bildete in Gegenwart von ATP einen stabilen Dimer. Die Stöchiometrieuntersuchungen an dem E599Q Dimer haben gezeigt, dass zwei Nukleotide inkorporiert waren. Nach einer Inkubation auf Eis in Abwesenheit von Mg²⁺ blieben zwei ATP Moleküle im Dimer erhalten. Wurde jedoch die NBD in Gegenwart von Mg²⁺ bei 30°C inkubiert, konnte ein Dimer isoliert werden, in dem ein ATP und ein ADP in das Molekül eingebaut waren. Obwohl die Inkubation auf mehrere Stunden verlängert wurde, konnte kein Dimer mit zwei ADP Molekülen isoliert wird. Dieses Ergebnis zeigte, dass zumindest ein ATP Molekül zur Erhaltung des Dimers erforderlich war. Hydrolyse beider Nukleotide führte zu Dissoziation des Komplexes.

Basierend auf diesen Ergebnissen konnte ein Modell für die ATP-Hydrolyse erstellt werden, in dem die Bindung der Nukleotide an die monomeren Untereinheiten eine Assoziation der NBD induziert. Zwei ATP Moleküle werden sequentiell hydrolysiert, bevor der Dimer mit gebundenen ADP Molekülen dissoziiert.

Im zweiten Teilprojekt dieser Arbeit wurde ein intrazellulärer Peptid ABC Transporter charakterisiert, der durch den Leserahmen *YLL048* im Hefegenom kodiert wird. In Analogie zu TAP transportiert YLL048p unter Hydrolyse von ATP Peptide in das Lumen des endoplasmatischen Reticulums. Durch den Einsatz von zufallsgerichteten Peptidbibliotheken wurde die Substratspezifität des Transporters im Detail untersucht. Dabei wurde gezeigt, dass der neu entdeckte Transporter eine Längenspezifität von 6 bis über 56 Aminosäuren aufweist. Ausserdem konnte gezeigt werden, dass Peptide mit D-Aminosäuren, die an unterschiedlichen Positionen eingeführt wurden, als Substrat erkannt werden. Eine mögliche physiologische Bedeutung des Peptidtransporters für die Hefezelle konnte nicht ermittelt werden. Die Deletion des *YLL048* Gens zeigte keinen Phänotyp. Stressfaktoren wie erhöhte Osmolarität oder Hitzeschock führten zu keiner erhöhten Transkription des Gens. Ferner konnte ausgeschlossen werden, dass die Transkriptionsfaktoren Pdr1p und Pdr3p die Expressionsrate von *YLL048* beeinflussen.

Im dritten Teilprojekt wurde ein autokriner Stimulationsassay entworfen, durch den in Hefe exprimierte TAP Mutanten auf Funktionalität überprüft werden sollten. Eine erfolgreiche Expression des Wildtyp-TAP-Komplexes in dem Hefestamm W303-1A konnte bereits etabliert werden. Um eine schnelle und effiziente Selektion von TAP Mutanten zu ermöglichen, wurde die Sekretion von Peptidpheromonen unter die Kontrolle der TAP Aktivität gestellt. Im Prinzip beruhte der Test auf dem Paarungsverhalten der Hefe, das durch die Peptidpheromone **a**- und α -Faktor vermittelt wird. Hefezellen des Paarungstyps *MATa* sezernieren den **a**-Faktor über den ABC Transporter Ste6 ins Medium, der die Hefezellen des *MAT α* -Paarungstyps zur Konjugation stimuliert. Umgekehrt sezernieren Hefezellen des Paarungstyps *MAT α* über den klassischen Sekretionsweg den α -Faktor. Der α -Faktor wird natürlicherweise als ein Vorläufermolekül von 120 Aminosäuren exprimiert, der über eine klassische Pre-pro-Sequenz verfügt. Nach ihrer Sekretion werden die Pheromone von G-Protein gekoppelten Rezeptoren Ste2 oder Ste3 auf der jeweiligen Zelloberfläche erkannt. Dadurch wird eine MAPK vermittelte Signaltransduktion in den Zellen induziert, die schliesslich zur Verschmelzung der Zellen unterschiedlichen Paarungstypes führt.

Da gezeigt werden konnte, dass der reife α -Faktor von TAP *in vitro* transportiert wurde, sollte die Sekretion des α -Faktors unter die Kontrolle des TAP-Transportes gestellt

werden. Dazu wurde im vorliegenden Versuchsansatz der reife α -Faktor in **a**-Zellen exprimiert. Um seine Sekretion über das ER und Golgi-Kompartiment zu unterbinden, wurde die klassische Pre-pro-Sequenz vom α -Faktor deletiert. Der cytoplasmatisch exprimierte α -Faktor sollte vom TAP-Komplex ins Periplasma gelangen und somit einen autokrinen Stimulus an der Zelloberfläche erzeugen. Für diesen Stimulationsassay standen Zellen zur Verfügung, deren aktivierte MAPK Kaskade in der Induktion von Genen endete, die das Wachstum der Hefezellen von Histidin Auxotrophie auf Prototrophie umstellen. Die Funktionalität der autokrinen Signalkaskade wurde durch extern zugeführten α -Faktor überprüft. Zugabe des α -Faktors in einer Konzentration von 100 nM führte zum Wachstum der Zellen in Abwesenheit von Histidin. Desweiteren konnte die cytoplasmatische Expression des α -Faktors gezeigt werden. Jedoch zeigte der TAP transformierte Hefestamm kein Wachstum in Abwesenheit von Histidin. Aus unbekanntem Gründen konnte keine Expression von TAP in dem verwendeten Stamm gezeigt werden. Anscheinend konnte der Hefe intrinsische YLL048 Peptidtransporter den α -Faktor ebenfalls nicht oder nicht effizient ins ER befördern, obwohl *in vitro* Transportexperimente gezeigt haben, dass YLL048p den α -Faktor als Substrat erkennt. Möglicherweise ist die cytoplasmatisch exprimierte Konzentration des α -Faktors zu gering, um effizient ins ER zu gelangen. Es ist auch vorstellbar, dass Proteasen im Cytosol den α -Faktor degradieren, bevor er ins ER gelangen kann.

8 Summary

The mechanism of peptide transport has been studied on two different ABC transporters of *S. cerevisiae*. Thereby, the aim of this PhD thesis was to characterise the transporter function on molecular level and shed light on the physiological role of these transporters.

The ABC gene *YLL048* encodes a novel intracellular transporter translocating peptides from the cytosol to the lumen of the ER. Deletion of the gene resulted in loss of peptide transport activity. The transport activity was fully restored after transformation of the deletion mutant by plasmid-encoded *YLL048*. Studying the substrate specificity using randomized peptide libraries it was demonstrated that peptides of the size from 6 to 56 amino acids are recognized. So far, no upper limit of the substrate size was obtained. Introduction of D-amino acids in various positions of a nonamer peptide did not impair transport activity. The physiological function of YLL048p is not well understood. The gene product is not essential for cell viability as the deletion mutant did not show any growth phenotype. To examine the possibility that *YLL048* encoded protein is part of a quality control of yeast cells involved in the unfolded protein response (UPR), upregulation of *YLL048* transcription by heat shock and stress conditions were investigated. We could not observe an influence of stress factors on *YLL048* mRNA level. Upregulation of gene expression by the transcription factors Pdr1p and Pdr3p was excluded.

The ABC transporter Mdl1p has been identified as peptide transporter of the inner mitochondrial membrane. This protein is required for the export of peptides with the size of 6 to 21 amino acids from the matrix into the intermembrane space. These peptides are generated by m-AAA proteases degrading non-assembled or misfolded membrane proteins. In order to understand the transport mechanism in detail, Mdl1p was expressed in *S. cerevisiae* and *E. coli*. Partially enriched protein was reconstituted into liposomes and was active in ATP binding. The association of the NBDs has been described as a central step of the ATPase cycle of ABC transporters, but it is still controversial how both motor domains cooperate and coordinate ATP hydrolysis. To address this question, the Mdl1p-NBD was overexpressed in *E. coli* and purified to homogeneity. The isolated NBD was active in ATP binding and hydrolysis with a turnover of 0.5 ATP per min and a K_m value of 0.2 mM. Isolated NBDs did not show cooperativity in ATPase activity. However, the ATPase activity was observed to be non-linearly dependent on protein concentration suggesting the active form of this enzyme is not a monomer. Very importantly, for the first time an ATP-induced dimer was observed after trapping the NBD by ortho-vanadate or BeF_x . The nucleotide composition of the trapped intermediate state was determined and two

Summary

ADP molecules were simultaneously bound per dimer. An ATP-induced dimer of the ATPase inactive mutant (E559Q) was observed already in the absence of ATPase inhibitor. The E599Q dimer contained two ATP molecules in the absence of Mg^{2+} at 4°C. Prolonged incubation at 30°C in the presence of Mg^{2+} induced a stable dimer in which one ATP and ADP molecule were trapped at the same time. Based on these experiments, a new cycle for ATPase activity of ABC transporters was proposed. Binding of ATP to two NBD monomers induces dimerization. Both nucleotides are hydrolysed sequentially. During the hydrolysis cycle the nucleotides cannot be released from the dimer. After hydrolysis of two ATP molecules the domains dissociate and start a new cycle.

9 Appendix

9.1 Thiol-specific labelling of NBDs to assay dimerization by FRET

Although gelfiltration was a useful method to detect dimer formation, the disadvantage of this method is the time required for separation of proteins. This makes it impossible to follow fast processes. To determine the association or dissociation kinetics of proteins, it is useful to measure the formation of the dimer in real-time e.g. by fluorescent resonance energy transfer (FRET). In FRET, nonradiative energy transfer occurs between two fluorophores. The energy transfer is based on an overlapping of the emission spectrum of the donor fluorophore with the excitation spectrum of the acceptor fluorophore. Because the efficiency of FRET decays with the sixth power of the donor-to-acceptor distance, the maximum separation allowing detectable FRET is about 100 Å. As energy transfer reports molecular proximity, it is possible to monitor dimerization of NBD by labelling each with two different fluorescent dyes.

The Mdl1p-NBD contains three cysteines, one of them is located three amino acids upstream of the Walker A sequence. From three dimensional structural prediction analysis this cysteine is highly embedded into the interior of the protein and probably not accessible for labelling. The other two cysteines are placed between the Q- and L-loop and should be accessible for derivatization by thiol-reactive dyes. One batch of the NBD was coupled to maleimide derivatized Oregon Green (OG) which has its excitation maximum at 490 nm and its emission maximum at 515 nm. The other batch of NBD was coupled to Texas Red (TR) which has its excitation maximum at 580 nm and its emission maximum at 600 nm. The TR-labelled NBD functions as acceptor whereas the OG-labelled NBD is the donor in FRET. After excitation at 490 nm the formation of the dimer consisting of two different dyes (50 %) is monitored by increasing emission at 600 nm of the acceptor or by quenching of donor fluorescence.

After labelling, the NBD was analysed for dimerization. In gelfiltration experiments labelled NBD and unmodified NBD were mixed in an equimolar ratio and trapped by BeF_x in the presence of MgATP (Fig.45). Only the unmodified NBDs formed a dimer. Obviously, the NBDs lost their ability to dimerize after the labelling reaction. To exclude that conditions during the labelling reaction had some negative effect, the NBDs were incubated with 0.1% methanol, which is the final concentration of methanol in the labelling reaction, mixed with an appropriate amount of glutathione and applied to a desalting column. After this procedure the NBDs remained active for dimerization (data not shown). As a control, the cysteines of the NBD were derivatized by iodacetamide, a thiol-reactive reagent, and again after this modification the NBDs lost their ability to dimerize (data not shown). It seems that some of the labelled cysteines or their molecular environment is critical for dimerization or ATP binding.

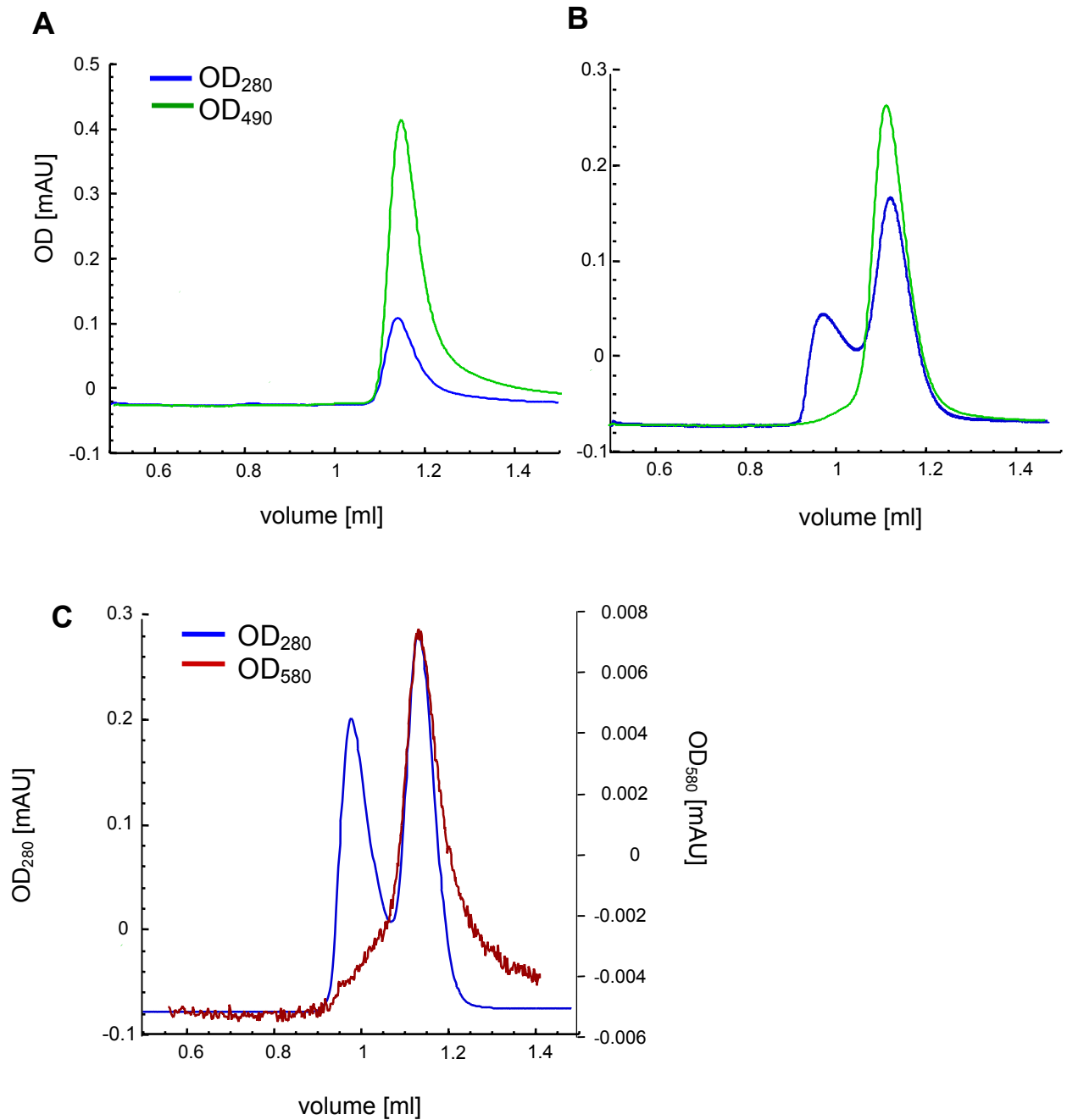


Fig.45 : Analytic gel filtration of fluorescent labelled wild-type NBD.

A: Oregon Green-labelled NBD (30 μ M) was applied to gel filtration (Superdex 75).

B: After preincubation of a 1:1 mixture of Oregon Green-labelled NBD (15 μ M) and non-labelled NBD with 1 mM BeF_x in the presence of 1 mM MgATP at 37°C, only the non-labelled NBD formed a dimer. The labelled NBD remained as a monomer as checked by OD 490 nm.

C: Incubation of Texas Red-labelled NBD (15 μ M) with an equimolar concentration of non-labelled NBD in the presence of 1 mM BeF_x and 1 mM MgATP at 37°C, showed dimer formation exclusively between non-labelled NBD. The labelled NBD remained as a monomer as checked by OD 580 nm.

9.2 Heterologous expression of transmembrane domain in *E. coli*

In bacterial systems the subunits of ABC transporters are mostly encoded as separate polypeptides e.g. HisQMP₂ or MALFGK₂ (Bavoil *et al.*, 1980; Ames and Lever, 1970). After their expression the NBD and TMD associate to a functional transport complex. Mdl1p is a half-size transporter in which a TMD is fused with a NBD in one polypeptide. However, we established the functional expression of the isolated NBD in *E. coli*. In the next step, we tried to express the TMD in *E. coli* as well. After expression and purification of both subunits we analysed whether NBDs and TMDs resemble the transport complex *in vitro*.

The TMD without the mitochondrial targeting sequence (59 aa to 422aa) was cloned into pET28b under the control of T7 promotor. This construct contains an N-terminal as well as a C-terminal His₆-tag. BL21(DE3) cells transformed with pET28-TMD were induced by IPTG. Inner membranes were isolated and solubilized with 30 mM DM, ultracentrifuged and the supernatant was applied to a Ni-IDA HiTrap column. After washing with 80 mM and 100 mM imidazole the membrane protein was eluted with 250 mM imidazole (Fig.46). The affinity purification of this construct was promising as an isolated peak was eluted by high imidazole concentrations. The eluted fractions were checked by Western blot using α -Ni-NTA alkaline phosphatase conjugate to detect His-tagged proteins. A single band of 33 kDa corresponding to the size of TMD was demonstrated. As α -Mdl1 is directed against the last C-terminal 15 amino acids of the protein, it does not recognize the transmembrane part as an epitope and could not be used. The purified fractions were applied to SDS-PAGE and the gel was silver stained revealing a high degree of impurities. Therefore, further chromatographies have to follow in order to obtain pure protein.

The TMD fractions were mixed with purified NBD and analysed for ATPase activity in the presence of two different peptides (R9LQK, R10T). No substrate stimulated ATPase could be observed (data not shown). This might be due to the inability of the NBD and TMD of Mdl1p to reorganize a full-length transporter after separate expression.

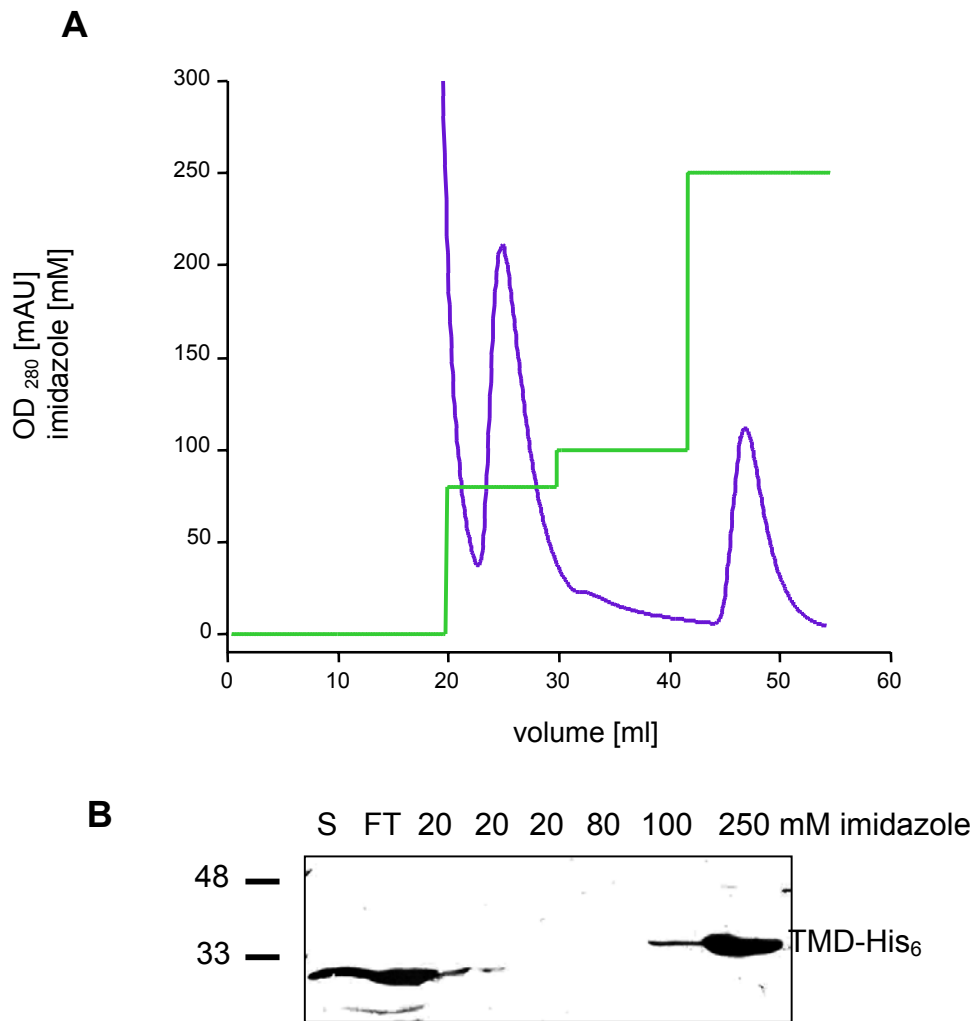


Fig.46: Heterologous expression of TMD in *E.coli* and purification by His-tag.

A: BL21(DE3) cells transformed with pET28-TMD were induced at OD 0.5 with 0.2 mM IPTG for 3 h at 30°C. After cell lysis debris were removed by 20.000 x g for 20 min and the supernatant was centrifuged by 100.000 x g for 1 h. The membrane pellet was solubilized with 30 mM DM for 1 h on ice, centrifuged at 20.000 x g for 15 min and the supernatant was applied to a Ni-IDA Hitrap column. The column was washed with a step gradient of 80 mM and 100 mM imidazole buffer containing 3 mM DM. Protein was eluted with 250 mM imidazole.

B: The fractions were analysed by SDS-PAGE and immunostaining with Ni-NTA alkaline phosphatase conjugate.

S: solubilized membranes, FT: flow through

9.3 Abbreviations

ABC	ATP-binding cassette
AHT	anhydrotetracycline
ADP	adenosine diphosphate
ATP	adenosine triphosphate
CDP	cytidine diphosphate
CTP	cytidine triphosphate
DMSO	dimethyl-sulphate
DTT	1,4-dithio-DL-threitol
EDTA	ethylenediamine tetraacetic acid
EGTA	ethylene glycol-bis(2-aminoethylether)- <i>N,N,N',N'</i> -tetraacetic acid
ER	endoplasmic reticulum
GDP	guanosine diphosphate
GTP	guanosine triphosphate
HEPES	<i>N</i> -(2-hydroxyethylpiperazine)- <i>N'</i> -2-ethanesulfonic acid
IDA	iminodiacetic acid
IPTG	isopropyl β -D-thiogalactopyranoside
LB	Luria broth
LEU	leucin
MHC	major histocompatibility complex
NBD	nucleotide binding domain
NTA	nitrilotriacetic acid
NP40	nonaethylenglycol- <i>p</i> -isooctophenyl ether
NTA	nitrilotriacetic acid
OD ₆₀₀	optical density at 600 nm
<i>o/n</i>	overnight
ORF	open reading frame
PAGE	polyacrylamide gel electrophoresis
PBS	phosphate-buffered saline
P-gp	P-glycoprotein
P _i	inorganic phosphate
PMSF	phenylmethonylsulfonyl fluoride

Appendix

RT	room temperature
SDS	sodium dodecyl sulphate
TBS	Tris-buffered saline
TCA	trichloroacetic acid
TMD	transmembrane domain
Tris	<i>tris</i> -(hydroxymethyl)aminomethane
UDP	uridine diphosphate
UTP	uridine triphosphate
YPD	yeast peptone dextrose
wt	wild type
MALDI-TOF	matrix-assisted laser desorption ionization - time of flight
TLC	thin layer chromatography
IMAC	immobilized metal affinity chromatography

10 References

1. Ames,G.F. and J.Lever. 1970. Components of histidine transport: histidine-binding proteins and hisP protein. *Proc Natl Acad Sci U S A* 66:1096-103.
2. Arnold,I. and T.Langer. 2002. Membrane protein degradation by AAA proteases in mitochondria. *Biochim Biophys Acta* 1592:89.
3. Baker,D., L.Hicke, M.Rexach, M.Schleyer, and R.Schekman. 1988. Reconstitution of SEC gene product-dependent intercompartmental protein transport. *Cell* 54:335-44.
4. Balzi,E. and A.Goffeau. 1995. Yeast multidrug resistance: the PDR network. *J Bioenerg Biomembr* 27:71-6.
5. Bauer,B.E., H.Wolfger, and K.Kuchler. 1999. Inventory and function of yeast ABC proteins: about sex, stress, pleiotropic drug and heavy metal resistance. *Biochim Biophys Acta* 1461:217-36.
6. Bavoil,P., M.Hofnung, and H.Nikaido. 1980. Identification of a cytoplasmic membrane-associated component of the maltose transport system of Escherichia coli. *J Biol Chem* 255:8366-9.
7. Bianchet,M.A., Y.H.Ko, L.M.Amzel, and P.L.Pedersen. 1997. Modeling of nucleotide binding domains of ABC transporter proteins based on a F1-ATPase/recA topology: structural model of the nucleotide binding domains of the cystic fibrosis transmembrane conductance regulator (CFTR). *J Bioenerg Biomembr* 29:503-24.

References

8. Blight, M.A., B. Menichi, and I.B. Holland. 1995. Evidence for post-transcriptional regulation of the synthesis of the *Escherichia coli* HlyB haemolysin translocator and production of polyclonal anti-HlyB antibody. *Mol Gen Genet* 247:73-85.
9. Blumer, K.J., J.E. Reneke, and J. Thorner. 1988. The STE2 gene product is the ligand-binding component of the alpha-factor receptor of *Saccharomyces cerevisiae*. *J Biol Chem* 263:10836-42.
10. Cross, F.R. 1988. DAF1, a mutant gene affecting size control, pheromone arrest, and cell cycle kinetics of *Saccharomyces cerevisiae*. *Mol Cell Biol* 8:4675-84.
11. Cui, Z., D. Hirata, E. Tsuchiya, H. Osada, and T. Miyakawa. 1996. The multidrug resistance-associated protein (MRP) subfamily (Yrs1/Yor1) of *Saccharomyces cerevisiae* is important for the tolerance to a broad range of organic anions. *J Biol Chem* 271:14712-6.
12. Daum, G., S.M. Gasser, and G. Schatz. 1982. Import of proteins into mitochondria. Energy-dependent, two-step processing of the intermembrane space enzyme cytochrome b2 by isolated yeast mitochondria. *J Biol Chem* 257:13075-80.
13. Dean, M. and R. Allikmets. 1995. Evolution of ATP-binding cassette transporter genes. *Curr Opin Genet Dev* 5:779-85.
14. Dean, M., R. Allikmets, B. Gerrard, C. Stewart, A. Kistler, B. Shafer, S. Michaelis, and J. Strathern. 1994. Mapping and sequencing of two yeast genes belonging to the ATP-binding cassette superfamily. *Yeast* 10:377-83.

-
15. Decottignies,A. and A.Goffeau. 1997. Complete inventory of the yeast ABC proteins. *Nat Genet* 15:137-45.
 16. Diederichs,K., J.Diez, G.Greller, C.Muller, J.Breed, C.Schnell, C.Vonrhein, W.Boos, and W.Welte. 2000. Crystal structure of MalK, the ATPase subunit of the trehalose/maltose ABC transporter of the archaeon *Thermococcus litoralis*. *EMBO J* 19:5951-61.
 17. Endres,M., W.Neupert, and M.Brunner. 1999. Transport of the ADP/ATP carrier of mitochondria from the TOM complex to the TIM22.54 complex. *EMBO J* 18:3214-21.
 18. Fetsch,E.E. and A.L.Davidson. 2002. Vanadate-catalyzed photocleavage of the signature motif of an ATP- binding cassette (ABC) transporter. *Proc Natl Acad Sci U S A* 99:9685-90.
 19. Fischer Lindahl,K. 1997. On naming H2 haplotypes: functional significance of MHC class Ib alleles. *Immunogenetics* 46:53-62.
 20. Fisher,A.J., C.A.Smith, J.B.Thoden, R.Smith, K.Sutoh, H.M.Holden, and I.Rayment. 1995. X-ray structures of the myosin motor domain of *Dictyostelium discoideum* complexed with MgADP.BeFx and MgADP.AIF4. *Biochemistry* 34:8960-72.
 21. Fritz,S., D.Rapaport, E.Klanner, W.Neupert, and B.Westermann. 2001. Connection of the mitochondrial outer and inner membranes by Fzo1 is critical for organellar fusion. *J Cell Biol* 152:683-92.

References

22. Gasser,S.M., A.Ohashi, G.Daum, P.C.Bohni, J.Gibson, G.A.Reid, T.Yonetani, and G.Schatz. 1982. Imported mitochondrial proteins cytochrome b2 and cytochrome c1 are processed in two steps. *Proc Natl Acad Sci U S A* 79:267-71.
23. Gaudet,R. and D.C.Wiley. 2001. Structure of the ABC ATPase domain of human TAP1, the transporter associated with antigen processing. *EMBO J* 20:4964-72.
24. Gavel,Y. and G.von Heijne. 1990. Cleavage-site motifs in mitochondrial targeting peptides. *Protein Eng* 4:33-7.
25. Goodno,C.C. 1982. Myosin active-site trapping with vanadate ion. *Methods Enzymol* 85:116-23.
26. Gorbulev,S., R.Abele, and R.Tampé. 2001. Allosteric crosstalk between peptide-binding, transport, and ATP hydrolysis of the ABC transporter TAP. *Proc Natl Acad Sci U S A* 98:3732-7.
27. Gottesman,M.M., C.A.Hrycyna, P.V.Schoenlein, U.A.Germann, and I.Pastan. 1995. Genetic analysis of the multidrug transporter. *Annu Rev Genet* 29:607-49.
28. Hartl,F.U., B.Schmidt, E.Wachter, H.Weiss, and W.Neupert. 1986. Transport into mitochondria and intramitochondrial sorting of the Fe/S protein of ubiquinol-cytochrome c reductase. *Cell* 47:939-51.
29. Heimpel,S., G.Basset, S.Odoy, and M.Klingenberg. 2001. Expression of the mitochondrial ADP/ATP carrier in *Escherichia coli*. Renaturation, reconstitution, and the effect of mutations on 10 positive residues. *J Biol Chem* 276:11499-506.

-
30. Henry,G.D., S.Maruta, M.Ikebe, and B.D.Sykes. 1993. Observation of multiple myosin subfragment 1-ADP-fluoroberyllate complexes by ^{19}F NMR spectroscopy. *Biochemistry* 32:10451-6.
 31. Hetteema,E.H., C.W.van Roermund, B.Distel, M.van den Berg, C.Vilela, C.Rodrigues-Pousada, R.J.Wanders, and H.F.Tabak. 1996. The ABC transporter proteins Pat1 and Pat2 are required for import of long-chain fatty acids into peroxisomes of *Saccharomyces cerevisiae*. *EMBO J* 15:3813-22.
 32. Higashio,H. and K.Kohno. 2002. A genetic link between the unfolded protein response and vesicle formation from the endoplasmic reticulum. *Biochem Biophys Res Commun* 296:568-74.
 33. Higgins,C.F. 1992. ABC transporters: from microorganisms to man. *Annu Rev Cell Biol* 8:67-113.
 34. Higgins,C.F. 1995. The ABC of channel regulation. *Cell* 82:693-6.
 35. Higgins,C.F. 2001. ABC transporters: physiology, structure and mechanism--an overview. *Res Microbiol* 152:205-10.
 36. Hogue,D.L., L.Liu, and V.Ling. 1999. Identification and characterization of a mammalian mitochondrial ATP- binding cassette membrane protein. *J Mol Biol* 285:379-89.
 37. Holland,I.B. and M.A.Blight. 1999. ABC-ATPases, adaptable energy generators fuelling transmembrane movement of a variety of molecules in organisms from bacteria to humans. *J Mol Biol* 293:381-99.

References

38. Hoof, T., A. Demmer, M.R. Hadam, J.R. Riordan, and B. Tumber. 1994. Cystic fibrosis-type mutational analysis in the ATP-binding cassette transporter signature of human P-glycoprotein MDR1. *J Biol Chem* 269:20575-83.
39. Hopfner, K.P., A. Karcher, D.S. Shin, L. Craig, L.M. Arthur, J.P. Carney, and J.A. Tainer. 2000. Structural biology of Rad50 ATPase: ATP-driven conformational control in DNA double-strand break repair and the ABC-ATPase superfamily. *Cell* 101:789-800.
40. Hrycyna, C.A., M. Ramachandra, U.A. Germann, P.W. Cheng, I. Pastan, and M.M. Gottesman. 1999. Both ATP sites of human P-glycoprotein are essential but not symmetric. *Biochemistry* 38:13887-99.
41. Hung, L.W., I.X. Wang, K. Nikaido, P.Q. Liu, G.F. Ames, and S.H. Kim. 1998. Crystal structure of the ATP-binding subunit of an ABC transporter. *Nature* 396:703-7.
42. Hunke, S., S. Dose, and E. Schneider. 1995. Vanadate and bafilomycin A1 are potent inhibitors of the ATPase activity of the reconstituted bacterial ATP-binding cassette transporter for maltose (MalFGK2). *Biochem Biophys Res Commun* 216:589-94.
43. Hunter, W.M. and F.C. Greenwood. 1964. A radio-immunoelectrophoretic assay for human growth hormone. *Biochem J* 91:43-56.
44. Jiang, F., M.T. Ryan, M. Schlame, M. Zhao, Z. Gu, M. Klingenberg, N. Pfanner, and M.L. Greenberg. 2000. Absence of cardiolipin in the *crd1* null mutant results in

-
- decreased mitochondrial membrane potential and reduced mitochondrial function. *J Biol Chem* 275:22387-94.
45. Jones,P.M. and A.M.George. 1999. Subunit interactions in ABC transporters: towards a functional architecture. *FEMS Microbiol Lett* 179:187-202.
46. Jones,P.M. and A.M.George. 2002. Mechanism of ABC transporters: A molecular dynamics simulation of a well characterised nucleotide-binding subunit. *Proc Natl Acad Sci U S A* 99:12639-44.
47. Julius,D., L.Blair, A.Brake, G.Sprague, and J.Thorner. 1983. Yeast alpha factor is processed from a larger precursor polypeptide: the essential role of a membrane-bound dipeptidyl aminopeptidase. *Cell* 32:839-52.
48. Katzmann,D.J., E.A.Epping, and W.S.Moye-Rowley. 1999. Mutational disruption of plasma membrane trafficking of *Saccharomyces cerevisiae* Yor1p, a homologue of mammalian multidrug resistance protein. *Mol Cell Biol* 19:2998-3009.
49. Kerr,I.D. 2002. Structure and association of ATP-binding cassette transporter nucleotide-binding domains. *Biochim Biophys Acta* 1561:47-64.
50. Kispal,G., P.Csere, C.Prohl, and R.Lill. 1999. The mitochondrial proteins Atm1p and Nfs1p are essential for biogenesis of cytosolic Fe/S proteins. *EMBO J* 18:3981-9.

References

51. Klanner,C., H.Prokisch, and T.Langer. 2001. MAP-1 and IAP-1, two novel AAA proteases with catalytic sites on opposite membrane surfaces in mitochondrial inner membrane of *Neurospora crassa*. *Mol Biol Cell* 12:2858-69.
52. Klopotoski,T. and A.Wiater. 1965. Synergism of aminotriazole and phosphate on the inhibition of yeast imidazole glycerol phosphate dehydratase. *Arch Biochem Biophys* 112:562-6.
53. Knop,M., K.Siegers, G.Pereira, W.Zachariae, B.Winsor, K.Nasmyth, and E.Schiebel. 1999. Epitope tagging of yeast genes using a PCR-based strategy: more tags and improved practical routines. *Yeast* 15:963-72.
54. Kolaczowska,A., M.Kolaczowski, A.Delahodde, and A.Goffeau. 2002. Functional dissection of Pdr1p, a regulator of multidrug resistance in *Saccharomyces cerevisiae*. *Mol Genet Genomics* 267:96-106.
55. Kolaczowski,M., A.Kolaczowska, J.Luczynski, S.Witek, and A.Goffeau. 1998. In vivo characterisation of the drug resistance profile of the major ABC transporters and other components of the yeast pleiotropic drug resistance network. *Microb Drug Resist* 4:143-58.
56. Koopmann,J.O., J.Albring, E.Huter, N.Bulbuc, P.Spee, J.Neefjes, G.J.Hammerling, and F.Momburg. 2000. Export of antigenic peptides from the endoplasmic reticulum intersects with retrograde protein translocation through the Sec61p channel. *Immunity* 13:117-27.

-
57. Kreimer,D.I., H.Malak, J.R.Lakowicz, S.Trakhanov, E.Villar, and V.L.Shnyrov. 2000. Thermodynamics and dynamics of histidine-binding protein, the water-soluble receptor of histidine permease. Implications for the transport of high and low affinity ligands. *Eur J Biochem* 267:4242-52.
 58. Kubrich,M., J.Rassow, W.Voos, N.Pfanner, and A.Honlinger. 1998. The import route of ADP/ATP carrier into mitochondria separates from the general import pathway of cleavable preproteins at the trans side of the outer membrane. *J Biol Chem* 273:16374-81.
 59. Kuchler,K., H.G.Dohlman, and J.Thorner. 1993. The a-factor transporter (STE6 gene product) and cell polarity in the yeast *Saccharomyces cerevisiae*. *J Cell Biol* 120:1203-15.
 60. Kuchler,K., R.E.Sterne, and J.Thorner. 1989. *Saccharomyces cerevisiae* STE6 gene product: a novel pathway for protein export in eukaryotic cells. *EMBO J* 8:3973-84.
 61. Kuchler,K. and J.Thorner. 1992. Functional expression of human *mdr1* in the yeast *Saccharomyces cerevisiae*. *Proc Natl Acad Sci U S A* 89:2302-6.
 62. Kurz,M., H.Martin, J.Rassow, N.Pfanner, and M.T.Ryan. 1999. Biogenesis of Tim proteins of the mitochondrial carrier import pathway: differential targeting mechanisms and crossing over with the main import pathway. *Mol Biol Cell* 10:2461-74.

References

63. Langer,T., M.Kaser, C.Klanner, and K.Leonhard. 2001. AAA proteases of mitochondria: quality control of membrane proteins and regulatory functions during mitochondrial biogenesis. *Biochem Soc Trans* 29:431-6.
64. Lankat-Buttgereit,B. and R.Tampé. 2002. The transporter associated with antigen processing: function and implications in human diseases. *Physiol Rev* 82:187-204.
65. Leighton,J. and G.Schatz. 1995. An ABC transporter in the mitochondrial inner membrane is required for normal growth of yeast. *EMBO J* 14:188-95.
66. Li,Z.S., M.Szczyпка, Y.P.Lu, D.J.Thiele, and P.A.Rea. 1996. The yeast cadmium factor protein (YCF1) is a vacuolar glutathione S- conjugate pump. *J Biol Chem* 271:6509-17.
67. Locher,K.P., A.T.Lee, and D.C.Rees. 2002. The E. coli BtuCD structure: a framework for ABC transporter architecture and mechanism. *Science* 296:1091-8.
68. Loo,T.W., M.C.Bartlett, and D.M.Clarke. 2002. The "LSGGQ" Motif in Each Nucleotide-binding Domain of Human P- glycoprotein Is Adjacent to the Opposing Walker A Sequence. *J Biol Chem* 277:41303-6.
69. Luciano,P., S.Vial, M.A.Vergnolle, S.D.Dyall, D.R.Robinson, and K.Tokatlidis. 2001. Functional reconstitution of the import of the yeast ADP/ATP carrier mediated by the TIM10 complex. *EMBO J* 20:4099-106.
70. Manfredi,J.P., C.Klein, J.J.Herrero, D.R.Byrd, J.Trueheart, W.T.Wiesler, D.M.Fowlkes, and J.R.Broach. 1996. Yeast alpha mating factor structure-activity

-
- relationship derived from genetically selected peptide agonists and antagonists of Ste2p. *Mol Cell Biol* 16:4700-9.
71. Mannella,C.A. 1992. The 'ins' and 'outs' of mitochondrial membrane channels. *Trends Biochem Sci* 17:315-20.
72. Maruta,S., G.D.Henry, B.D.Sykes, and M.Ikebe. 1993. Formation of the stable myosin-ADP-aluminum fluoride and myosin-ADP- beryllium fluoride complexes and their analysis using ^{19}F NMR. *J Biol Chem* 268:7093-100.
73. McGrath,J.P. and A.Varshavsky. 1989. The yeast STE6 gene encodes a homologue of the mammalian multidrug resistance P-glycoprotein. *Nature* 340:400-4.
74. McKinney,J.D., F.Chang, N.Heintz, and F.R.Cross. 1993. Negative regulation of FAR1 at the Start of the yeast cell cycle. *Genes Dev* 7:833-43.
75. Meisinger,C., T.Sommer, and N.Pfanner. 2000. Purification of *Saccharomyces cerevisiae* mitochondria devoid of microsomal and cytosolic contaminations. *Anal Biochem* 287:339-42.
76. Michaelis,S. and C.Berkower. 1995. Sequence comparison of yeast ATP-binding cassette proteins. *Cold Spring Harb Symp Quant Biol* 60:291-307.
77. Moody,J.E., L.Millen, D.Binns, J.F.Hunt, and P.J.Thomas. 2002. Cooperative, ATP-dependent association of the nucleotide binding cassettes during the catalytic cycle of ATP-binding cassette transporters. *J Biol Chem* 277:21111-4.

References

78. Morbach,S., S.Tebbe, and E.Schneider. 1993. The ATP-binding cassette (ABC) transporter for maltose/maltodextrins of *Salmonella typhimurium*. Characterization of the ATPase activity associated with the purified MalK subunit. *J Biol Chem* 268:18617-21.
79. Neupert,W. 1997. Protein import into mitochondria. *Annu Rev Biochem* 66:863-917.
80. Nikaido,H. 2002. How are the ABC transporters energized? *Proc Natl Acad Sci U S A* 99:9609-10.
81. Nikaido,K. and G.F.Ames. 1999. One intact ATP-binding subunit is sufficient to support ATP hydrolysis and translocation in an ABC transporter, the histidine permease. *J Biol Chem* 274:26727-35.
82. Nikaido,K., P.Q.Liu, and G.F.Ames. 1997. Purification and characterization of HisP, the ATP-binding subunit of a traffic ATPase (ABC transporter), the histidine permease of *Salmonella typhimurium*. Solubility, dimerization, and ATPase activity. *J Biol Chem* 272:27745-52.
83. Ortiz,D.F., M.V.St Pierre, A.Abdulmessih, and I.M.Arias. 1997. A yeast ATP-binding cassette-type protein mediating ATP-dependent bile acid transport. *J Biol Chem* 272:15358-65.
84. Palmisano,A., V.Zara, A.Honlinger, A.Vozza, P.J.Dekker, N.Pfanner, and F.Palmieri. 1998. Targeting and assembly of the oxoglutarate carrier: general

-
- principles for biogenesis of carrier proteins of the mitochondrial inner membrane. *Biochem J* 333:151-8.
85. Peter, M., A. Gartner, J. Horecka, G. Ammerer, and I. Herskowitz. 1993. FAR1 links the signal transduction pathway to the cell cycle machinery in yeast. *Cell* 73:747-60.
86. Phan, B. and E. Reisler. 1992. Inhibition of myosin ATPase by beryllium fluoride. *Biochemistry* 31:4787-93.
87. Roberts, C. J., C. K. Raymond, C. T. Yamashiro, and T. H. Stevens. 1991. Methods for studying the yeast vacuole. *Methods Enzymol* 194:644-61.
88. Römisch, K. and R. Schekman. 1992. Distinct processes mediate glycoprotein and glycopeptide export from the endoplasmic reticulum in *Saccharomyces cerevisiae*. *Proc Natl Acad Sci U S A* 89:7227-31.
89. Sankaran, B., S. Bhagat, and A. E. Senior. 1997. Inhibition of P-glycoprotein ATPase activity by beryllium fluoride. *Biochemistry* 36:6847-53.
90. Schatz, G. and B. Dobberstein. 1996. Common principles of protein translocation across membranes. *Science* 271:1519-26.
91. Schiestl, R. H. and R. D. Gietz. 1989. High efficiency transformation of intact yeast cells using single stranded nucleic acids as a carrier. *Curr Genet* 16:339-46.
92. Schmitt, M. E., T. A. Brown, and B. L. Trumpower. 1990. A rapid and simple method for preparation of RNA from *Saccharomyces cerevisiae*. *Nucleic Acids Res* 18:3091-2.

References

93. Schneider,E. and S.Hunke. 1998. ATP-binding-cassette (ABC) transport systems: functional and structural aspects of the ATP-hydrolyzing subunits/domains. *FEMS Microbiol Rev* 22:1-20.
94. Segui-Real,B., G.Kispal, R.Lill, and W.Neupert. 1993. Functional independence of the protein translocation machineries in mitochondrial outer and inner membranes: passage of preproteins through the intermembrane space. *EMBO J* 12:2211-8.
95. Senior,A.E., M.K.al-Shawi, and I.L.Urbatsch. 1995. The catalytic cycle of P-glycoprotein. *FEBS Lett* 377:285-9.
96. Shani,N., A.Sapag, P.A.Watkins, and D.Valle. 1996. An *S. cerevisiae* peroxisomal transporter, orthologous to the human adrenoleukodystrophy protein, appears to be a heterodimer of two half ABC transporters: Pxa1p and Pxa2p. *Ann N Y Acad Sci* 804:770-2.
97. Shani,N., P.A.Watkins, and D.Valle. 1995. PXA1, a possible *Saccharomyces cerevisiae* ortholog of the human adrenoleukodystrophy gene. *Proc Natl Acad Sci U S A* 92:6012-6.
98. Shanklin,J. 2000. Overexpression and purification of the *Escherichia coli* inner membrane enzyme acyl-acyl carrier protein synthase in an active form. *Protein Expr Purif* 18:355-60.
99. Sharma,S. and A.L.Davidson. 2000. Vanadate-induced trapping of nucleotides by purified maltose transport complex requires ATP hydrolysis. *J Bacteriol* 182:6570-6.

-
100. Shibuya,H., K.Kondo, N.Kimura, and S.Maruta. 2002. Formation and Characterization of Kinesin.ADP.Fluorometal Complexes. *J Biochem (Tokyo)* 132:573-9.
 101. Shirihai,O.S., T.Gregory, C.Yu, S.H.Orkin, and M.J.Weiss. 2000. ABC-me: a novel mitochondrial transporter induced by GATA-1 during erythroid differentiation. *EMBO J* 19:2492-502.
 102. Smith,C.A. and I.Rayment. 1995. X-ray structure of the magnesium(II)-pyrophosphate complex of the truncated head of Dictyostelium discoideum myosin to 2.7 Å resolution. *Biochemistry* 34:8973-81.
 103. Smith,P.C., N.Karpowich, L.Millen, J.E.Moody, J.Rosen, P.J.Thomas, and J.F.Hunt. 2002. ATP binding to the motor domain from an ABC transporter drives formation of a nucleotide sandwich dimer. *Mol Cell* 10:139-49.
 104. Sprague,G.F., Jr., L.C.Blair, and J.Thorner. 1983. Cell interactions and regulation of cell type in the yeast *Saccharomyces cerevisiae*. *Annu Rev Microbiol* 37:623-60.
 105. Szczypka,M.S., J.A.Wemmie, W.S.Moye-Rowley, and D.J.Thiele. 1994. A yeast metal resistance protein similar to human cystic fibrosis transmembrane conductance regulator (CFTR) and multidrug resistance- associated protein. *J Biol Chem* 269:22853-7.
 106. Taglicht,D. and S.Michaelis. 1998. *Saccharomyces cerevisiae* ABC proteins and their relevance to human health and disease. *Methods Enzymol* 292:130-62.

References

107. Trueheart, J., J.D. Boeke, and G.R. Fink. 1987. Two genes required for cell fusion during yeast conjugation: evidence for a pheromone-induced surface protein. *Mol Cell Biol* 7:2316-28.
108. Urbatsch, I.L., L. Beaudet, I. Carrier, and P. Gros. 1998. Mutations in either nucleotide-binding site of P-glycoprotein (Mdr3) prevent vanadate trapping of nucleotide at both sites. *Biochemistry* 37:4592-602.
109. Urbatsch, I.L., M. Julien, I. Carrier, M.E. Rousseau, R. Cayrol, and P. Gros. 2000a. Mutational analysis of conserved carboxylate residues in the nucleotide binding sites of P-glycoprotein. *Biochemistry* 39:14138-49
110. Urbatsch, I.L., K. Gimi, S. Wilke-Mounts, and A.E. Senior. 2000b. Conserved walker A Ser residues in the catalytic sites of P-glycoprotein are critical for catalysis and involved primarily at the transition state step. *J Biol Chem* 275:25031-8.
111. Urbatsch, I.L., B. Sankaran, S. Bhagat, and A.E. Senior. 1995a. Both P-glycoprotein nucleotide-binding sites are catalytically active. *J Biol Chem* 270:26956-61.
112. Urbatsch, I.L., B. Sankaran, J. Weber, and A.E. Senior. 1995b. P-glycoprotein is stably inhibited by vanadate-induced trapping of nucleotide at a single catalytic site. *J Biol Chem* 270:19383-90.
113. Urlinger, S., K. Kuchler, T.H. Meyer, S. Uebel, and R. Tampé. 1997. Intracellular location, complex formation, and function of the transporter associated with antigen processing in yeast. *Eur J Biochem* 245:266-72.

-
114. Van Der Heide, T. and B. Poolman. 2002. ABC transporters: one, two or four extracytoplasmic substrate-binding sites? *EMBO J Rep* 3:938-43.
 115. van Veen, H.W., C.F. Higgins, and W.N. Konings. 2001. Multidrug transport by ATP binding cassette transporters: a proposed two-cylinder engine mechanism. *Res Microbiol* 152:365-74.
 116. van Veen, H.W., A. Margolles, M. Muller, C.F. Higgins, and W.N. Konings. 2000. The homodimeric ATP-binding cassette transporter LmrA mediates multidrug transport by an alternating two-site (two-cylinder engine) mechanism. *EMBO J* 19:2503-14.
 117. von Heijne, G. 1986. Mitochondrial targeting sequences may form amphiphilic helices. *EMBO J* 5:1335-42.
 118. Walker, J.E., M. Saraste, and N.J. Gay. 1982. E. coli F1-ATPase interacts with a membrane protein component of a proton channel. *Nature* 298:867-9.
 119. Wiedemann, N., N. Pfanner, and M.T. Ryan. 2001. The three modules of ADP/ATP carrier cooperate in receptor recruitment and translocation into mitochondria. *EMBO J* 20:951-60.
 120. Wieland, F.T., M.L. Gleason, T.A. Serafini, and J.E. Rothman. 1987. The rate of bulk flow from the endoplasmic reticulum to the cell surface. *Cell* 50:289-300.
 121. Young, L., K. Leonhard, T. Tatsuta, J. Trowsdale, and T. Langer. 2001. Role of the ABC transporter Mdl1 in peptide export from mitochondria. *Science* 291:2135-8.

References

122. Zhang,F., D.L.Hogue, L.Liu, C.L.Fisher, D.Hui, S.Childs, and V.Ling. 2000. M-ABC2, a new human mitochondrial ATP-binding cassette membrane protein. *FEBS Lett* 478:89-94.
123. Zinser,E. and G.Daum. 1995. Isolation and biochemical characterization of organelles from the yeast, *Saccharomyces cerevisiae*. *Yeast* 11:493-536.

11 Curriculum vitae

Name: Janas, Eva

Born: 02.12.1972, Kedzerzen, Poland

Nationality: German

Education

10/98-12/02 Doctoral student studying for Ph.D. at the University of Frankfurt, Institute for Biochemistry; University of Marburg, Institute for Physiological Chemistry; Max-Planck-Institute for Biochemistry, Martinsried.

Ph.D. thesis on "Intracellular Peptide Trafficking in *Saccharomyces cerevisiae*"

10/98-12/98 Research visit at the University and Biocenter of Vienna, Department of Molecular Genetics, supported by an EMBO short termed fellowship.

10/92-07/98 Master's degree and bachelor's degree (with honour) in Biology at the University of Bonn. Diploma thesis on "Relevance of Penicillin Binding Proteins for the Induction of chromosomal encoded β -Lactamase AmpC of *Enterobacteriaceae*". This work was carried out at the medical and pharmacological Institute of Microbiology, University of Bonn.

04/96-05/96 Practical work at the Pharma Research Center, Bayer AG in Wuppertal.

09/83-05/92 Graduated (with honour) at Hildegardis grammar school, Hagen

Conferences

2002 Selected short talk at the international meeting "Transporters 2002", Seon

2001/1999 Poster presentation at the 2nd and 3rd FEBS Advanced Lecture Course "ATP-Binding Cassette Proteins: From Multidrug Resistance to Genetic disease", Gosau

Academic teachers

Prof. Tampé (Frankfurt), Prof. Entian (Frankfurt), Prof. Kuchler (Vienna), Prof. Wiedemann (Bonn), Prof. Trüper (Bonn), Prof. Sandhoff (Bonn)

Danksagung

Ich möchte mich bei Prof. Tampé für die intensive Betreuung und Förderung sowie die zahlreichen fruchtbaren Diskussionen bedanken.

Prof. Entian danke ich für die Übernahme des Koreferates.

Prof. Kuchler danke ich für die Zusammenarbeit und Unterstützung. Besonders bedanken möchte ich mich bei Hubert Wolfger, der mich in Wien betreut hat. Nicole Foeger, Chantal Schwartz und Michael Schuster möchte ich für die geniale Zeit in Wien danken.

Allen Mitgliedern der Arbeitsgruppe Tampé danke ich für ihre Hilfsbereitschaft und angenehme Arbeitsatmosphäre.

Besonderer Dank gilt der Münchner Doktorandengruppe, die mich herzlich aufgenommen hat. Ich bedanke mich bei Kurt Pawlitschko für die Einarbeitung ins Projekt. Ulf Rädler, Lars Neumann und Stefan Ammer danke ich für die Hilfe und Motivation und für die vielen lustigen Wochenendaktionen.

Herzlicher Dank gilt der Marburger Gruppe. Dabei möchte ich Christian May für die experimentelle Unterstützung danken und dem technischen Personal, vor allem Nicole Löwer, für die Mitarbeit am Projekt.

Den Mitgliedern der Arbeitsgruppe in Frankfurt danke ich für ihre Kollegialität und Unterstützung. Matthias Hofacker danke ich besonders für die enge und erfolgreiche Zusammenarbeit im Mdl-Projekt. Min Chen danke ich für ihre Diskussionsbereitschaft und kreativen Anmerkungen sowie. Sander Smits für seine Vorschläge. Robin Klemm, Suman Lata und Christine Le Gal danke ich für ihre Unterstützung. Chris van der Does, Hans Bäumert, Silke Beismann-Driemeyer, Ulf, Sander, Kurt und Lars danke für das Korrekturlesen. Lizhong He und vielen anderen danke ich für die Hilfe am Computer.

Der grösste Dank gilt meiner Mutter, die mir das Studium und die Promotion ermöglicht hat.